UNIVERSITEIT VAN PRETORIA
UNIVERSITY OF PRETORIA
YUNIBESITHI YA PRETORIA

A Comparison of Radiotherapy Techniques for the Irradiation of the Whole Scalp

by

Emma Viviers

Submitted in partial fulfilment of the requirements for the Degree Masters of Science MSc in Medical Physics In the Faculty of Health Sciences

University of Pretoria
Pretoria

November 2010

Student Number 21329975

Preface

Particular thanks are given to Katinka Ferreira, at Steve Biko Academic Hospital, who assisted me with many of the practical aspects of this project. Thanks are also given to Mrs Evelyn Farrant for her continued motivation to complete this dissertation. Gratitude is extended to the patient who first prompted this study and best wishes are offered for complete remission without complications.

Contents

Contents

List of Tables

List of Tables

List of Figures

List of Figures

List of Figures

List of Abbreviations

BEV	Beam's Eye View
CT	Computed Tomography
d_{MAX}	Depth of Maximum Dose
DVH	Dose Volume Histogram
d_x	Depth of x% of Maximum Dose
EDR	Extended Dose Range
HDR	High Dose Rate
IMRT	Intensity Modulated Radiotherapy
Linac	Linear Accelerator
MeV	Mega Electron Volts
MLC	Multi-Leaved Collimator
mu	Monitor Units
MV	Megavolts
OEV	Observer's Eye View
PDD	Percentage Depth Dose
PTV	Planned Target Volume
R_P	Practical Range
SAD	Source Axis Distance
SSD	Source Surface Distance
TEP	Tissue Equivalent Plastic
TLD	Thermoluminescent Dosimeter
TPS	Treatment Planning System

CHAPTER I: INTRODUCTION

A patient was treated for a synovial sarcoma of the scalp, a soft tissue sarcoma, at Steve Biko Academic Hospital in September 2006. Due to time constraints, which prevented the thorough investigation of other modalities, Intensity Modulated Radiotherapy (IMRT) was chosen to deliver this treatment. Total scalp irradiation is required for several other superficial malignancies such as angiosarcomas, melanomas and cutaneous lymphomas.

It was found in the literature that several different techniques for the irradiation of the whole scalp have been proposed. However, there have not been any studies performed which thoroughly compare different treatment modalities and the accuracy of their delivery.

Radiotherapy of the entire scalp provides a challenge to several aspects of the treatment. The scalp is an extremely concave surface, which presents a number of technical obstacles to the treatment planning process. The scalp also has a target volume which is very close to the surface of the patient. This is within the region of electronic dis-equilibrium for external beam therapy. The calculation of dose in this region demands accurate beam modelling by the planning system and additionally requires rigorous quality control procedures to ensure that the calculated dose matches the predicted dose.

External beam radiotherapy using photon beams is generally performed using static conformal beams which are targeted towards a common isocentre. However, if the scalp is treated in this manner, then a dose which is sufficient to kill the tumour, will over irradiate the brain and other critical structures. The exit dose from these beams will also overlap with the entrance dose from the opposite beams. It is difficult to match these beams to reduce this overlap whilst still providing adequate target coverage.

This can be partially overcome using electron beam therapy. However, electron beams are normally delivered using an applicator which is close to the patient's skin. Hence a common isocentre cannot be used, without colliding with the patient. Each electron beam

must additionally be blocked in regions where the field will overlap with an adjacent field. To deliver dose using traditional electron applicators results in a technically demanding and time consuming daily treatment setup, with a high risk of overlap resulting in unacceptably high doses.

In addition to difficulties posed by irradiating a highly spherical object, there are technical problems with the patient setup. The patient generally has to lie in a prone position with a mask to prevent movement. This position results in a highly restricted, claustrophobic treatment which requires good patient cooperation, especially during long treatment times, such as those experienced with IMRT.

Each treatment modality has logistical problems which must also be evaluated. The use of treatment aids such as masks, bolus or blocks requires personnel time and the use of disposable resources. Alternatively techniques such as IMRT require specialized linear accelerators and planning systems which may not be available to all clinics.

It can therefore be seen that a thorough investigation of different treatment modalities to treat the whole scalp can be invaluable in optimizing dose distribution parameters, patient comfort and resource management.

There have been several papers published which propose different solutions to this complex problem. Some of the more popular treatment techniques have been the use of a combination of lateral opposing electron and photon fields with brain blocking, or multiple electron field 'sets' to smudge match lines[1]. Photon IMRT using a conventional linac with a multi-leaved collimator (MLC) has been proposed as an elegant isocentric solution [2]. A combination of electron and or photon arcs has been proposed to address the problem of the concave surface [3]. High dose rate (HDR) brachytherapy catheters have been demonstrated by several authors. [4]

[1] Able (1991:1063), De Boer (2005:S555), Mellenberg (1991:1063), Tung (1993:153)
[2] Pearce (2005:S66)
[3] Kinard (1996:351)
[4] Holmes (2006:104), Liebmann (2007:211), Nakamura (2003:198), Ozyar (2002:1286)

However, several of these letters and papers have strongly promoted the use of a particular technique over another, without an experimental comparison with alternative modalities [5].

One paper showed the results of a thorough analysis (measured and computational) of static electron, arced electron and IMRT photon treatments [6]. However, this paper was unfortunately based on the treatment of a unilateral scalp target volume and, as such, the results cannot be widely applied to total scalp irradiation. Others have compared existing techniques based purely on the dose distributions *predicted* by the planning systems [7].

This is particularly problematic in the region of the scalp where tangential fields, air gaps, high dose gradients and electronic buildup may not be accurately predicted by the treatment planning systems.

Despite the number of papers which have been published on this treatment, none have compared multiple, commonly available, techniques, with an analysis of both the calculated and the delivered dose distributions, as well as resource and personnel input requirements, to truly evaluate the best modality for total scalp irradiation.

The aim of this project was to evaluate several different treatment techniques, the majority of which were applied using equipment which is standard in most radiotherapy units.

[5] Able (1991:1063), Bedford (2005:1549), de Boer (2005:S555), Hardcastle (2008:5061), Holmes (2006:104), Mellenberg (1991:1063), Nakamura (2003:198), Ozyar (2002:1286), Pearce (2005:S66), Tung (1993:153)
[6] Able (1991:1063)
[7] Nakamura (2003:198), Pearce (2005:S66), Wojcicka (2009:255)

The treatment techniques that were evaluated were:

- Electron isocentric arced fields
- Parallel opposed photon fields with opposing blocked electron fields
- Intensity modulated non-coplanar photon fields
- High dose rate brachytherapy using catheters with a fixed mould

Matched shielded multiple electron fields were not considered in this evaluation as the technique is too cumbersome to deliver accurately without overlap or cold spots.

All of the plans were developed to treat an anthropomorphic 'Rando' phantom head. A phantom head was used to provide consistency across all treatment modalities. It allows an evaluation throughout the treated area, particularly for dose measurements to the brain. There is not a huge variation in skull shape between individuals so the plan assessment is likely to be applicable to patient treatments. By using a phantom, it may not be possible to review all problems which are likely to be encountered in a clinical environment. However, it would be neither practical nor ethical to perform this evaluation on a patient.

The plans were optimized and in some cases several plans of each type were generated. The plans were evaluated in terms of the dose distributions produced, the personnel and machine time required for all steps of the procedure and the equipment required for delivery. Additionally, the accuracy of plan delivery was assessed using thermoluminescent dosimetry (TLD) and film dosimetry techniques.

CHAPTER II: MATERIALS AND METHODS

1. INTRODUCTION

All of the plans were developed to treat an anthropomorphic phantom head. The phantom consists of slices of tissue equivalent plastic encasing a human skull. The phantom head was scanned at 1cm slice separation and thickness using the Siemens Sensation 4 computed tomography (CT) scanner at Steve Biko Academic Hospital. The CT scans were performed using the cushions, thermoplastic masks, applicator tubes and bolus material which were to be used in the treatment process. A prone cushion was manufactured from plastic foam to be used for the duration of the study. Additionally, marks were made on the phantom to ensure reproducibility of the mask and isocentre setup during treatment.

Before planning an electron arc treatment, the arc applicator was first commissioned and data entered into the XiO planning system. The commissioning process employed the use of Wellhöfer Dosimetrie scanning software.

For all of the external beam techniques with electrons and photons, the CMS Focus XiO planning system was used. For the brachytherapy technique, the Varian BrachyVision planning system was used. The external beam treatments were delivered using Siemens Oncor linear accelerators with 1 cm MLCs. An additional electron arc applicator was employed for the electron arc treatment. The HDR treatment was delivered using a GammaMed+ HDR unit with a 5 Ci Iridium 192 source.

The plans were each optimised using personnel expertise, inverse planning and trial and error processes.

The first factor for comparison of the plans was the accuracy with which each plan could be delivered. This involved a dosimetric analysis of each treatment as well as an evaluation of setup difficulties. The dosimetric analysis of the plans was performed using film dosimetry and TLD dosimetry.

The next factor for comparison was the resultant dose distribution predicted by the planning system. The plans were assessed in terms of the dose coverage of the scalp planned target volume (PTV) and the maximum doses received by the phantom head. Five plans were optimized and 1 cm transverse slices printed with the PTV, brain and isodose lines marked. All of the plans were normalized to give a nominal dose of 100 cGy. Dose volume histograms (DVHs) were also printed. These printed plans were given to 19 radiotherapy personnel to rank in order of preference in a blind study.

The final factor for comparison was the ease with which each plan could be delivered. This part of the evaluation included the preparation time and specialised labour required for each treatment aid, such as the manufacture of electron shields, HDR moulds or bolus material. It also included the time and expertise required for the planning of each treatment and the patient setup and delivery time.

CHAPTER II: MATERIALS AND METHODS

2. ELECTRON ARC COMMISSIONING

The electron arc applicator had not been previously used so all data needed to be measured for the planning system. For this a 'Blue Phantom' water bath (~48cm^3) was employed, as shown in Fig 1. Two 3 mm radius, 0.13 cc ion chambers (6538, 6539) were used to measure the reference output and a field measurement respectively. This equipment was used in conjunction with a CU500E Electrometer and drive control unit and Scanditronix Wellhöfer Omni-Pro 6.4A scanning software. A Siemens Oncor linear accelerator (linac) 'Hobbes' was used to make these measurements. This linac has electron energies 5, 7, 8, 10, 12, 14 MeV. The electron arc applicator license was not enabled on this linear accelerator so an applicator interlock was overridden during measurements.

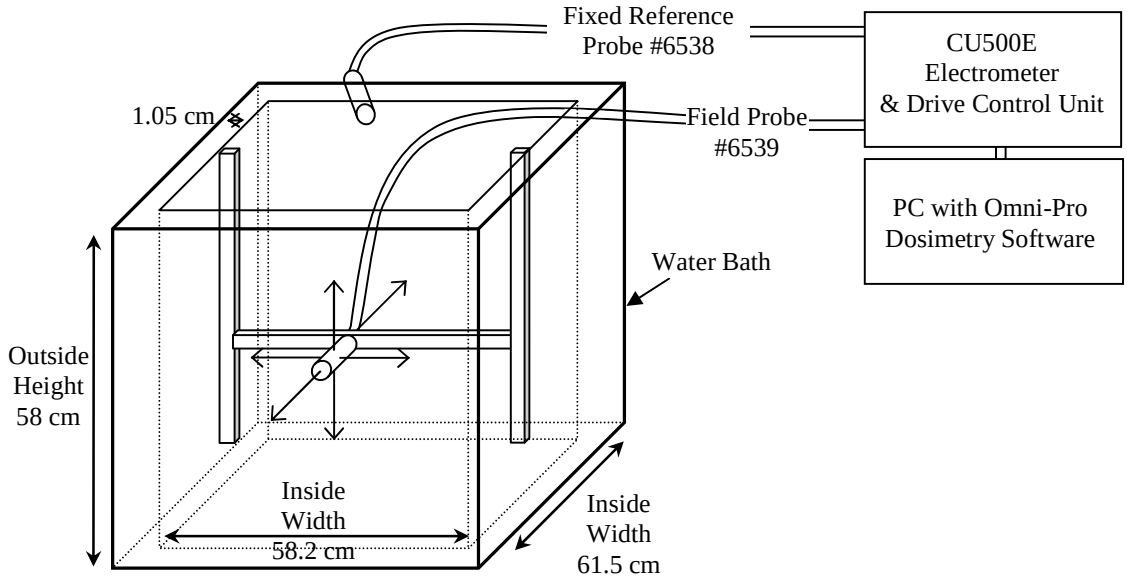

Fig 1 - Water bath used to commission electron arc applicator

The electron arc applicator had physical dimensions of 41x171 mm, for a source surface distance (SSD) of 72.5 cm. This projected a field of 60x250 mm at the isocentre of 100 cm. With a collimator rotation of 0° the inplane dimension was 250 mm and the crossplane dimension 60 mm.

The water bath level was checked using the scanning field probe. The water level was set to an SSD of 100 cm. The lowest electron energy at d_{MAX} was used to determine the gain of the electrometer. Profiles were scanned automatically to determine the exact position of the central axis. Percentage depth dose (PDD) curves were then acquired for all energies to determine the depths of the isodoses required for profile scanning.

The PDDs were acquired down to a depth of R_P+100mm where R_P is the practical range for the electrons. Inplane and crossplane profiles were acquired at the depths of d_{MAX}, d_{90}, d_{80} and d_{50}. Here d_{MAX} is the depth of the maximum dose and d_x is the depth of the x % dose. The PDD and profile scans were repeated at SSDs of 80, 90, 110 cm. These PDD curves are shown in Fig 2.

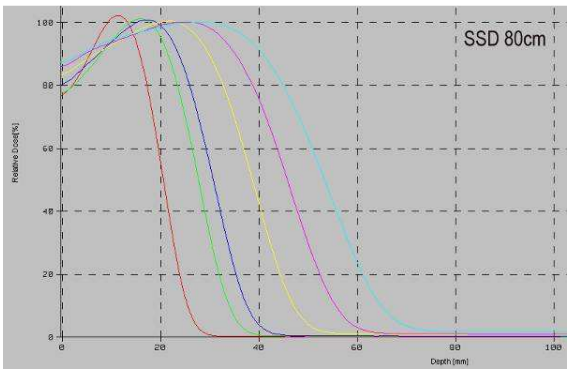

SSD 80 cm

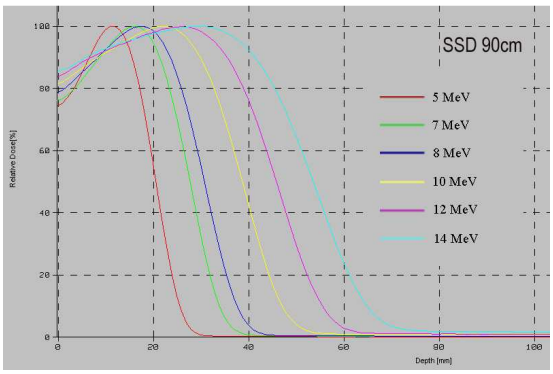

SSD 90 cm

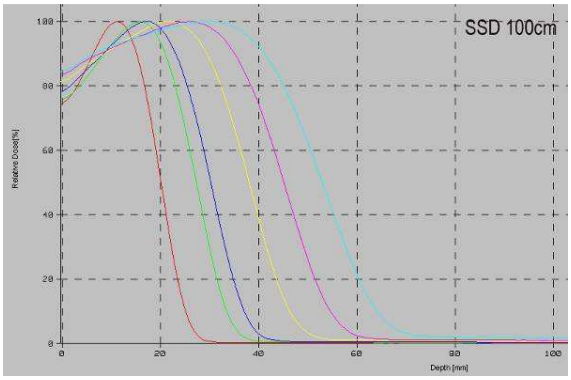

SSD 100 cm

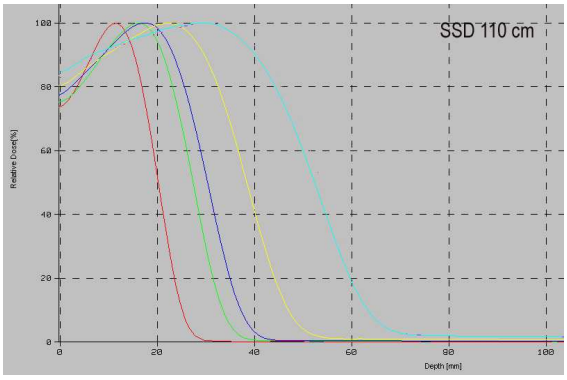

SSD 110 cm

Fig 2 – PDDs measured for all electron energies with the electron arc applicator

After ionization to dose conversion, the electron ranges measured are shown in Table 1.

Energy	SSD cm	Field Size d_0	d_{MAX}	d_{90}	d_{80}	d_{50}	R_P	R_P+100
5 MeV	80	200x45	11.0	15.3	17.0	20.4	25.6	125.6
7 MeV	80	200x45	15.6	21.1	23.2	27.6	34.2	134.2
8 MeV	80	200x45	16.8	23.3	25.7	30.6	37.9	79.7
10 MeV	80	200x45	21.2	29.6	32.6	38.6	47.4	147.4
12 MeV	80	200x45	24.6	35.0	38.7	45.7	55.9	155.9
14 MeV	80	200x45	27.7	40.6	44.9	53.3	65.4	165.4
5 MeV	90	225x54	11.2	15.4	17.0	20.4	25.6	125.6
7 MeV	90	225x54	15.7	21.2	23.3	27.6	34.2	134.2
8 MeV	90	225x54	17.0	23.4	25.8	30.6	37.9	137.9
10 MeV	90	225x54	21.6	29.7	32.7	38.6	47.4	147.4
12 MeV	90	225x54	25.4	35.4	38.8	45.7	55.8	155.8
14 MeV	90	225x54	29.0	41.2	45.4	53.5	65.1	165.1
5 MeV	100	250x60	10.8	15.1	16.7	20.1	25.2	125.2
7 MeV	100	250x60	15.4	20.9	22.9	27.2	33.7	133.7
8 MeV	100	250x60	16.8	23.0	25.4	30.2	37.3	137.3
10 MeV	100	250x60	21.3	29.7	32.2	38.0	46.7	146.7
12 MeV	100	250x60	25.4	35.0	38.3	45.0	54.8	154.8
14 MeV	100	250x60	29.7	41.1	45.1	52.9	64.4	164.4
5 MeV	110	275x66	11.1	15.2	16.8	20.2	25.3	125.3
7 MeV	110	275x66	15.7	21.1	23.1	27.3	33.7	133.7
8 MeV	110	275x66	17.1	23.3	25.5	30.3	37.4	137.4
10 MeV	110	275x66	21.9	29.6	32.5	38.4	47.1	147.1
12 MeV	110	275x66	25.4*	34.5*	38.1*	45.0*	54.8*	154.7*
14 MeV	100	275x66	28.8	40.1	44.2	52.3	63.8	163.8

*Table 1 – Electron ranges measured for electron arc applicator(*extrapolated values)*

Using the electron ranges measured previously, the d_{MAX} was determined for all relevant SSDs for both the arc applicator and the 10x10 cm reference applicator. Outputs were then measured using the large water bath, a PTW Unidos electrometer (T10002-20009) and a 0.6 cc waterproof farmer ionization chamber (TW300013-2678). Outputs were measured at SSDs of 75-110 cm at 5 cm intervals for the electron arc applicator. These readings were then compared with the output values for a 10x10 applicator at d_{MAX} for an SSD of 100cm to give an absolute output value in cGy / mu (monitor units). For each measurement, the probe was positioned at a depth of d_{SET} = d_{MAX} + (chamber radius/2) so that the effective depth of measurement was equal to d_{MAX}. Table 2 shows the doses measured at each SSD and the output in cGy/mu. All of the readings were relative readings made with no temperature and pressure corrections.

Arc Applicator 6x25cm:

SSD *cm*	Energy *MeV*	d_{SET} mm	Measure *mGy*	Output *cGy/mu*
75	5	11.2	751.6	1.664
75	7	15.7	772.6	1.661
75	8	16.9	777.3	1.658
75	10	21.3	783.9	1.665
75	12	24.7	791.3	1.676
75	14	27.8	794.9	1.671
80	5	11.1	634.1	1.404
80	7	15.7	661.0	1.421
80	8	16.9	670.8	1.431
80	10	21.3	677.6	1.439
80	12	24.7	687.2	1.455
80	14	27.8	692.8	1.457

SSD *cm*	Energy *MeV*	d_{SET} *mm*	Measure *mGy*	Output *cGy/mu*
95	5	11.2	391.5	0.867
95	7	15.6	426.0	0.916
95	8	17.0	442.9	0.945
95	10	21.5	462.5	0.982
95	12	25.5	477.2	1.011
95	14	29.5	481.8	1.013
100	5	10.9	334.0	0.739
100	7	15.5	373.4	0.803
100	8	16.9	389.1	0.830
100	10	21.4	408.0	0.867
100	12	25.5	422.5	0.895
100	14	29.8	430.2	0.905

SSD *cm*	Energy *MeV*	d_{SET} mm	Measure *mGy*	Output *cGy/mu*
85	5	11.2	536.9	1.189
85	7	15.7	569.2	1.224
85	8	17.0	581.9	1.242
85	10	21.4	595.0	1.264
85	12	25.1	604.9	1.281
85	14	28.4	611.6	1.286
90	5	11.3	459.1	1.016
90	7	15.8	492.1	1.058
90	8	17.1	510.1	1.088
90	10	21.6	523.0	1.111
90	12	25.5	535.6	1.134
90	14	29.1	541.4	1.138

SSD *cm*	Energy *MeV*	d_{SET} *mm*	Measure *mGy*	Output *cGy/mu*
105	5	11.0	289.2	0.640
105	7	15.7	326.2	0.701
105	8	17.0	342.3	0.730
105	10	21.7	364.9	0.775
105	12	25.5	378.8	0.802
105	14	29.9	388.1	0.816
110	5	11.2	250.2	0.554
110	7	15.8	286.3	0.616
110	8	17.2	303.4	0.647
110	10	22.0	325.9	0.692
110	12	25.6	339.2	0.718
110	14	30.0	350.0	0.736

Reference Applicator 10x10cm:

SSD *cm*	Energy *MeV*	d_{SET} mm	Measure *mGy*	Output *cGy/mu*
100	5	8.3	451.7	1.000
100	7	13.3	465.1	1.000
100	8	16.0	468.7	1.000

SSD *cm*	Energy *MeV*	d_{SET} *mm*	Measure *mGy*	Output *cGy/mu*
100	10	20.4	470.8	1.000
100	12	24.0	472.2	1.000
100	14	25.4	475.6	1.000

Table 2 – Outputs, depths and doses for electron arc applicator

The effective SSD was calculated using Khan F (2003:317). The short applicator results in wider scatter, hence a significantly reduced effective SSD. This gave the results shown in Table 3 which were entered into the planning system:

Energy	d_{MAX} (mm)	Effective SSD (cm)
5 MeV	10.8	68.5
7 MeV	15.4	75.3
8 MeV	16.8	78.9

Energy	d_{MAX} (mm)	Effective SSD (cm)
10 MeV	21.3	84.9
12 MeV	25.4	87.6
14 MeV	29.7	90.3

Table 3 – Effective SSDs for electron arc applicator

Table 4 summarises the electron outputs for the electron arc applicator. Fig 3 shows the inverse square law dependence of the outputs with SSD and the inverse relationship between the level of dose reduction with SSD and the electron energy. This is due to the preferential attenuation of lower energy electrons in the air gap between the applicator and the patient surface.

	Actual (cGy/mu)							
Energy	75	80	85	90	95	100	105	110
5	1.664	1.404	1.189	1.016	0.867	0.739	0.640	0.554
7	1.661	1.421	1.224	1.058	0.916	0.803	0.701	0.616
8	1.658	1.431	1.242	1.088	0.945	0.830	0.730	0.647
10	1.665	1.439	1.264	1.111	0.982	0.867	0.775	0.692
12	1.676	1.455	1.281	1.134	1.011	0.895	0.802	0.718
14	1.671	1.457	1.286	1.138	1.013	0.905	0.816	0.736

Table 4 – Summary of electron outputs for arc applicator

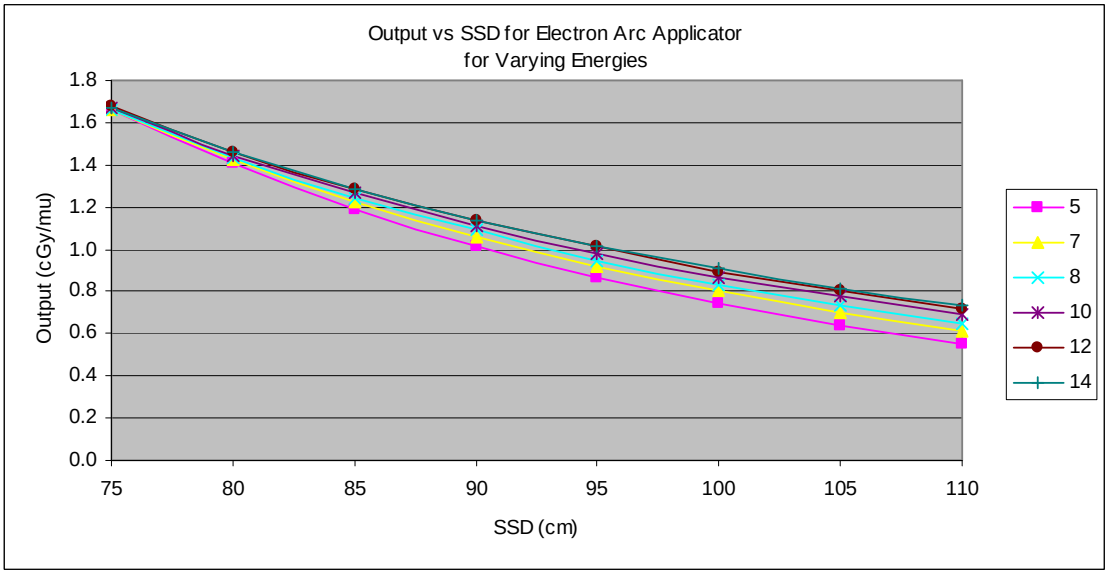

Fig 3 – Output versus SSD for electron arc applicator

All of this information was entered into the Source File Maintenance section of the XiO planning system. Both constant source surface (SSD) and constant source axis distance (SAD) were selected as possible treatment types in the planning system. However, the software has not been written by CMS Focus to calculate SAD electron treatments. The measured and calculated profiles were displayed by the Source File Maintenance module. By changing the ΣθX values and the coulomb scattering correction, the pencil beam modelled profiles were adjusted to most closely match the measured profile. A coulomb scattering correction of 2 was used for all profiles. The ΣθX values which gave the most accurate modelling are shown in Table 5:

Energy	5 MeV	7 MeV	8 MeV	10 MeV	12 MeV	14 MeV
ΣθX	0.055	0.035	0.030	0.025	0.020	0.015

Table 5 – Beam modelling factors for the electron arc applicator

An example of the measured and calculated profiles for 7 MeV is shown in Fig 4. Additionally, the relative intensities at the cone edge could be manually adjusted. The final profile adjustment is shown in Fig 5 and was used for all energies. The arc applicator was thus commissioned for all energies.

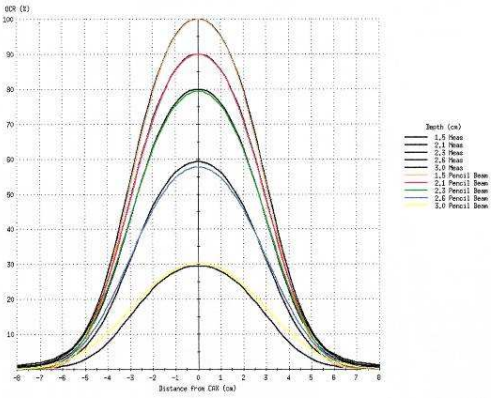

Fig 4 - Calculated and measured dose profiles 7 MeV for electron arc applicator

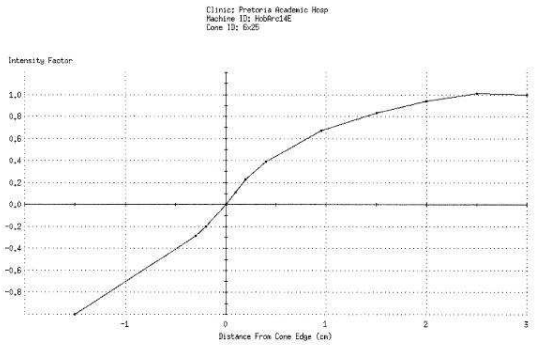

Fig 5 – Relative beam intensity at cone edge for electron arc applicator

CHAPTER II: MATERIALS AND METHODS

3. PLAN GENERATION

Table 6 shows the plans which were generated for the phantom, to deliver a uniform dose to the Scalp PTV whilst avoiding the brain.

Type	TPS	Plan Name	Bolus	Block	
HDR	BrachyVision	HDR	N	N	24 Catheters
IMRT	XiO	Slow IMRT	Y	N	247 Segments
		No Bolus IMRT	N	N	246 Segments
		Quick IMRT	Y	N	125 Segments
X & e- Parallel Opposed	XiO	eXOpp	N	Y	4 blocks
Electron Arc	XiO	ArcAP	N	N	One Arc
		Block Ears Arc AP	N	Y	Arc Ears Blocked
		Bolus Ears Arc AP	Y	N	Arc Ears Bolused
		Arc LR Inf Sup	N	Y	Arc Split into Inferior & Superior Treatments

Table 6 – Plans generated for phantom head

Several plans were developed for the electron arc and the IMRT plan types. This is because each plan resulted in logistical differences as well as dose distribution preferences. They would therefore all have to be considered for evaluation.

CHAPTER II: MATERIALS AND METHODS

3. PLAN GENERATION, 3.1 HDR

The first plan generated employed HDR brachytherapy. The dose was delivered using multiple catheters placed from anterior to posterior into which the source was inserted. A thermoplastic mask was made to fit the phantom head. Excess mask was trimmed to reduce patient discomfort. This was repeated to give two layers, as seen in Fig 6, to give a larger standoff between the catheters and the phantom surface. Two plastic tubes were used for each catheter. The smaller tube was threaded inside the larger tube, as seen in Fig 6, using oil lubrication to give a stable applicator for catheter placement and to give an increased catheter standoff.

The tubes were fitted to the thermoplastic mask using super glue and superglue filler. It was found that this gave more superior fixation than superglue alone, a hot glue gun, melted thermoplastic mask or threaded ties. The catheter ends were sealed using melted thermoplastic. This ensured reliable catheter positioning and visibility for digitization on the planning system.

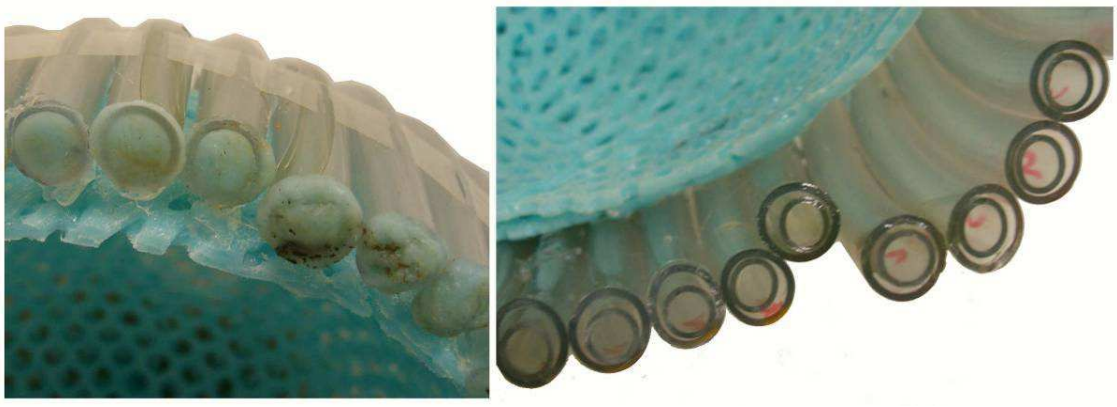

Catheter ends sealed with thermoplastic material

Double layer mask & double plastic tubing visible

Fig 6 – Plastic tubing and thermoplastic mask used for HDR plan

The optimum standoff was determined previously on the planning system. Using a prototype shown in Fig 7, it was found that catheters placed too close to the head gave a rapid dose drop off which did not allow for enough penetration to cover the entire PTV. Catheters placed at an increased standoff gave more uniform coverage but at the expense of overall brain dose. Additionally, the tightest curvature of the tubes which would allow free passage of the HDR catheters was determined previously as a circle of diameter 8 cm. This restricted the use of catheters placed around the ears as shown in Fig 7.

Prototype with short catheter standoff Final scalp applicator

Fig 7 – Catheter placement on phantom head

The CT scan was acquired following standard protocol for head and neck radiotherapy. The phantom was scanned while the head mask and catheters were in place. The mask position was marked on the phantom for reproducibility during treatment. The treatment planning system used was SomaVision Brachytherapy Planning v7-3-10 “BrachyVision”.

The phantom bony structures, scalp (PTV), eyes and brain were contoured using standard tools. The catheters were then individually tracked into the system. The catheter positions in the planning system are shown in Fig 8.

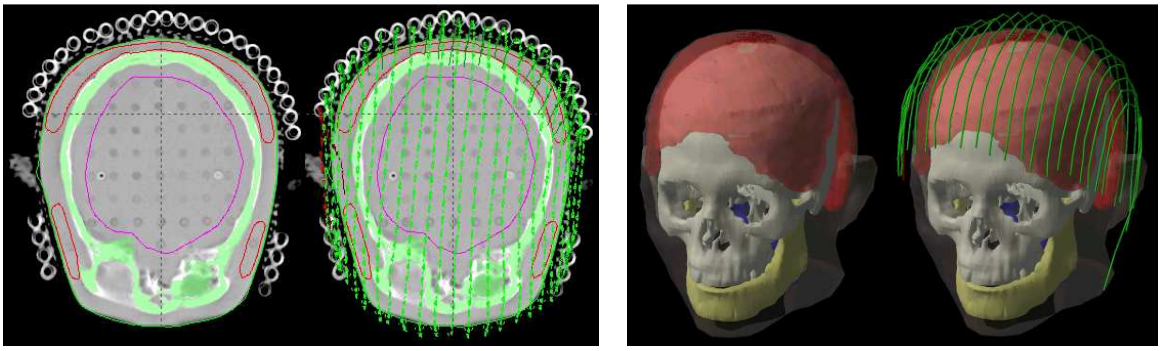

Transverse CT image showing catheters Observer's view of catheter position

Fig 8 – Catheter position in brachytherapy planning system

Inverse planning optimization software was used to generate the dwell times to give a dose of 50-70Gy to the scalp PTV contoured. The inverse planning limits were adjusted several times to find the optimum values for the desired distribution. The final limits selected are shown in Table 7.

Organ	Percentage (%)	Dose (Gy)	Limit	Weight
Scalp	5%	76 Gy	Max	1.0
Scalp	95%	56 Gy	Min	1.0
Brain	10%	38 Gy	Max	1.0

Table 7 – Inverse planning prescription for HDR brachytherapy

The phantom was placed in a vertical position to simulate a patient sitting in a chair. The mask and catheter applicator was placed on to the phantom head to correspond with marks made during the CT scan. The plan was delivered to the phantom with films and TLDs placed between slices for dosimetry purposes. The plan was exported to the GammaMed+ HDR brachytherapy control unit. It was generated for 24 channels, but unfortunately only two catheters were available for placement into the catheter tubing. The plan was therefore delivered in 12 consecutive deliveries, to two channels at a time. This resulted in room entry between each delivery and room entry between each channel-check run. The total 'irradiation' time of 268 seconds therefore took approximately 30

minutes to deliver. This could be avoided in a patient delivery by purchasing an additional 22 catheters. The mask and catheters were removed from the phantom in a dark room to avoid accidental film exposure. The films were then removed and developed at the same time as calibration films. The TLDs were removed and were read at the same time as calibration TLDs.

CHAPTER II: MATERIALS AND METHODS
3. PLAN GENERATION, 3.2 IMRT

All other plans were generated using the CMS Focus XiO planning system. Two sets of IMRT data were input. The first employed the use of wax bolus material, as seen in Fig 9, to pull hot spots away from the phantom into the bolus. This was the method employed in the pilot study on the patient with the synovial sarcoma.

Fig 9 – Wax bolus used for IMRT plan

The use of wax bolus was both time consuming to manufacture and uncomfortable for the patient, so an additional CT and contour set was acquired without bolus material. The beam configuration for the IMRT plans was optimised to avoid critical structures and

give a fairly uniform coverage of the PTV. An energy of 6 MV was employed to minimise beam penetration into the brain and reduce skin sparing. The jaw size was automatically adjusted to cover the target with a 5 mm margin.

The optimal isocentric beam configuration was found to be two lateral oblique fields and three oblique fields rotated in the coronal plane as shown in Table 8, Fig 10 and Fig 11.

	Ant to Post	Cranial Caudal	Post to Ant	R Post Oblique	L Post Oblique
Field Size	190x164	210x168	160x170	210x164	200x163
Gantry	230º	280º	30º	45º	315º
Collimator	0º	0º	0º	0º	0º
Couch	90º	90º	90º	0º	0º

Table 8 – Beam configuration for IMRT

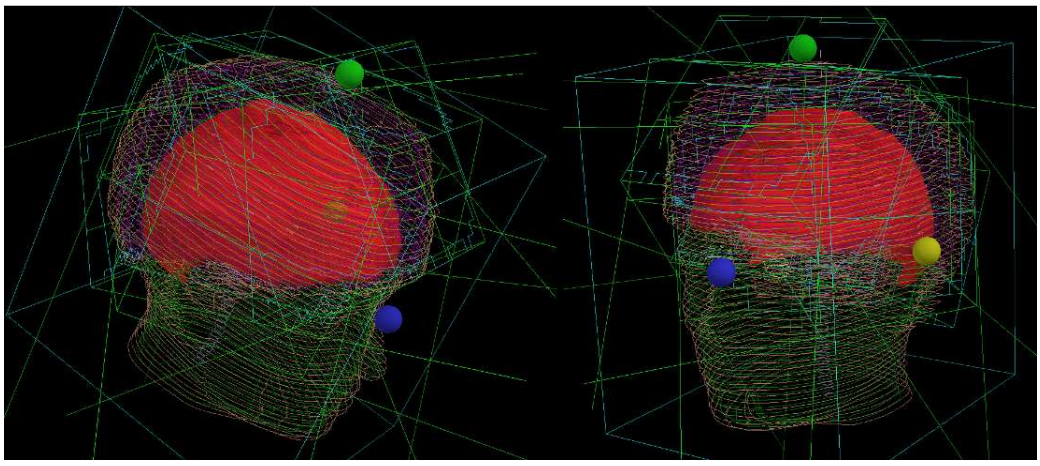

Fig 10 – Observer's eye view (OEV) of beam configuration used for IMRT plans

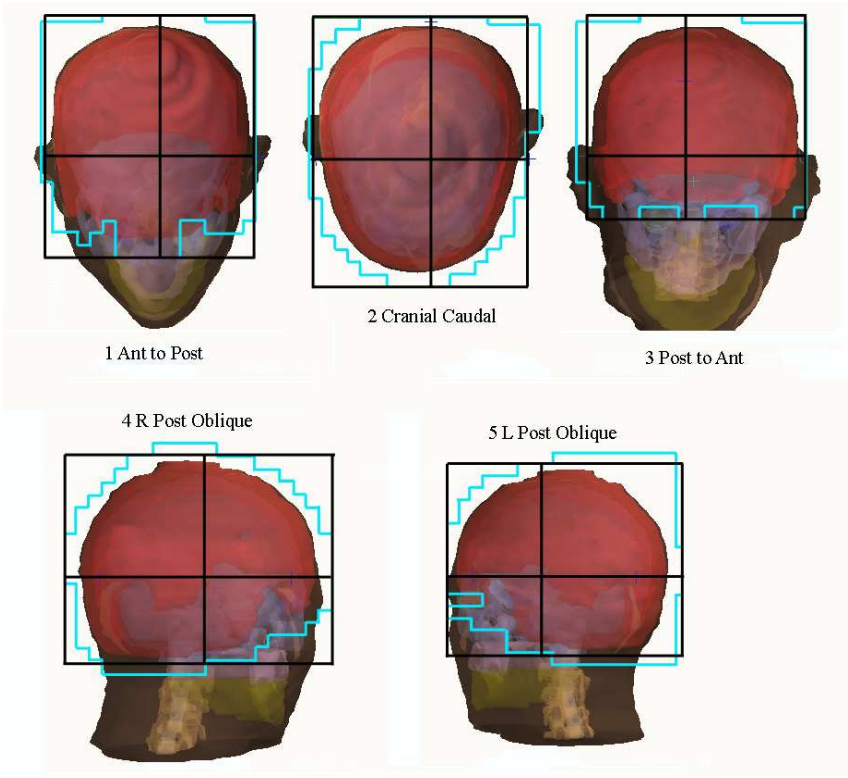

Fig 11 - Beam's eye view (BEV) of configuration used for IMRT plans

The IMRT inverse planning limits employed were a convergence criterion of 0.01%, a step increment of 1 cm and <100 iterations. The best inverse planning prescription was found to be the values shown in Table 9 for a prescription dose of 100 cGy. These criteria were used for all the IMRT plans.

Structure	Rank	Objective	Dose (cGy)	Volume (%)	Power
Scalp PTV	1	Max	132	0	3.0
		Goal	104	100	1.0
		Min	100	100	3.5
Brain	2	Max	30	0	2.2
		Dose Volume	20	100	2.0
Spinal Cord	3	Max	80	100	2.0
R Eye	4	Max	20	0	1.0
L Eye	5	Max	20	0	1.0

Table 9 – Inverse planning prescription for IMRT

The MLC segments were optimised using the inverse planning algorithm. Examples of the resultant beam fluences are shown in Fig 12.

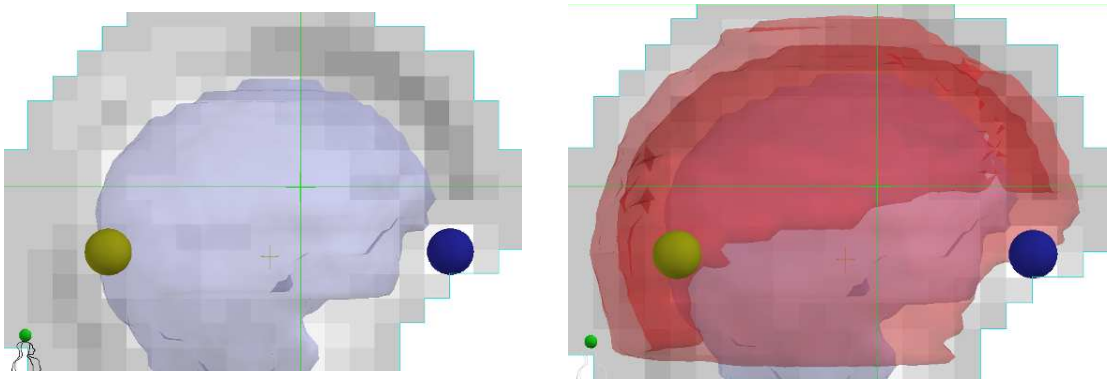

Fluence map avoiding brain Fluence map covering PTV

Fig 12 – Example of fluence maps used for IMRT fields

Three IMRT plans were generated for comparison:

i. 'Slow IMRT' plan with 20 discrete intensity levels, a minimum segment size of 1 cm, 247 segments and 1092 mu, using the wax bolus.
ii. 'No Bolus IMRT' a slow plan of 246 segments and 1124 mu, without the bolus.
iii. 'Quick IMRT' plan which employed the bolus, had 10 discrete intensity levels, a minimum segment size of 2cm, 125 segments and 931 mu, to shorten the delivery time.

The Slow IMRT plan was treated using the 'Obelix' Siemens Oncor linear accelerator. The mask and bolus was placed on to the phantom head to correspond with marks made during the CT scan. The mask was fixed to the head tray and cushion support in a prone position as originally scanned. The plan was delivered to the phantom with films and TLDs placed between slices. There were no logistical difficulties encountered with the plan delivery. The bolus was removed from the phantom in a dark room to avoid accidental film exposure. The films were then removed and developed at the same time as calibration films. The TLDs were removed and were read at the same time as calibration TLDs.

The Quick IMRT plan was treated using the 'Obelix' Siemens Oncor linear accelerator without the phantom, in order to establish the treatment time for the faster treatment. The IMRT plan without bolus was not treated as any reproducibility errors would be redundant as they would be highlighted by the Slow IMRT plan.

CHAPTER II: MATERIALS AND METHODS

3. PLAN GENERATION, 3.4 ELECTRON PHOTON PARALLEL OPPOSED

A plan was generated on the XiO planning system for the phantom without bolus, using parallel opposed lateral electron and photon beams. The electron beams were generated using a 20x20 cm applicator to give sufficient PTV coverage. An energy of 5 MeV was found to provide adequate penetration without over-irradiating the brain. The photon beam jaws were adjusted to cover the PTV with a 0.5cm margin. The photon beams had blocks to shield the brain and were used to treat the superior portion of the scalp. The electron beams had shielding over the photon field overlap to treat the lateral portions of the scalp. Each field was setup using an SSD technique so that the block scaling would be identical. The beam weighting was adjusted manually to give the best isodose distribution. This resulted in the plan summary shown in Table 10.

	Right Lateral Electron	Left Lateral Electron	Right Lateral Photon	Left Lateral Photon
Energy	5 MeV	5 MeV	6 MV	6 MV
Open Field Size mm	200 x 200	200 x 200	190 x 150	190 x 150
Gantry	90º	270º	90º	270º
Collimator	0º	0º	0º	0º
Couch	0º	0º	0º	0º
mu	50	52	85	85

Table 10 – Beam configuration for electron and photon parallel opposed plan

An example of the beam blocking for the left lateral beam is shown in Fig 13.

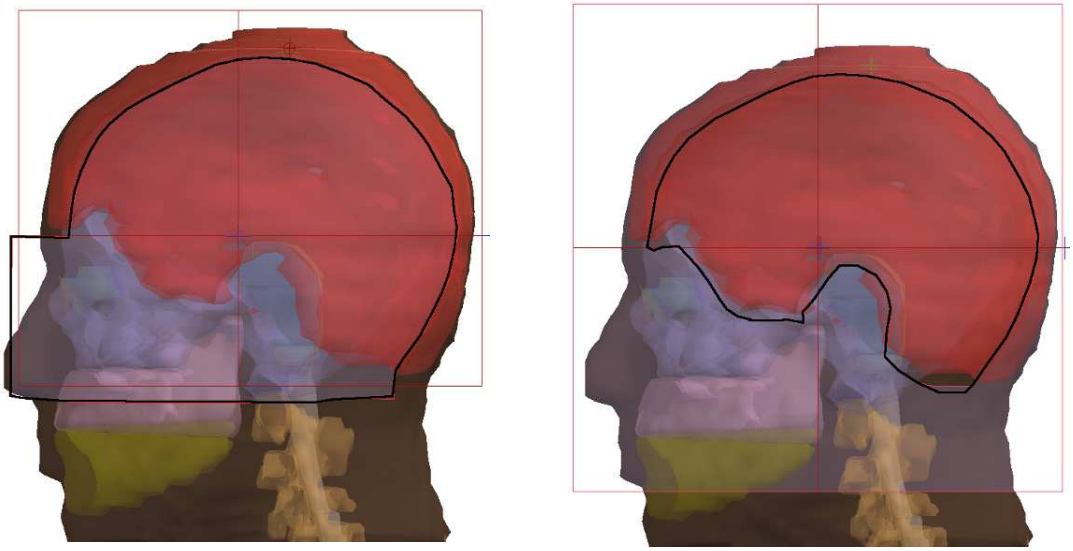

Photon field with brain blocked

Electron Field with Photon Overlap Blocked

Fig 13 – Beam blocking for electron and photon parallel opposed plan

The blocks were drawn manually and copied between beams to ensure an accurate match. Beam's eye views (BEVs) were printed at the distance of the block to verify the block once it was cut. For the electron applicator the BEV was printed at a distance of 951 mm, which corresponded to the bottom of the applicator. For the photons the BEV was printed at a distance of 562 mm, which corresponded to the top of the tray, as the blocks were mounted on top of the trays. The BEVs were also printed at 100 cm for the manufacture of the blocks.

The 100 cm BEV for the electron blocks was marked on to a 1 cm thick polystyrene sheet. The sheet was cut using hot wire in a non-divergent manner. The sheet was then secured to the 20x20 cm applicator mould as shown in Fig 14.

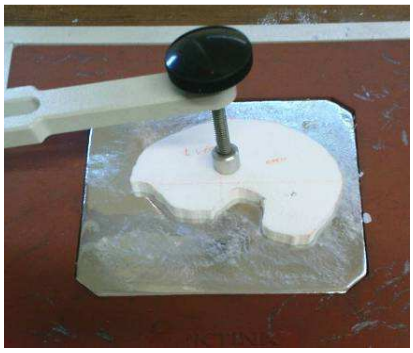

Fig 14 - Cerrobend block mould for electron shielding

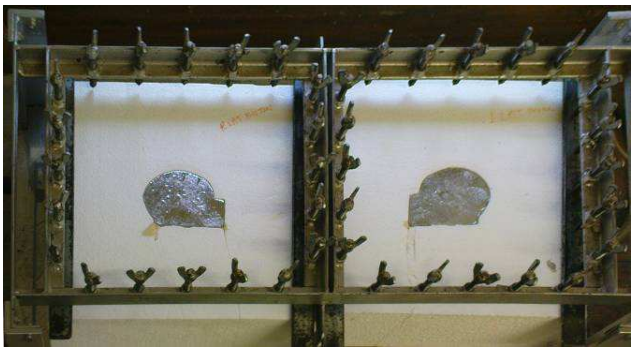

Fig 15 – Cerrobend block moulds for photon shielding

Cerrobend was poured into the mould and left for 2 hours to harden. The polystyrene was then removed and the cerrobend cut-out was removed from the rubber applicator mould. Electron cut-outs used in this manner may have beam edges spoiled with wax to smooth the edges adjacent to other fields. However, the block was cut in a non-divergent manner which will introduce some beam spoiling at the edges.

The photon blocks were cut using a divergent block-cutting apparatus. A polystyrene sheet was mounted at 562 mm from the hot wire attachment, to correspond to the top of the tray. The 100 cm BEV printout was mounted on a light source at 1000 mm from the hot wire attachment. The polystyrene was then cut using the hot wire whilst tracing the BEV printout. The polystyrene mould was then placed into a device shown in Fig 15 to compress it against the base to minimise leakage. Cerrobend was then poured into the mould and left for 6 hours to harden. All of the cerrobend blocks were filed to remove any excess. The final block size and position was checked against the BEV printouts at the height of the mounting.

The plan was treated using the ‘Hobbes’ Siemens Oncor linear accelerator. The mask was placed on to the phantom head to correspond with marks made during the CT scan. The mask was fixed to the head tray and cushion support in a prone position as originally scanned.

The image in Fig 16 shows the light field for the photon field, which was marked on the mask. The electron block was fixed to the applicator with tape. It was found that it caused considerable sag to the end of the applicator. This can be seen in Fig 17.

Fig 16 – Photon field for electron photon parallel opposed plan

Fig 17 – Electron applicator for electron photon parallel opposed plan

The sag was overcome by adjusting the couch height so that the electron field matched the marks made on the mask for the photon field edge. It was not possible to compensate for the change in divergence or the misalignment between the primary jaws and the applicator end. However, it was found that there are additional supports that can be fixed to the applicator to prevent sag from heavy blocks.

The TLDs and film are radiation type and energy sensitive. It was therefore not possible to deliver this dual-modality plan in its entirety and be able to convert the readings to dose directly. Consequently, the plan was delivered to the phantom with films and TLDs placed between slices in three parts: the plan was delivered using the photon fields only to one set of film and TLDs; the plan was then delivered using the electron fields only to another set of film and TLDs; finally, the plan was delivered to another set of film and TLDs using both modalities, to qualitatively assess any hot or cold spots in regions of overlap. After irradiation, the mask was removed from the phantom in a dark room to avoid accidental film exposure. The films were then removed and developed at the same time as calibration films. The TLDs were removed and were read at the same time as calibration TLDs

CHAPTER II: MATERIALS AND METHODS

3. PLAN GENERATION, 3.4 ELECTRON ARCS

Once the applicator had been commissioned, plans were generated using the arc applicator in the XiO planning system. There were considerable difficulties with this planning process. Although an arc applicator could be selected in the Source File Maintenance module, the calculation software has not been written in order to use this applicator in an arc treatment. Another difficulty encountered, was that the electron applicator could not be used in an SAD treatment, despite the fact that there was sufficient distance between the applicator and the patient. To overcome these limitations, plans were generated for multiple single fields with 10^{o} separation and equal monitor units, to simulate the distribution which would be achieved using an arced treatment. It is likely that a planning system which enables arced treatment would consider the dose calculation in a similar manner. A final difficulty was encountered as the XiO electron treatment module uses the beam entry point relative to the surface of the patient as a reference for the beam placement, not the isocentre. Each beam therefore had to be entered in a systematic manner until each beam placement gave the equivalent of an isocentric set-up. The SSD of each field was set as 100 cm minus the depth to isocentre. The field reference point was chosen at the depth to the centre of the scalp volume of interest (VOI) for that beam. This significantly increased the time taken to plan these treatments.

Several treatments were planned using the electron arc applicator as each gave different dose distributions and had additional treatment aids required which could impact the final plan assessment. All of them were planned using 5 MeV as this energy gave the best distribution over the scalp. The arced treatments which were planned are shown in Table 11.

Plan Name	Plan Description
Arc AP	An arc rotating about an axis going between the ears, from the front, at eyebrow level, to the back, at the base of the skull
Block Ears Arc AP	An arc rotating about an axis going between the ears, from the front, at eyebrow level, to the back, at the base of the skull, with the ears blocked
Bolus Ears Arc AP	An arc rotating about an axis going between the ears, from the front, at eyebrow level, to the back, at the base of the skull, with the ears bloused
ArcLR	An arc rotating about an axis going down spine.
ArcLR InfSup	An arc rotating about an axis going down spine, split into two fields. Superior portion rotation around entire skull. Inferior portion rotated around hairline only, excluding face and eyes

Table 11 – Arced electron plans

The anterior to posterior arced field employed 22 beams at 10º degree gantry angle increments between 30º and 180º. The applicator was used in an open configuration without any block. Fig 18 shows the positioning of the beams. A couch angle of 90º was used to enable this gantry rotation. No change in couch or collimator angle was required during this planned treatment.

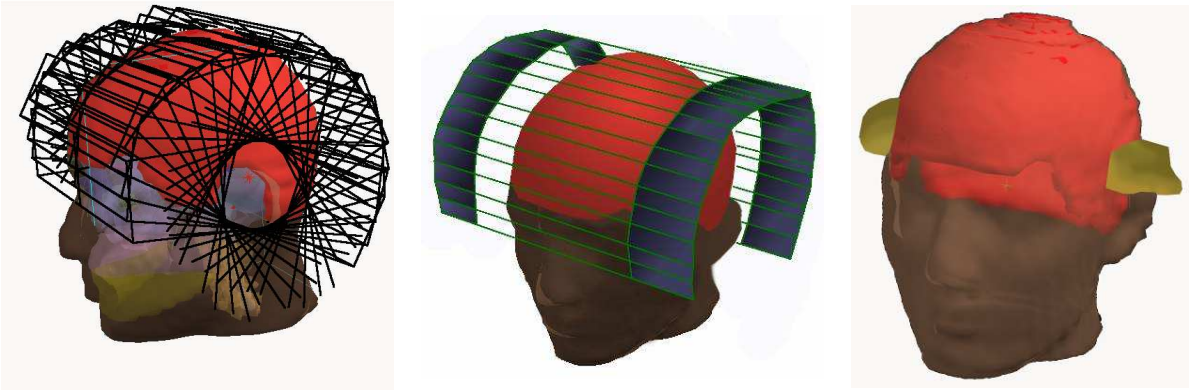

Beam Configuration Blocked Field Edges Bolused Ears

Fig 18 – Beam configuration and treatment aids used in electron arc plans

It was found that this plan gave a very high dose to the ears. A block was therefore used on all fields to reduce the dose to the ears. The block prevented transmission through the lateral edges of the applicator as seen in Fig 18.

The same aim was achieved using bolus over the ears as seen in Fig 18 to help reduce the ear dose whilst eliminating block manufacture time. The shape of the head is more spherical than conical. This makes it difficult to get a uniform dose distribution. These three plans were all generated using the same 22 beam configuration to simulate the arced treatment.

A plan was then generated using 36 beams rotating about a central axis approximately parallel to the spine with 10º gantry angle increments. This plan required a couch angle of 0º. The beam configuration is shown in Fig 19. However, in order to deliver dose to the region above the eyebrows, dose was also delivered to the eyes and face. The plan was then split into two sets of beams. The superior set employed 36 beams covering a full 360º rotation around the skull, with the inferior portion of the beam blocked as shown in the figure 19. The inferior set of beams was blocked in the superior direction to avoid overlap with the superior beam set. It was also blocked inferiorly to avoid unnecessary irradiation to the spine below the scalp. These blocks are shown in Fig 19. It was only used over an arc of 270º at 10º gantry angle increments from 220º, through 0º, to 130 º.

This limited rotation treated the posterior section of the inferior scalp without delivering dose to the lower jaw. Although this appeared to be an unnecessarily complex plan, it did produce a superior distribution and would be fairly simple to treat on the linear accelerator.

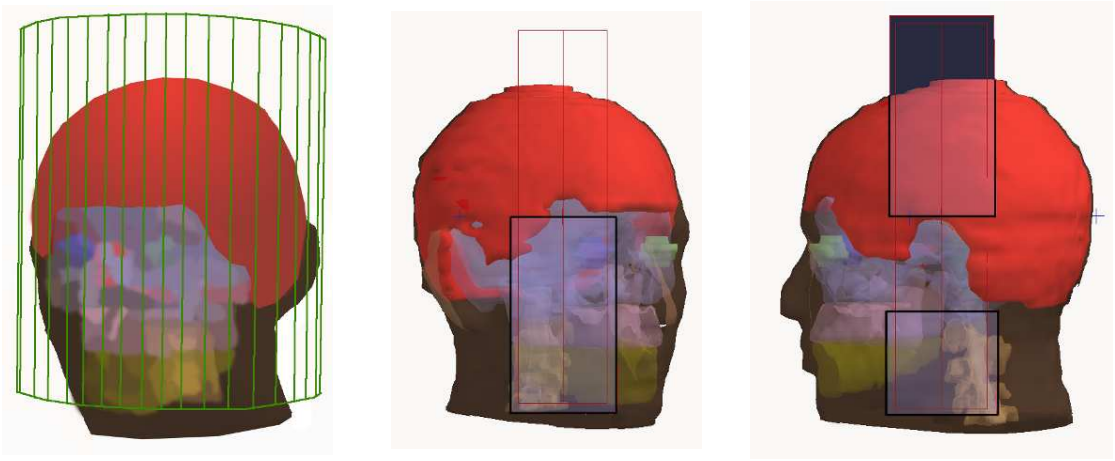

Left-Right Beam Placement Superior Beam's Eye View Inferior Beam's Eye View

Fig 19 – Beam configuration for left to right arced electron plans

In order to treat using an arc applicator on the linear accelerators, it was necessary to override the accessory fault as the applicator license was not activated on the linac used. The ArcAP treatment was evaluated on the linac using TLDs and film dosimetry. The other arced AP treatments would take a similar time to treat as the total monitor units were comparable. The arced treatment from left to right, split into two parts inferiorly and superiorly, would take approximately twice the time to deliver.

Fig 20 shows that posterior fields would have gone through the Perspex head tray. Therefore, fields between 180º and 260º were treated using the mesh carbon fibre headboard, with the perspex head tray removed. The position without the head tray was verified using the treatment marks on the phantom and the mask. This could be circumvented by scanning the patient for this setup with the mask attached to the mesh headboard initially. As can be seen in the Fig 21, the gantry angle of 230º went directly through the end of the headboard.

Whilst insignificant at 6 MV, at 5 MeV this may have produced a significant loss of dose from this field. The gantry angles between 180º and 260º also went through the sponge head support. This will be discussed in the results.

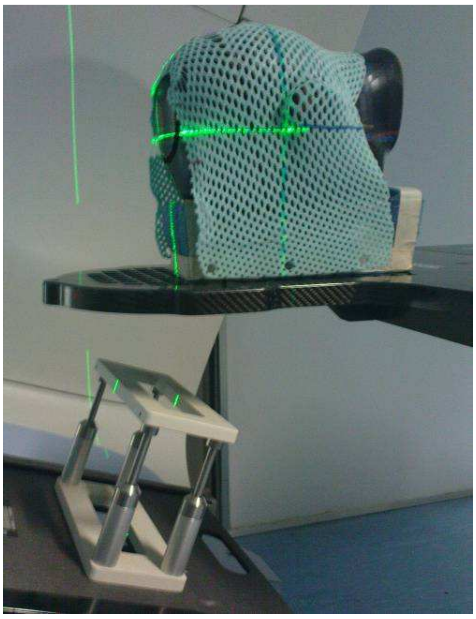

Fig 20 – Electron arc anterior angles treated without head tray

Fig 21 – Electron arc field 230º gantry goes through carbon fibre end

CHAPTER II: MATERIALS AND METHODS

4. FILM DOSIMETRY

All plans were compared for the accuracy of delivery using film dosimetry. Firstly calibration films were irradiated at multiple known doses then an optical density to dose conversion was effected. Calibration films were used from the same pack and were irradiated and developed at the same time as the plan films. This enabled processor and film variables to be eliminated.

For the HDR calibration film, plans were generated for single fraction doses of 20, 40, 60, 80, 100 and 130 cGy. The applicator "Sorbot 30V" was used to get a long straight rod. A reference line was generated parallel to the rod at a distance of 2 cm. The plan was optimized deliver the fraction dose required to the 2 cm reference line. This resulted in a distribution which was uniform at 2 cm with non-parallel isodose lines at other distances, as shown in Fig 22.

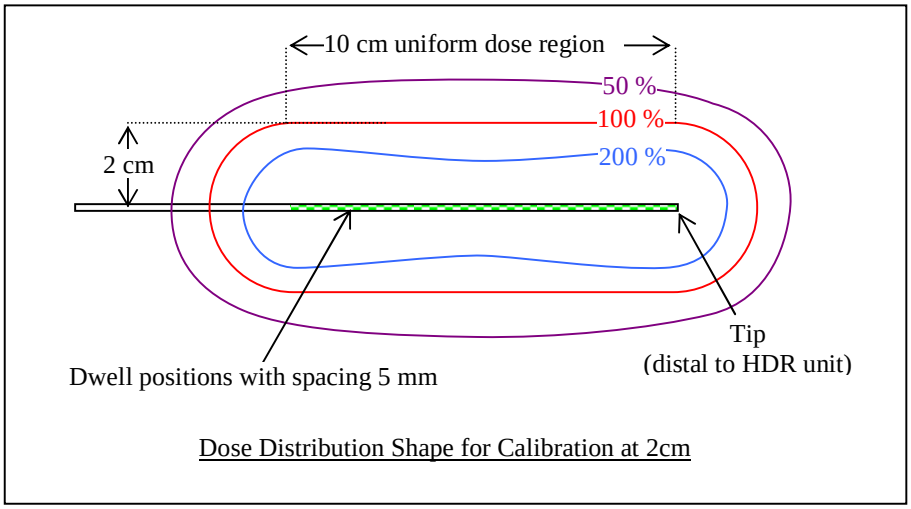

Fig 22 – Dose shape for HDR film calibration

This distribution was achieved using non-equal dwell times. An example of these source times is shown in Table 12 for a 10 Ci source strength to give a dose of 40 cGy

Position cm	Time s	Position cm	Time s	Position cm	Time s
0.0	3.6	5.0	1.3	10.0	1.2
0.5	2.7	5.5	1.2	10.5	1.1
1.0	1.7	6.0	1.2	11.0	1.1
1.5	1.2	6.5	1.1	11.5	1.2
2.0	1.0	7.0	1.1	12.0	1.3
2.5	1.0	7.5	1.1	12.5	1.6
3.0	1.1	8.0	1.2	13.0	2.4
3.5	1.1	8.5	1.2	13.5	3.5
4.0	1.2	9.0	1.2		
4.5	1.3	9.5	1.2		

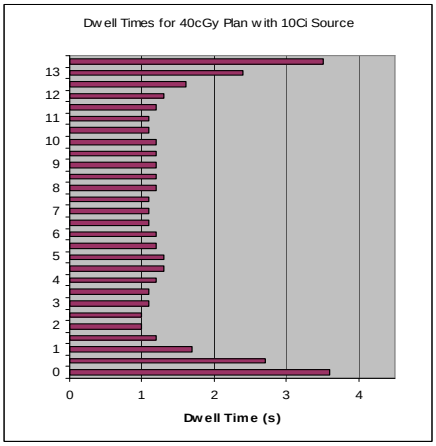

Table 12 – Dwell times for HDR calibration film

The doses received by points in the reference line at distances 3-10.5 cm from the tip were noted for the calibration films. These values were not exactly equal to the fraction doses prescribed. An example of the dose to the reference line is shown in Table 13 at 1 cm intervals for a prescription of 40 cGy. This discrepancy is due to the optimization algorithm used by the planning system and, to a lesser extent, the resolution of the treatment times. The mean of the actual dose calculated to the reference line was used for the optical density to dose conversion.

Distance from tip (cm)	3	4	5	6	7	8	9	10
Dose (cGy)	39.1	39.2	39.4	39.2	39.0	39.0	39.1	39.2

Table 13 – Doses to dose points for HDR calibration film

The applicator was used without the spacers or plastic tubing. Kodak extended dose range (EDR) pre-packaged film was placed on top of 4 cm sheets of tissue equivalent plastic (TEP) material. A 2 cm sheet of bolus material was placed on top of the film. An incision

was made on the top of this bolus and the applicator was placed in the incision so that the centre of the rod was on the surface of the bolus material. A 2 cm sheet of bolus was placed on top of the rod to provide backscatter and secure the rod in position.

The setup is shown in Fig 23. The film was irradiated with the first planned dose of ~20 cGy. This film was then removed and a new film was irradiated. In this manner, films were irradiated with doses from ~20 cGy to ~130 cGy.

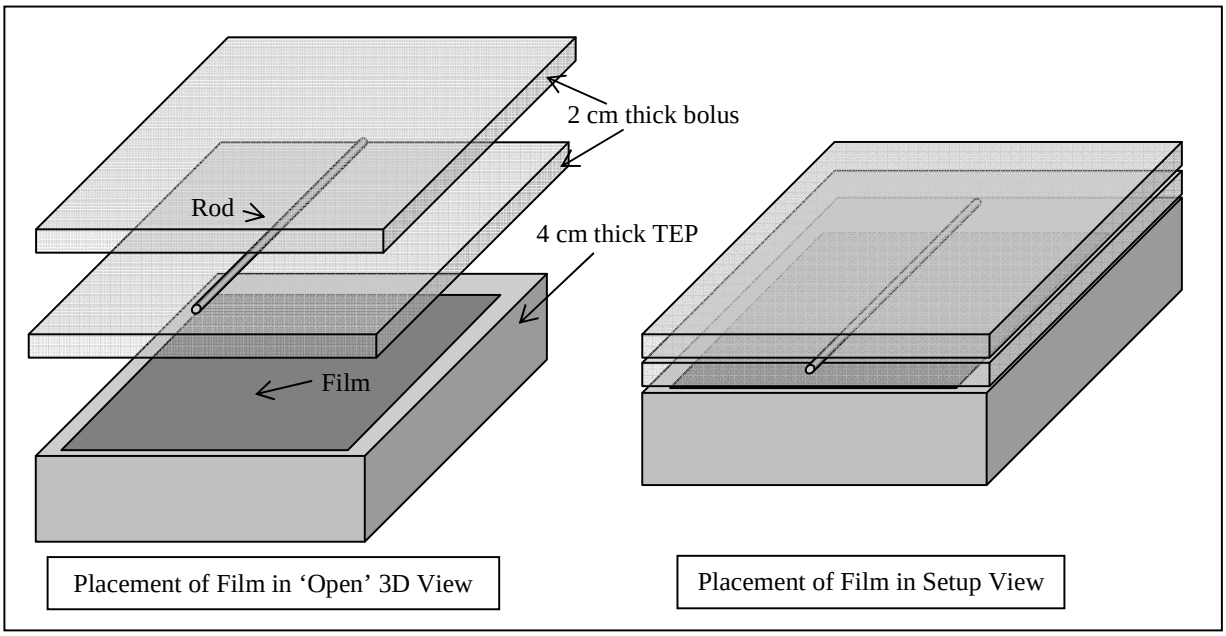

Fig 23 – Placement of film for calibration with HDR brachytherapy

For the external beam calibration films, films were placed in TEP at a depth of d_{MAX} for the energy employed, with an SSD setup and a 10x10 cm field. For the linacs used this corresponds to an output of 1 cGy per monitor unit (mu). Approximately 10 cm of TEP was used to provide backscatter. Doses of 20, 40, 60, 80 and 100 cGy were delivered to separate films. The same energy and radiation type was used to irradiate the calibration films and the phantom plans. For the electron and parallel opposed photon plans, calibration films were irradiated for both electrons and photons.

The optical density of the film was measured using a Wellhöfer Dosimetrie WP102 densitometer. The background adjustment was adjusted to give an optical density reading of zero when no film was present. The reading rate was set to ‘fast’ and the output level of the densitometer was set to ‘density’. This output level does not amplify the reading, allowing a higher optical density to be measured. The optical density of each film was measured at six different points within the region of maximum density.

Additionally, a background reading (of film and fog density) was made at six points on a non-irradiated film. All of these readings were used to generate optical density to dose conversions for each energy and radiation type employed.

The reproducibility of the dose distributions calculated by the planning systems was tested using an anthropomorphic head. Kodak EDR pre-packaged film was used to measure the isodose distribution. The film and envelope was cut to the exact size of the head slice of interest, in a dark room. Three marks were cut into the film edge to coincide with marking on the phantom. These marks were later used to localize and orientate the film. The edge of the envelope was then light sealed using black insulating tape. The film was then placed in the phantom and the edge of the slice was light sealed using black insulating tape. This film was placed in the first three, most superior, head slices and denoted as films 1,2 and 3 as shown in Fig 24.

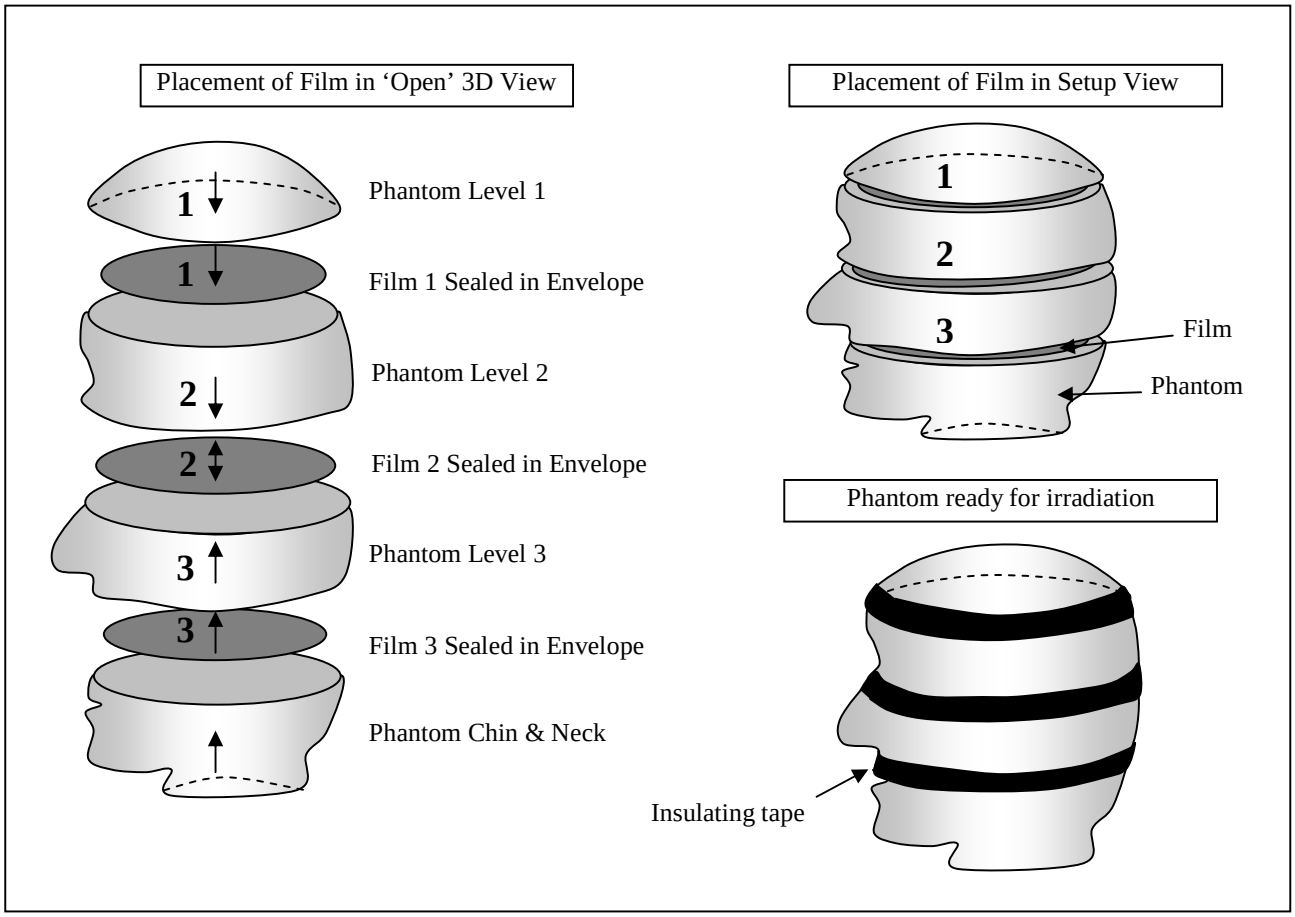

Fig 24 – Placement of film in 'Rando' phantom

Fig 25 shows the position of the three films, relative to coronal and sagittal CT images.

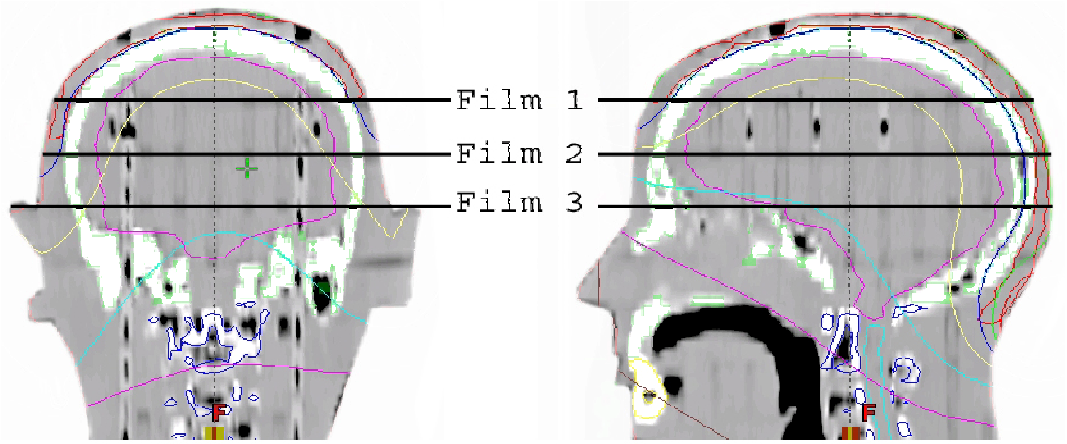

Fig 25 – Film position on CT orthogonal views

The plans generated for the treatment of the scalp were then delivered to test their reproducibility. Only one of each plan type was analysed for reproducibility. The plans which were analysed are shown in Table 14.

Plan	Description
IMRT	A 6MV photon IMRT plan with 247 segments and bolus
HDR	The catheter HDR plan
X Ray & e	X Ray and electron blocked parallel opposed
Electron Arc	An electron arc which arced from anterior to posterior

Table 14 – Plans assessed with film and TLD dosimetry

The ‘treated’ films were removed from the phantom head and the film envelopes in a dark room. They were then processed at the same time as the calibration films described earlier. Not all dose distributions could be exported from the planning systems due to licensing restrictions. The film dosimetry was therefore performed by superimposing a 1.5 cm grid on to the plan and the phantom films using the plastic markers embedded in the phantom as the centre of each grid point. The grids used for the three films are shown in Fig 26. These 250 grid points were used as the measurement points for the film dosimetry and the dose calculation points for the plan.

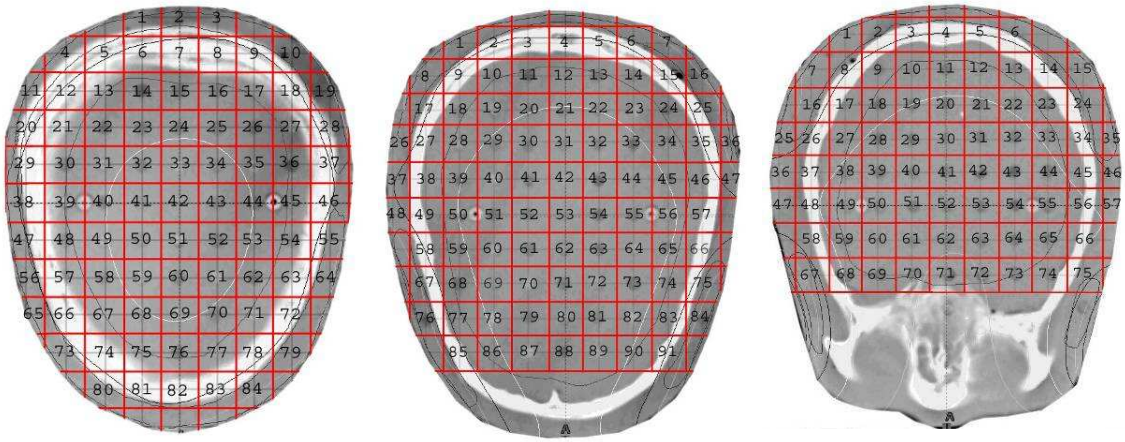

Slice 1 Slice 2 Slice 3

Fig 26 – Grids used for film dosimetry

The optical density of the phantom films was measured using the Wellhöfer Dosimetrie densitometer as previously described. The optical density readings were converted to dose values using the calibration films. The measured dose values were then compared with the doses calculated by the planning system.

CHAPTER II: MATERIALS AND METHODS

5. TLD DOSIMETRY

The TLDs were irradiated using the HDR source and the external beam sources in order to generate calibration files for comparison with the TLDs irradiated in the phantom. Prior to the irradiation of the TLDs they were annealed in an oven for one hour at 400º C and 24 hours at 80º C.

To irradiate the calibration TLDs for comparison with the HDR phantom plan, the following protocol was used. The plans used to deliver a uniform dose at 2 cm, for the film dosimetry, were used to deliver calibration doses for the TLDs. The applicator rod was placed in an incision in 2 cm of bolus so that the centre of the rod was at the bolus surface. Four TLDs were placed underneath on a 2 cm sheet of bolus. Several centimetres of TEP were placed on either side to provide scatter. The use of bolus instead of TEP adjacent to the TLDs was to minimize the air gap surrounding them. The TLDs were placed at 1.5 cm intervals parallel to the rod, at distances 3.0, 4.5, 6.0, and 7.5 cm from the tip. The uniform dose region occurred from 2-12 cm from the tip so all TLDs were well within this region. The experimental setup is shown in Fig 27.

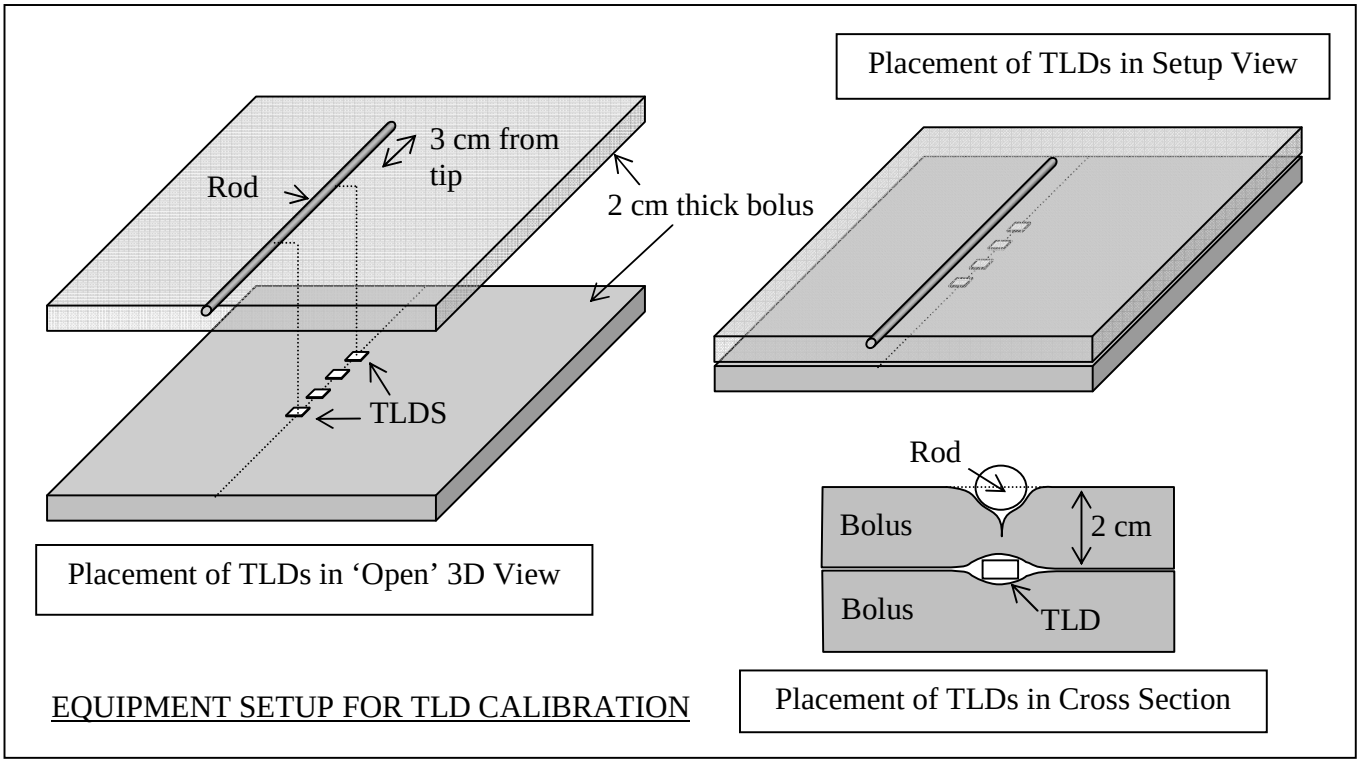

Fig 27 – Equipment setup for TLD calibration

Initially five TLDs were irradiated with a dose of 60 cGy and were used to generate the calibration file. Then four TLDs were irradiated with the first planned dose of ~40 cGy. These TLDs were then removed and four new TLDS were irradiated with the next plan. In this manner, four TLDs were irradiated with each dose ~40, 60, 80 cGy. These TLDs were used to check the calibration file and to find the system variability. Four TLDs were also left un-irradiated to provide a background 'annealed' reading.

The TLDs were read using Rexon UL 320 software, without nitrogen for all readings. A calibration file was generated with an exposure of 60 cGy, a coefficient of variance for exposed TLDs less than nine and annealed TLDs less than 30. The five 60 cGy calibration TLDs were used to generate the exposed readings and the four unexposed TLDs were used to generate the annealed readings. The glow curve employed is shown in Fig 28. The calibration file created in this manner was used to convert all subsequent TLD readings to dose for the phantom readings.

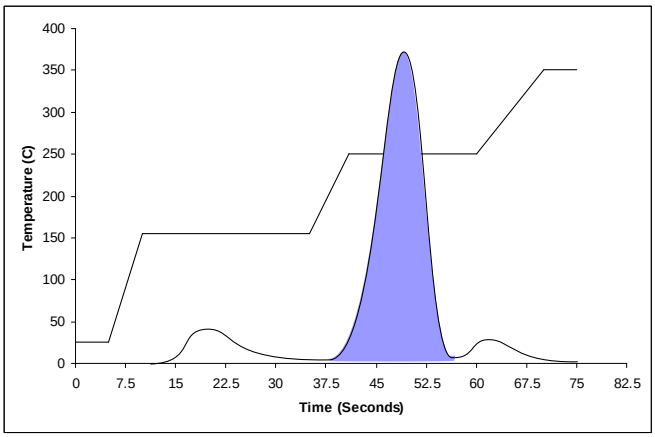

Fig 28 - Glow Curve used for TLD Readings

For the external beam TLD calibrations, TLDs were placed in TEP at a depth of d_{MAX} with an SSD setup. 1 cm of bolus was used behind the TLDs to minimise air gaps. Approximately 10 cm of TEP was used to provide backscatter. 50 cGy was delivered to eight TLDs using a 10x10 cm field. The same energy and radiation type was used to irradiate the TLDs as was required by the phantom plans.

For the electron and parallel opposed photon plans, TLDs were irradiated for both electrons and photons. Eight TLDs were left un-irradiated for the background annealed calibration reading.

For each treatment plan delivered to the phantom, 12 TLDs were placed inside the phantom head. Four TLDs were placed on each slice in a small gap machined to minimize air gaps. The exact positions are shown in Fig 29.

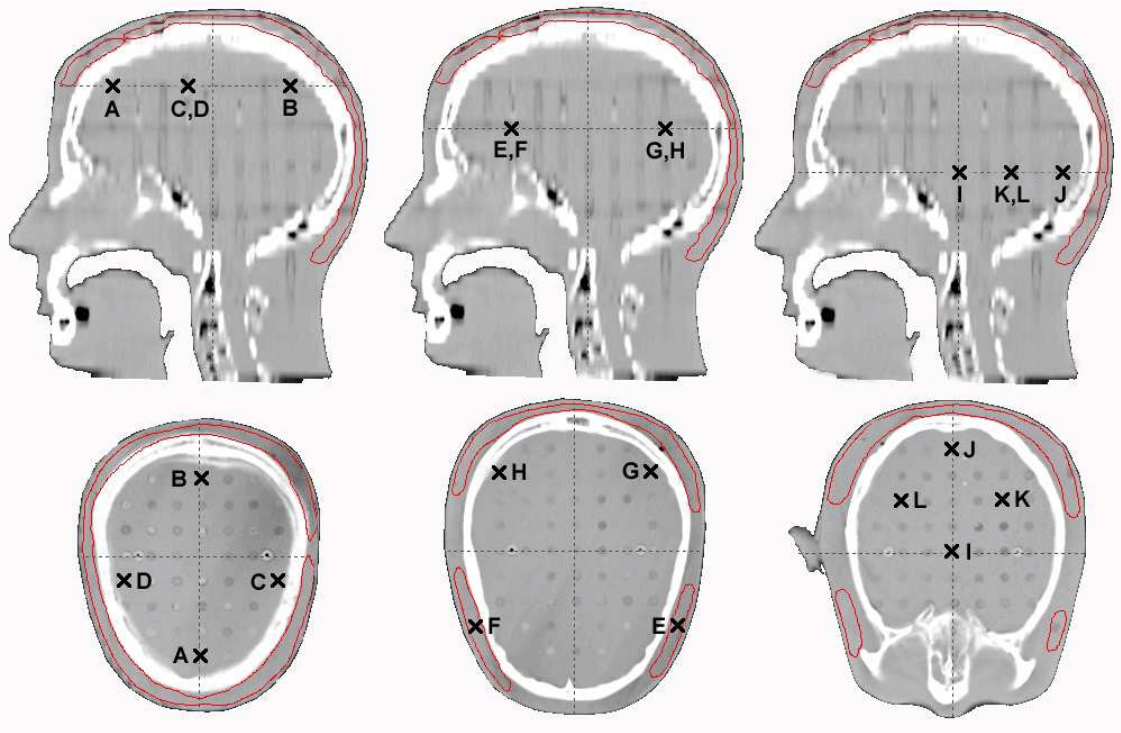

Fig 29 - TLD Positions in the Phantom

The points were chosen to measure over most of the treatment volume including measurements of both the target and the brain doses. The same points were used for all phantom plans. The TLDs were read using the same procedure described previously. The dose to each of these points was calculated on the planning system. A comparison was then made between the calculated dose and the dose measured using the calibration file for that particular energy and radiation type.

CHAPTER II: MATERIALS AND METHODS

6. PLAN EVALUATION

The plans were evaluated by timing each part of the treatment process including planning, delivery and treatment aid manufacture. They were also assessed in terms of specialist equipment or personnel skills required and difficulties unique to each treatment type. The reproducibility of the treatment delivery was measured using the film dosimetry and the TLD dosimetry.

Finally, the resultant dose distributions were assessed to determine the plans which provided the best target coverage whilst avoiding the organs at risk. This plan evaluation was performed by generating transverse dose distribution images which were identical in format regardless of the planning system employed. Bolus and catheters visible on the transverse slices were deleted from the image. This ensured that an assessment could be made without any bias towards any particular technique. In order to be able to rank the plans in order of preference, only five plans were considered. The plan of each type which produced the best distribution was chosen for the evaluation. The plans considered for evaluation are shown in Table 15.

Type	TPS	Plan Name	Bolus	Block
HDR	BrachyVision	HDR	N	N
IMRT	XiO	Slow IMRT	Y	N
		No Bolus IMRT	N	N
X & e- Parallel Opposed	XiO	eXOpp	N	Y
Electron Arc	XiO	Arc LR Inf Sup	N	Y

Table 15 – Plans used for dose distribution evaluation

Two IMRT plans were evaluated as the use of bolus had a significant impact on the timing, practical preparation and dose distributions for the two treatments. For each plan, two colour sheets were printed. Examples of these sheets are shown in Fig 30. These sheets were given to the personnel chosen to evaluate the plans.

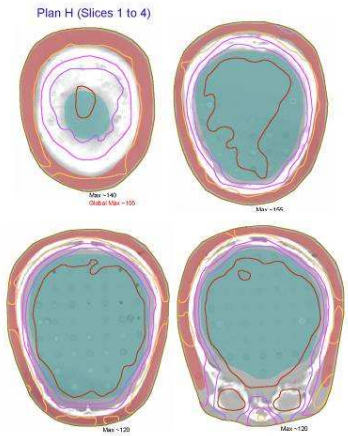

Transverse Slices 1-4

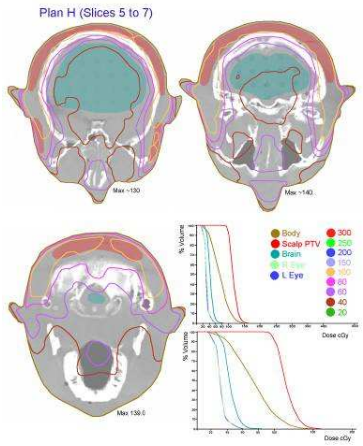

Transverse Slices 5-7 & DVH

Fig 30 – Examples of dose distribution sheets used for plan evaluation

Each printout showed the following information:

- Seven 2 cm transverse slices over the treatment volume
- Dose distributions normalized to give reasonable coverage with the 100 cGy isodose line
- Isodose lines 20, 40, 60, 80, 100, 150, 200, 250, 300 cGy where relevant
- Shaded Brain and Scalp PTV regions
- Maximum dose per slice and global maximum within the patient (not the bolus)
- DVHs showing PTV, brain, body and eye doses, scaled to 200 and 500cGy

The plans were given to the following 19 personnel:

- 11 Radiation Oncologists (8 Private Practice, 3 Government Department)
- 6 Planning Radiographers (2 Private Practice, 4 Government Department)
- 2 Physicists (2 Government Department)

They were asked to rank the plans in order of preference from one to five. The plan ranking was used to assess the popularity of each plan relative to the others. They were also given the handout shown in Fig 31 to aid in the evaluation.

These plans have been generated to simulate the treatment of the whole scalp. They are from different planning systems using varying treatment modalities and energies. The slice separation is 2 cm. The DVHs have been renormalized to give 100% dose to 90% of the PTV volume. Some plans have wax build up or bolus which is not shown here. Where the maximum dose is in the bolus, the maximum dose to the body is estimated. Two identical DVHs are shown, for each plan, scaled to 200 & 500cGy.

The scalp target volume is shown as solid shading in red

The brain OAR is shown as solid shading in light blue

.

ASSUME AN ARBITRARY DOSE OF

100cGy for the PTV

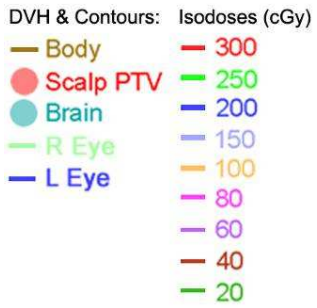

PLEASE RANK PLANS 1-5 WHERE 1 IS BEST PLAN, 5 IS WORST

ALL PLANS CAN BE RENORMALISED, SO BASE RANKING ON RELATIVE DISTRIBUTION ONLY

Plan Letter	Plan Ranking (1-5) 1 Best
D	
F	
G	
H	
I	

Fig 31 – Plan evaluation instruction sheet

CHAPTER III: RESULTS

1. PLANNED ISODOSE DISTRIBUTIONS 1.1 HDR

The plans were optimised as far as possible for the modalities employed. The dose distributions show 2 cm slices through the phantom head for a nominal prescribed dose of 100 cGy. The scalp is shown as a dark pink shaded region and the brain is shaded blue.

Fig 32 shows the dose distribution on the first four slices of the HDR plan

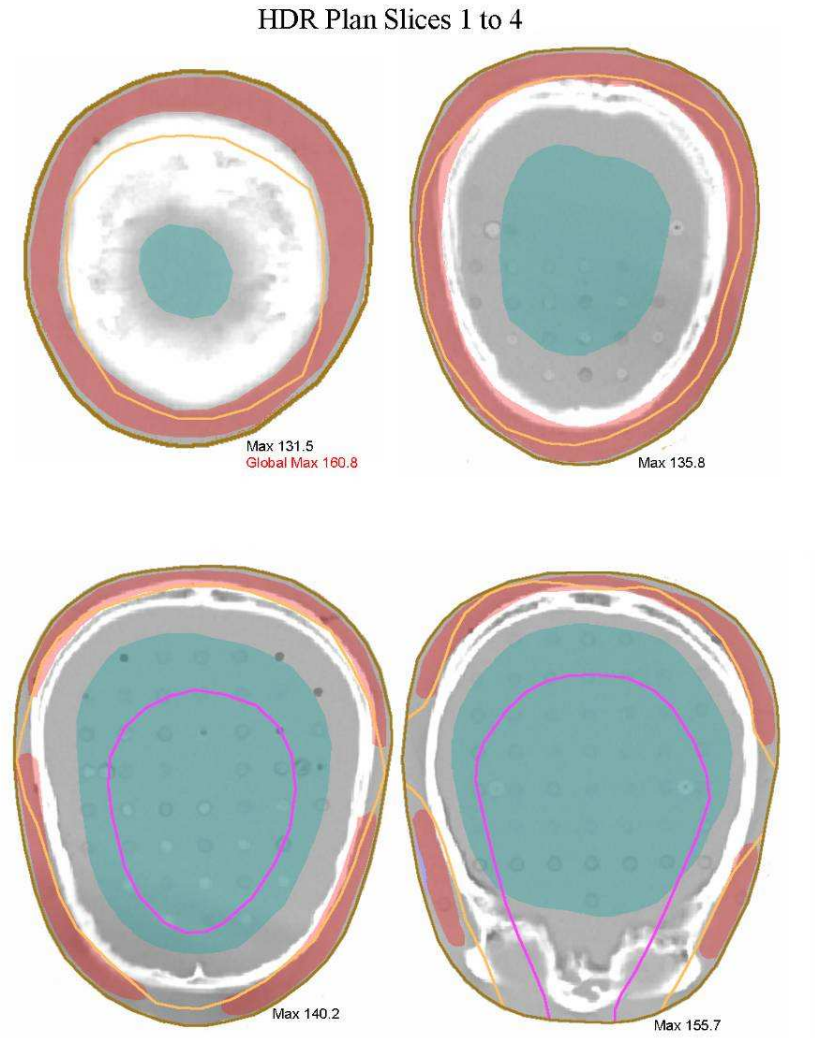

Fig 32 – HDR Plan Slices 1 to 4

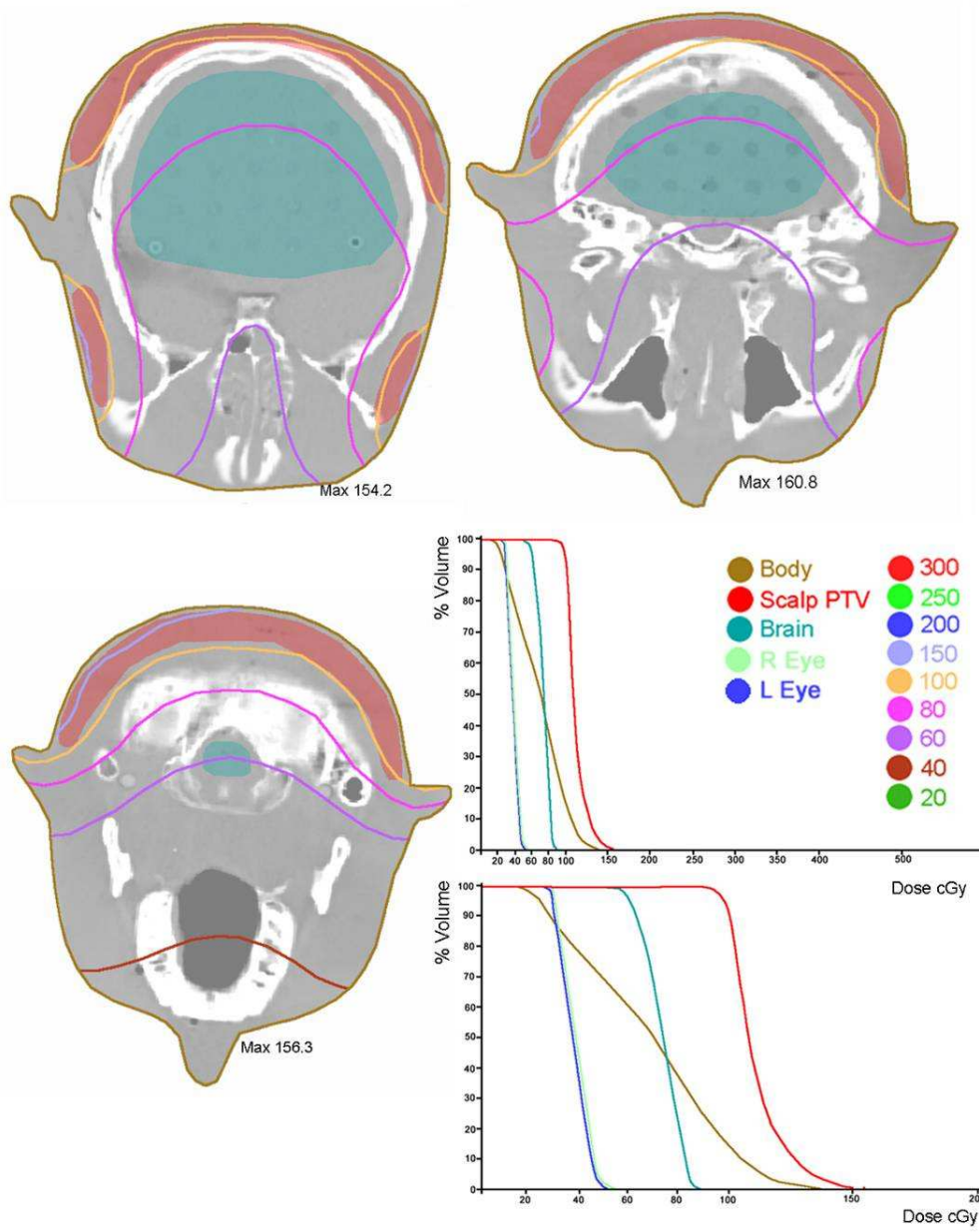

Fig 33 – HDR Plan Slices 5 to 7 and DVH

Figs 32-33 show that the HDR plan gave a very high dose to the organs at risk despite optimising the catheter distance from the skull. The dose to the scalp is fairly uniform but any further improvement would result in an increased brain dose.

CHAPTER III: RESULTS

1. PLANNED ISODOSE DISTRIBUTIONS 1.2 IMRT

Three IMRT plans were generated to compare the improvement obtained by adding bolus or increasing the number of segments and the treatment time. Fig 34 shows the dose distribution on the first four slices of the slow IMRT plan with bolus

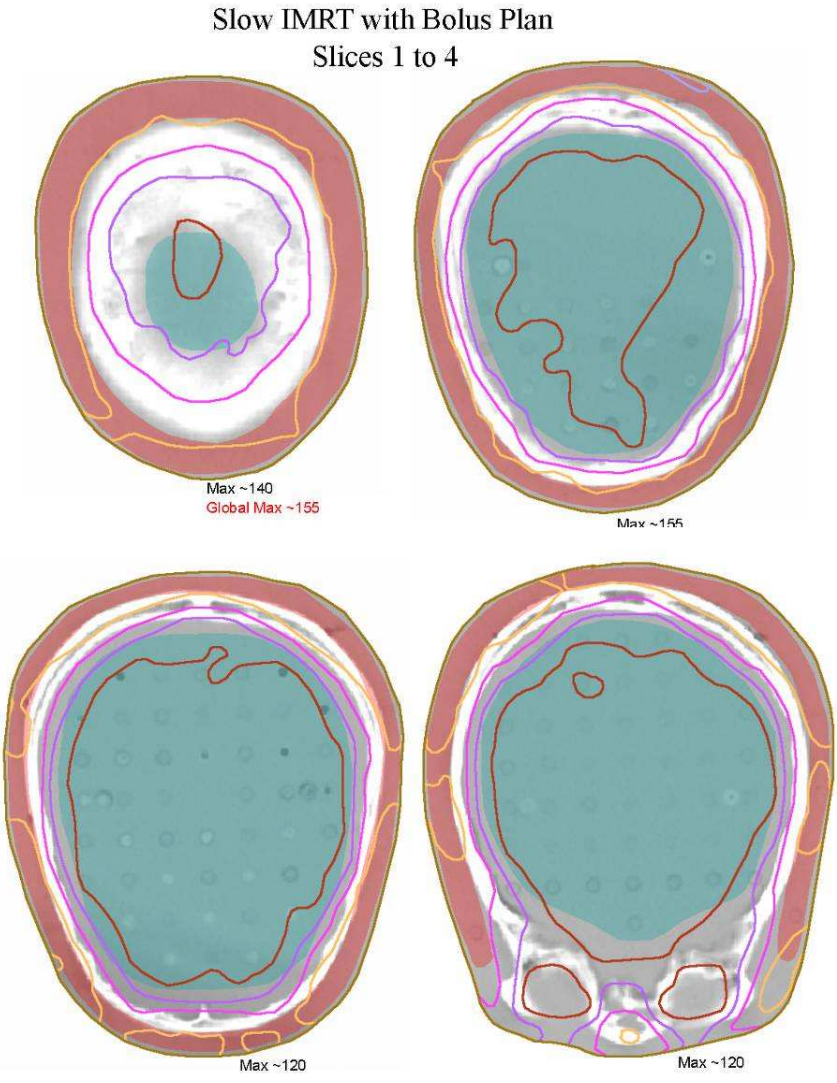

Fig 34 - Slow IMRT Plan with Bolus, Slices 1 to 4

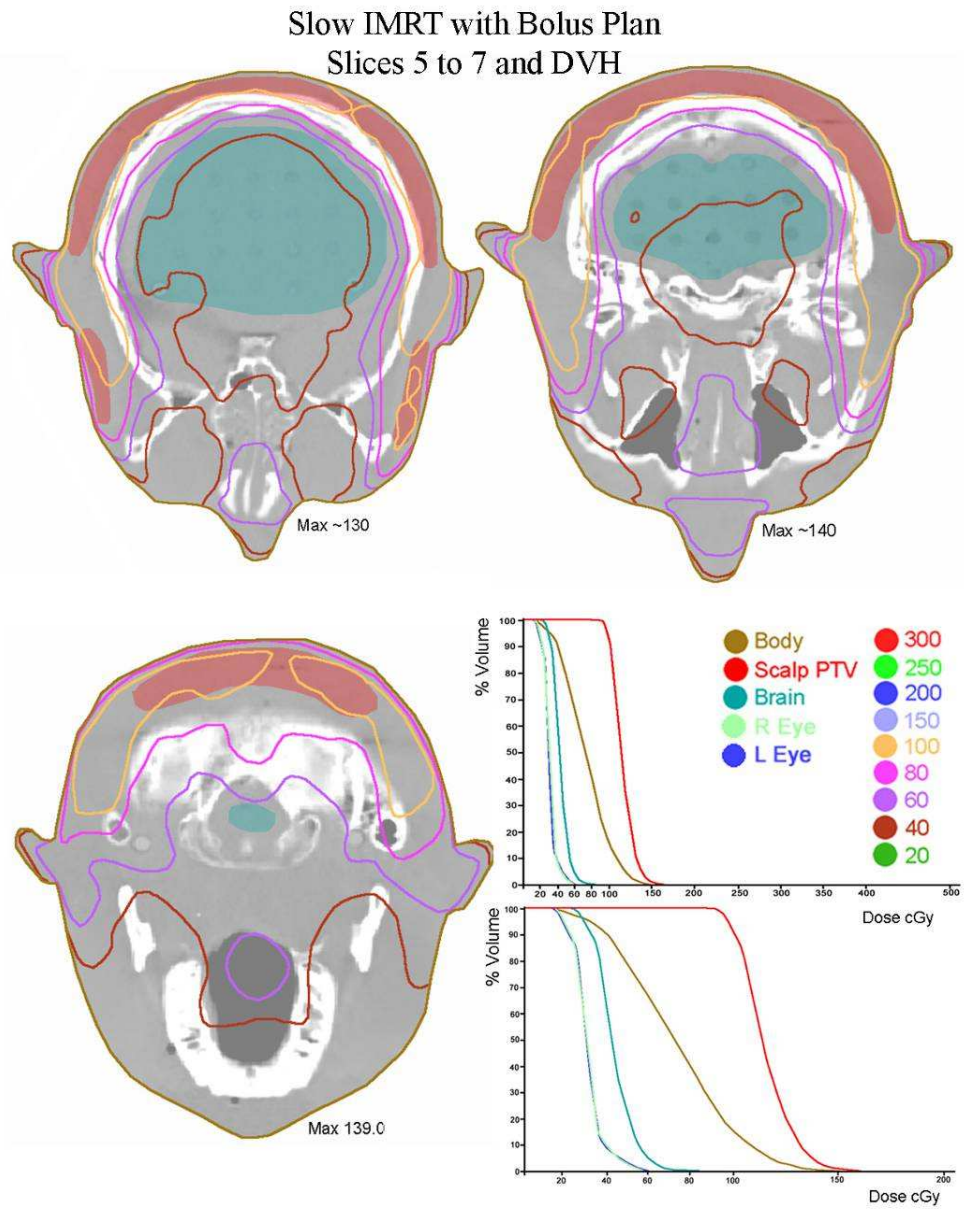

Fig 35 - Slow IMRT Plan with Bolus, Slices 5 to 7 and DVH

Figs 34-35 show that the IMRT plan gave much lower dose to the organs at risk. The use of bolus enabled the dose to be pulled closer to the skin by having the electron build up region inside the wax. The dose to the scalp is quite inhomogeneous as anticipated with IMRT, but good coverage is obtained.

Fig 36 shows the dose distribution on the first four slices of the slow IMRT plan without bolus

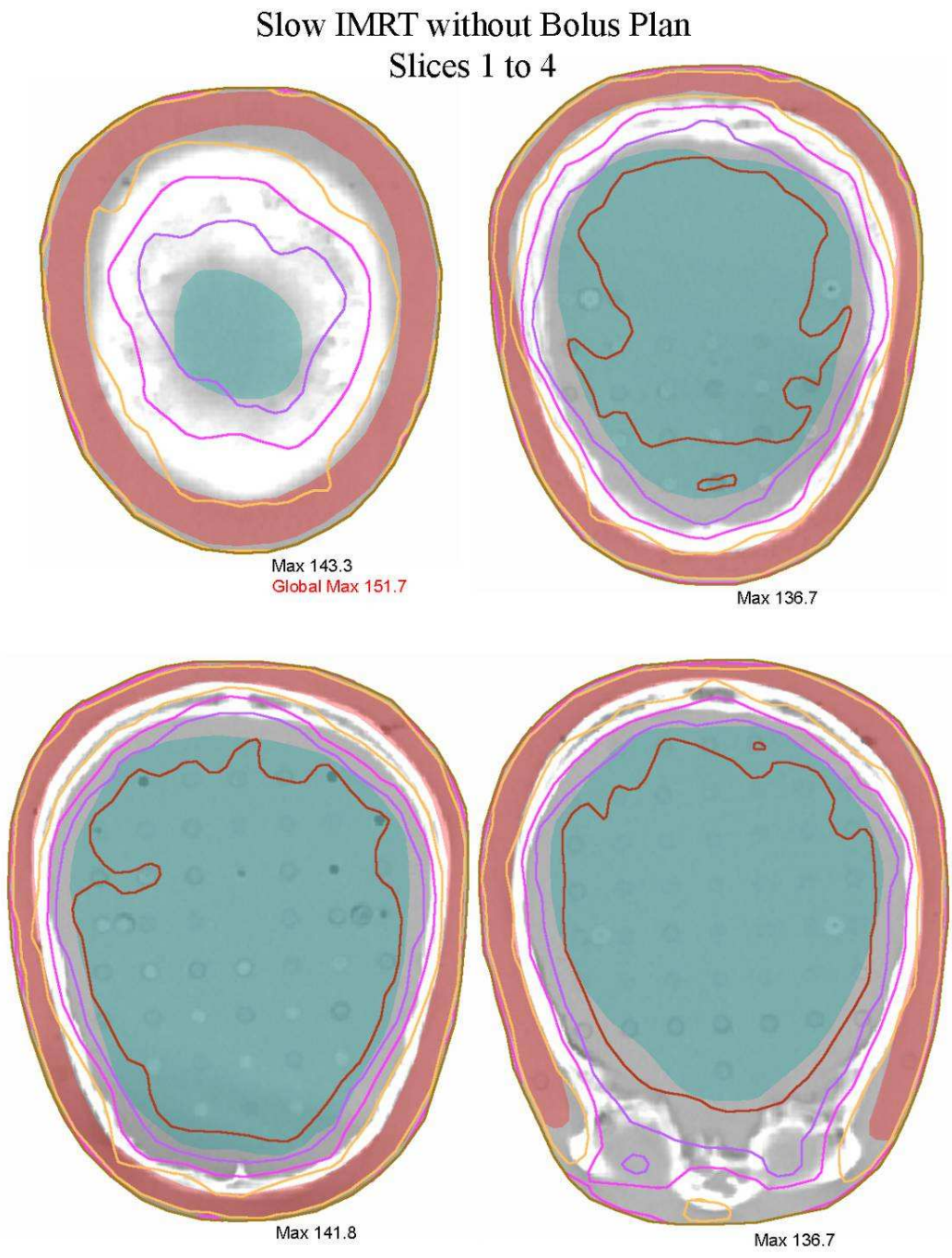

Fig 36 - Slow IMRT Plan without Bolus, Slices 1 to 4

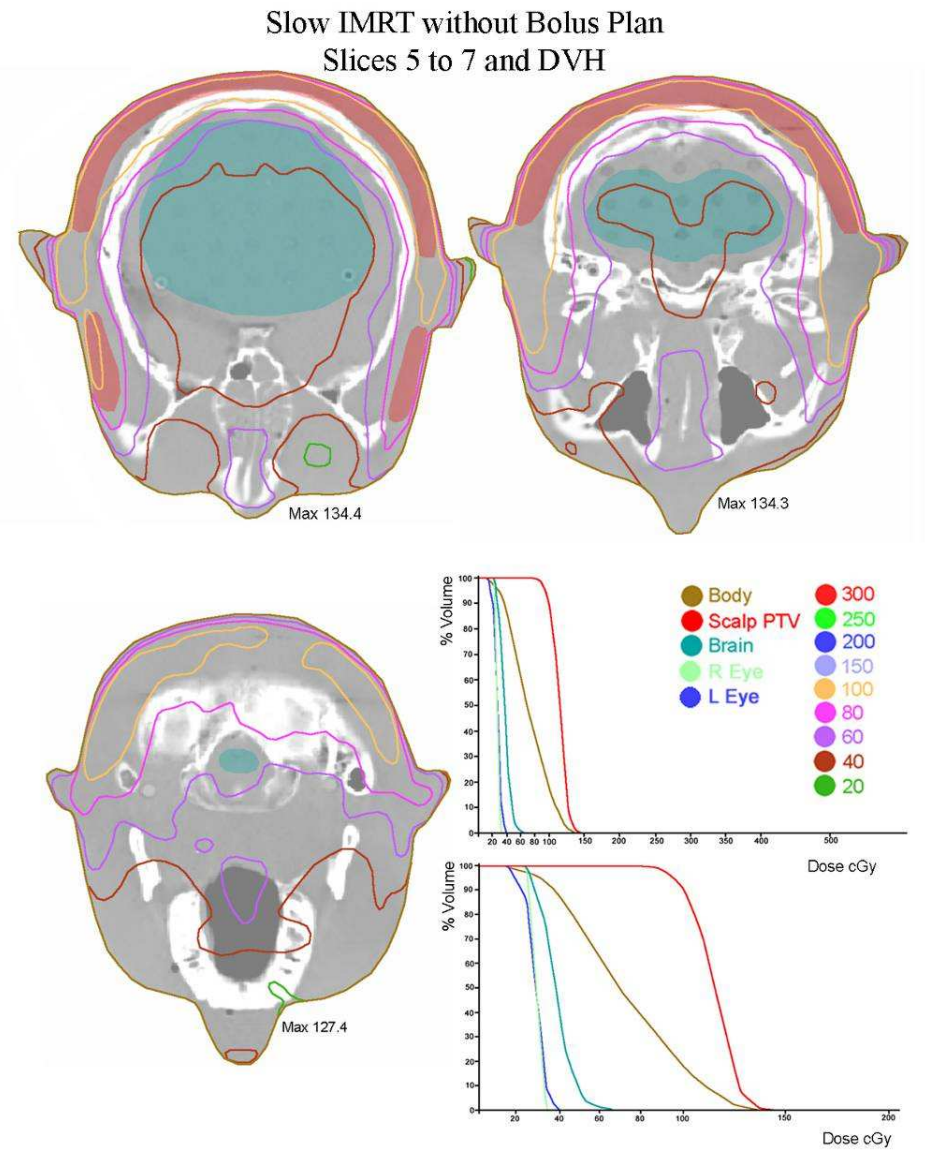

Fig 37 - Slow IMRT Plan without Bolus, Slices 5 to 7 and DVH

Figs 36-37 show that the use of bolus creates little difference to the plan. Although the skin sparing is more significant in this plan, the use of dose from a depth of zero increases the dose drop off due to the inverse square law and enables a much lower dose to be delivered to the brain. The benefit of the use of bolus appears to be negated by the increased organ at risk doses.

Fig 38 shows the dose distribution on the first four slices of the fast IMRT plan with bolus

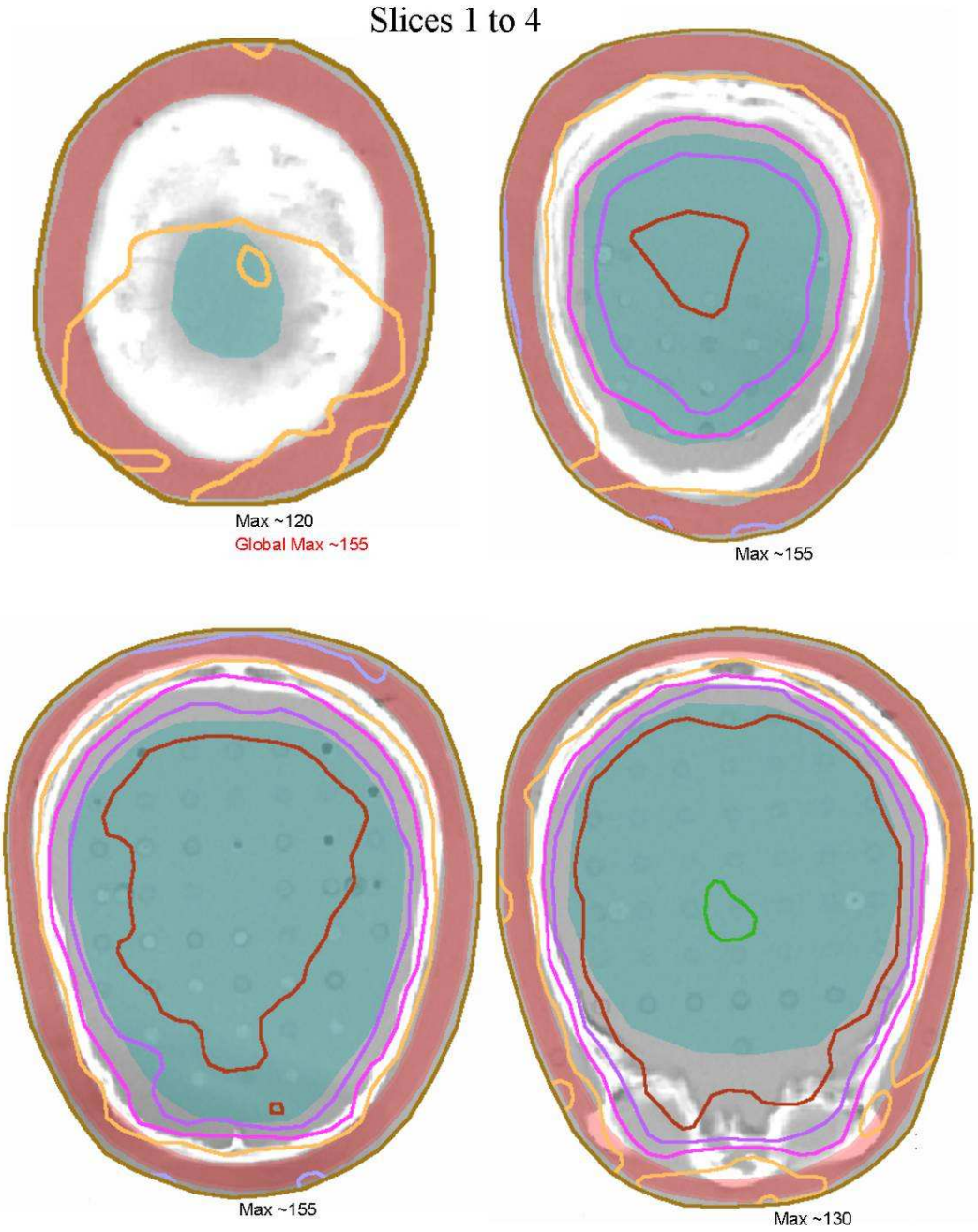

Fig 38 - Fast IMRT Plan with Bolus, Slices 1 to 4

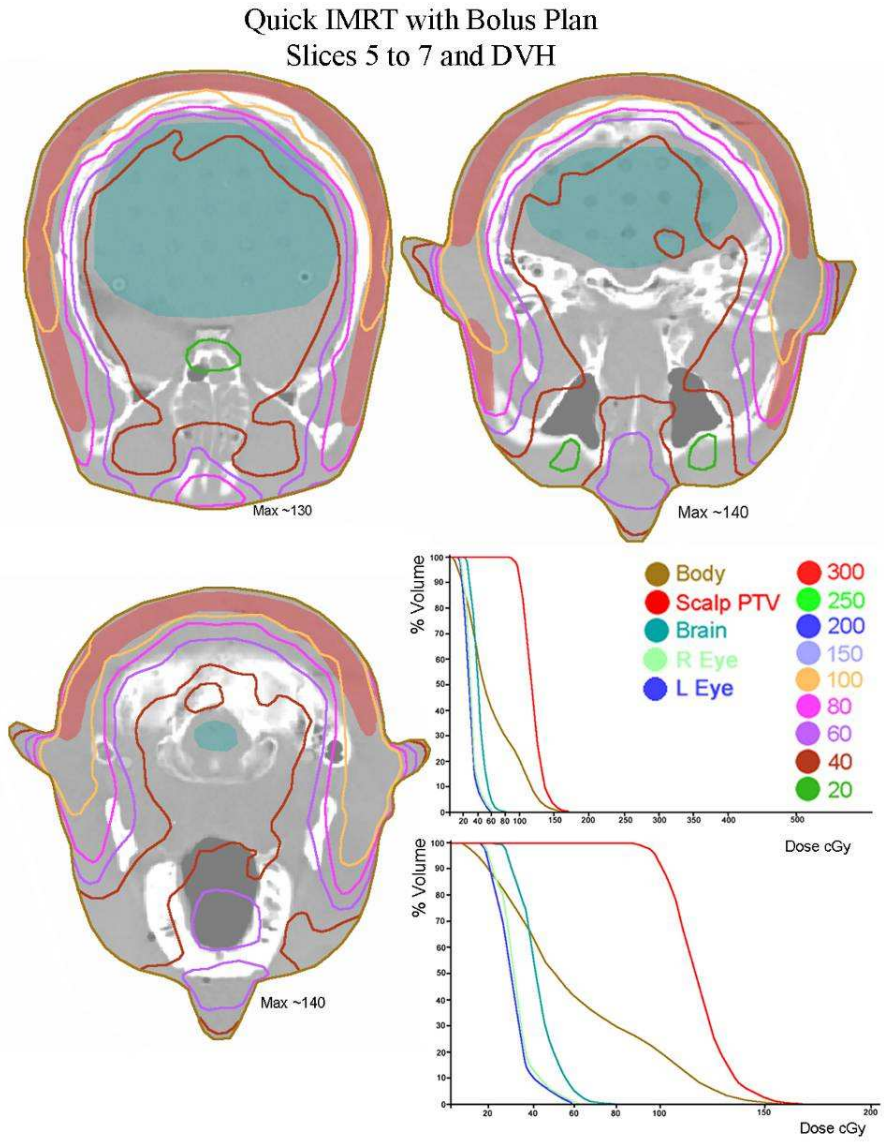

Fig 39 - Fast IMRT Plan with Bolus, Slices 5 to 7 and DVH

Figs 38-39 show that the reduction in the number of segments from 247 to 125 and a halving of the number of intensity levels made no appreciable difference to the plan. The faster plan shows a marginal increase in hot spots within the target. However, the dose maximums, dose distributions and DVHs are virtually identical to those obtained with the slower IMRT plan with bolus.

CHAPTER III: RESULTS

1. PLANNED ISODOSE DISTRIBUTIONS 1.3 ELECTRON PHOTON OPPOSED

Fig 40 shows the dose distribution on the first four slices of the electron and photon parallel opposed plan

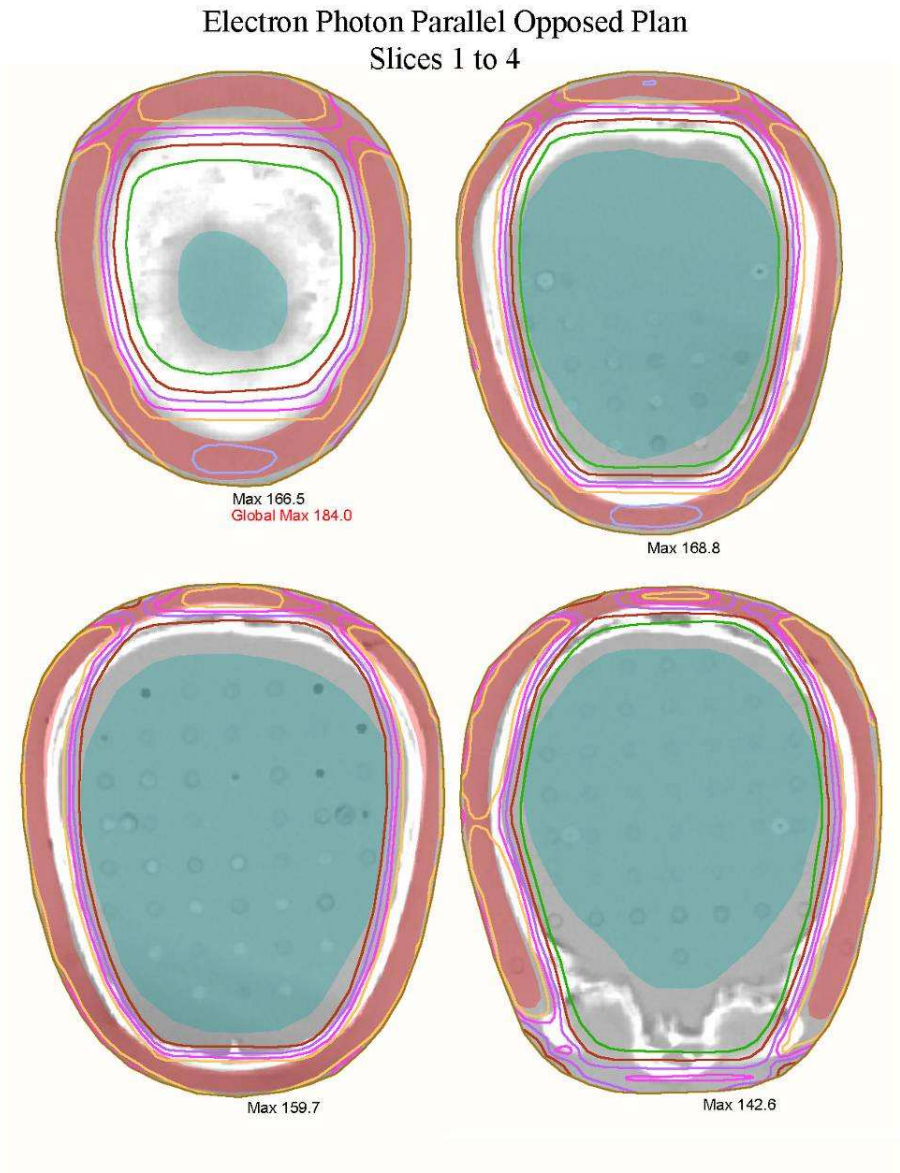

Fig 40 - Electron Photon Parallel Opposed Plan, Slices 1 to 4

The distribution shows cold spots in the posterior lateral regions of the PTV. This is due to the build up region of the photon fields. Little difference was obtained by increasing the energy of the photon fields as the increased exit dose was not able to compensate for the increase in skin sparing. Bolus made only a marginal difference so was not evaluated due to the significant difference that this would make to the patient setup. Finally the cold spots could be improved slightly by reducing the size of the electron block to have a small area of overlap in this region. However, such a plan was not evaluated, as it was beyond the scope of this project.

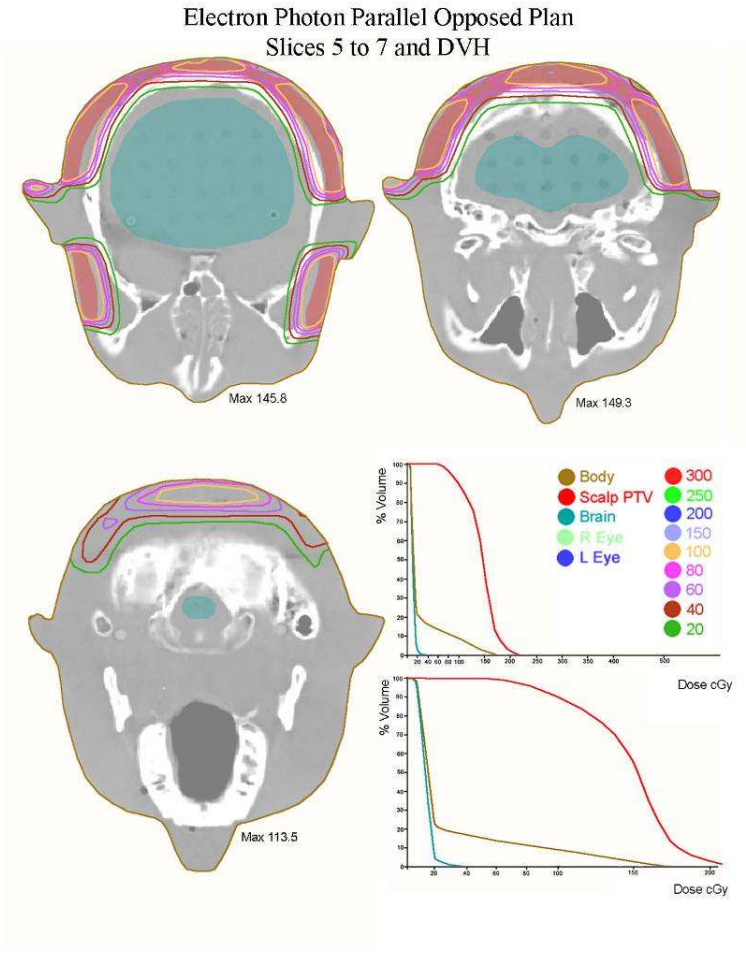

Fig 41 - Electron Photon Parallel Opposed Plan, Slices 5 to 7 and DVH

Figs 40-41 show that the dose to the organs at risk is very low but at the expense of a very inhomogeneous dose to the PTV. The global maximum of this plan was very high at 184 cGy.

CHAPTER III: RESULTS

1. PLANNED ISODOSE DISTRIBUTIONS 1.4 ELECTRON ARC

The electron arc treatment technique was first planned using an electron arc from anterior to posterior. It was found that this plan gave a prohibitively high dose to the ears. Two plans which employed either a block or a bolus to reduce the dose to the ears were therefore considered. Fig 42 shows the dose distribution on these anterior to posterior electron arc plans.

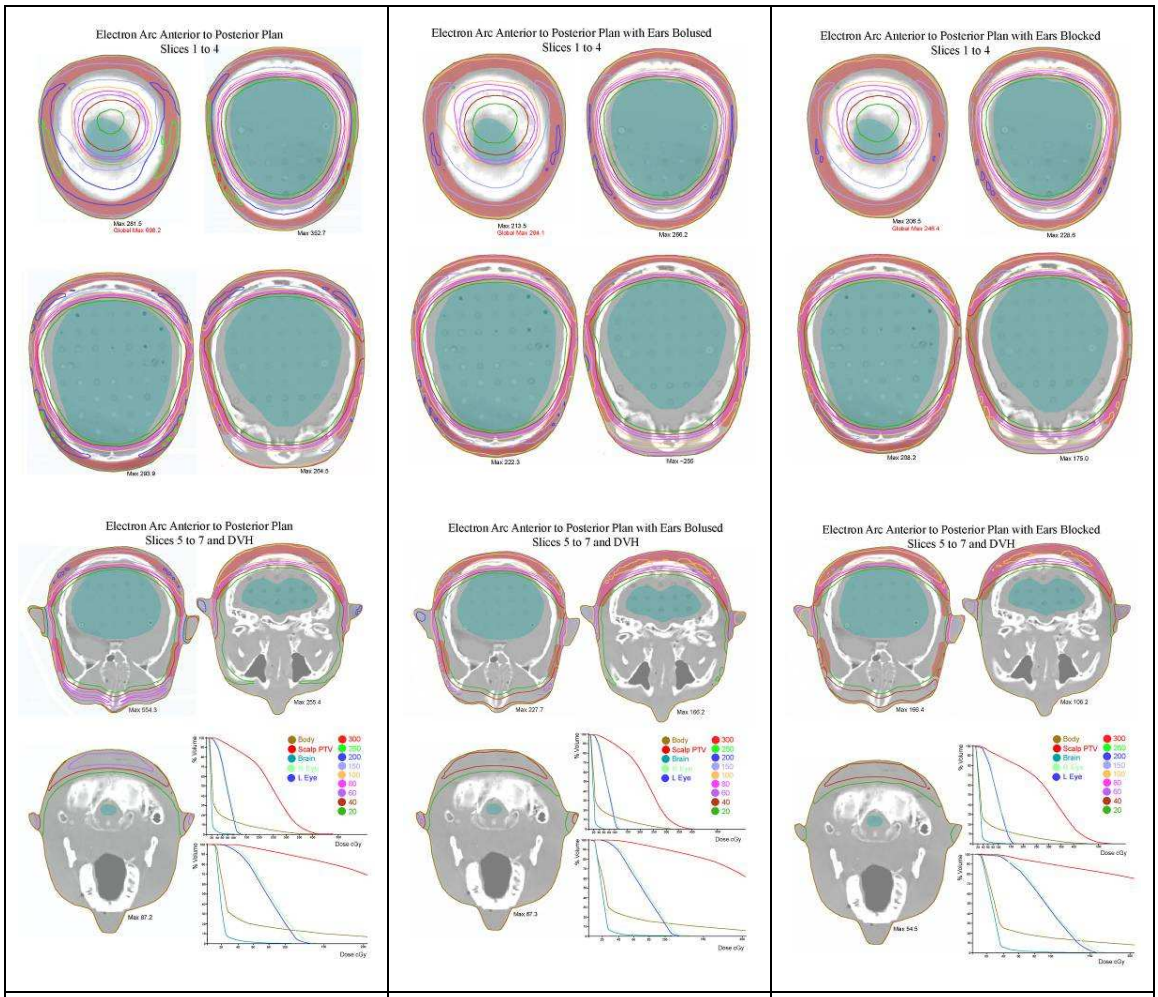

Arc AP Plan	Arc AP with Bolus	Arc AP with Blocks

Fig 42 – Arc anterior to posterior dose distributions

It can be seen that these plans produced hot spots of between 250-700% outside the target volume, which automatically eliminated these plans from further evaluation. This was due to both the over irradiation of the ears and the inability of this beam configuration to deliver dose to the lateral portions of the PTV.

A plan was then generated using an arc from left to right which more accurately reproduced the shape of the skull, as this applicator works best for cylindrical volumes. Fig 43 shows the dose distributions resulting from this plan.

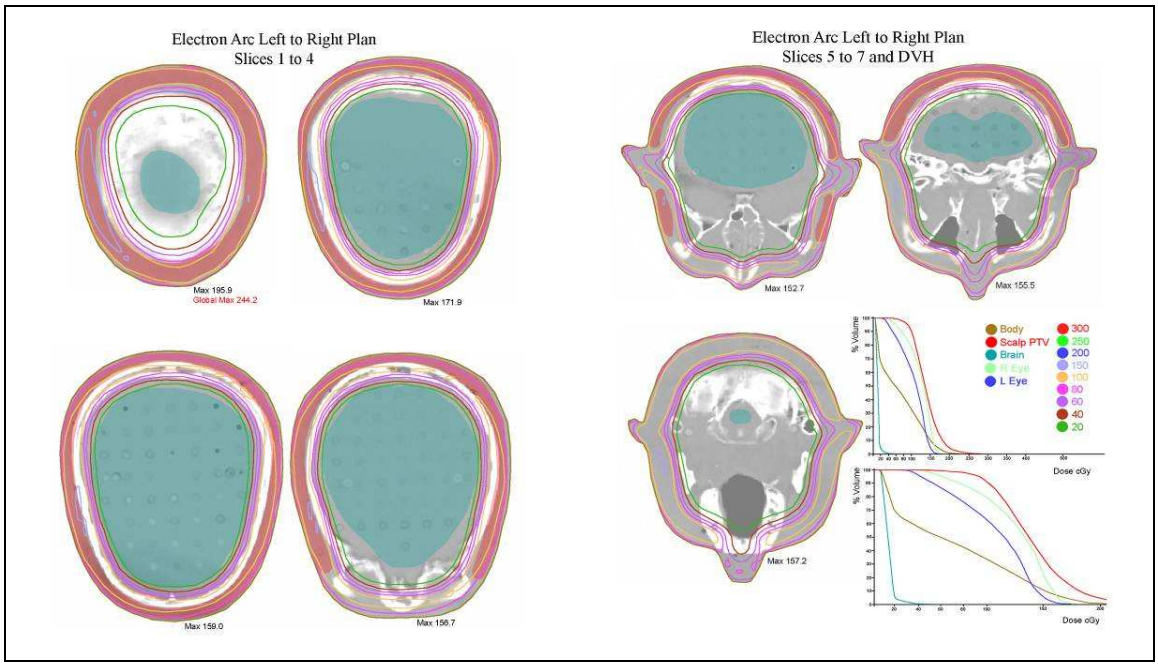

Fig 43 - Electron Arc Left to Right Dose Distributions

In order to treat the anterior region of the PTV is was necessary to generate a full 360º arc. It was therefore not possible, using this plan, to deliver the dose to the PTV without delivering the prescription dose to the eyes. Despite the low dose to the brain, this plan could not be employed due to the dose limit of the eyes. Additionally, this plan resulted in a dose of 244% to the phantom.

The plan was therefore split into two parts. A superior part was delivered using a full 360º arc. An inferior part was then delivered using a blocked field to the posterior region of the skull whilst avoiding the face and eyes.

Fig 44 shows the dose distribution on the first four slices of the electron arc plan, delivered from left to right and split into a superior full arc and an inferior blocked partial arc.

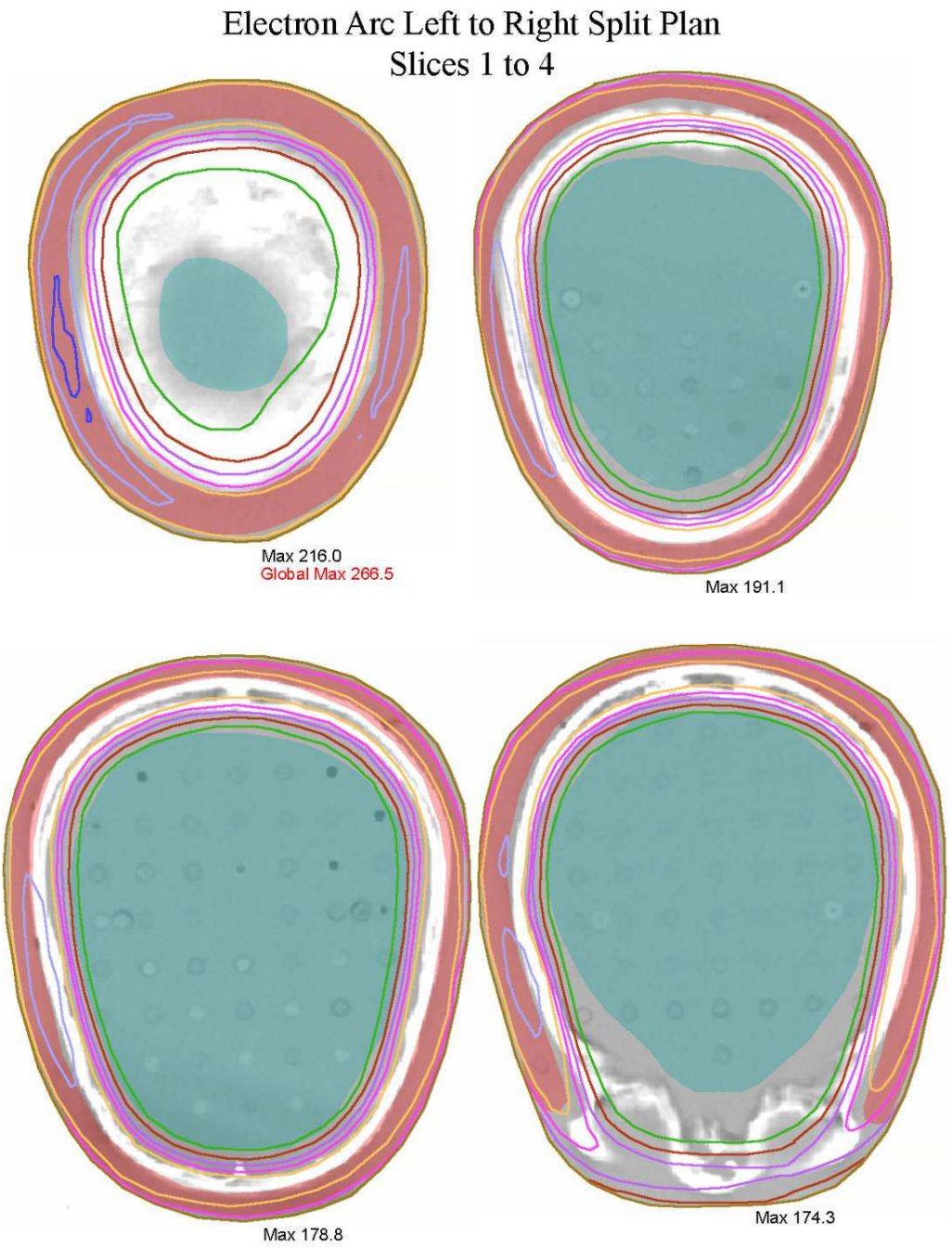

Fig 44 - Electron Arc Left to Right Split Plan, Slices 1 to 4

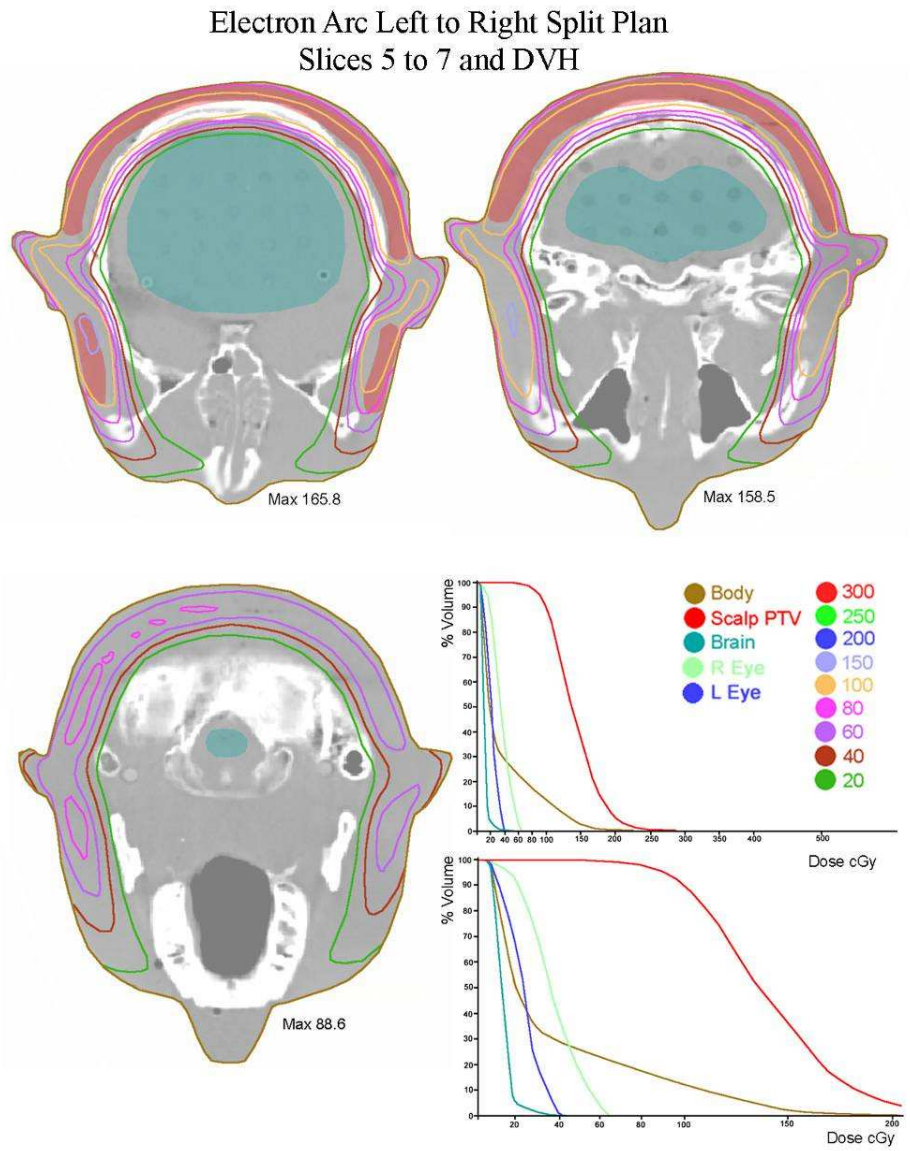

Fig 45 - Electron Arc Left to Right Split Plan, Slices 5 to 7 and DVH

Figs 44-45 show that this plan is able to deliver a very low dose to the organs at risk. The dose to the PTV is very inhomogeneous with a high global maximum of 267%. However, the high dose regions are all within the target volume and it can be seen on the DVH that most of the body organ receives a very low dose.

CHAPTER III: RESULTS

2. FILM DOSIMETRY 2.1 VARIABILITY

The reproducibility of dose values recorded using film dosimetry was investigated prior to using it to detect dose distributions in the phantom. The optical density of each HDR irradiated calibration film was measured at six different points within the region of maximum density. Additionally, a background reading (of film and fog density) was made at six points on a non-irradiated film.

The readings in Table 16 show the optical densities measured for each film. These calibration films were irradiated and processed at the same time as the phantom films, to avoid any processor related variations.

Dose cGy	Average	Reading 1	Reading 2	Reading 3	Reading 4	Reading 5	Reading 6
0.0	**12.2**	12.3	13.0	12.1	11.4	12.4	11.8
19.8	**67.2**	62.6	67.7	68.0	67.9	67.7	69.2
39.3	**114.6**	113.9	112.6	112.0	115.2	115.9	118.1
58.8	**145.7**	144.9	145.3	145.1	145.9	145.9	146.8
78.6	**172.5**	176.7	172.1	172.2	171.3	170.2	172.2
98.4	**195.0**	194.1	197.1	196.0	195.2	196.7	191.1
127.6	>Range	>Range	>Range	>Range	>Range	>Range	>Range

Table 16 – Optical density values for HDR calibration film

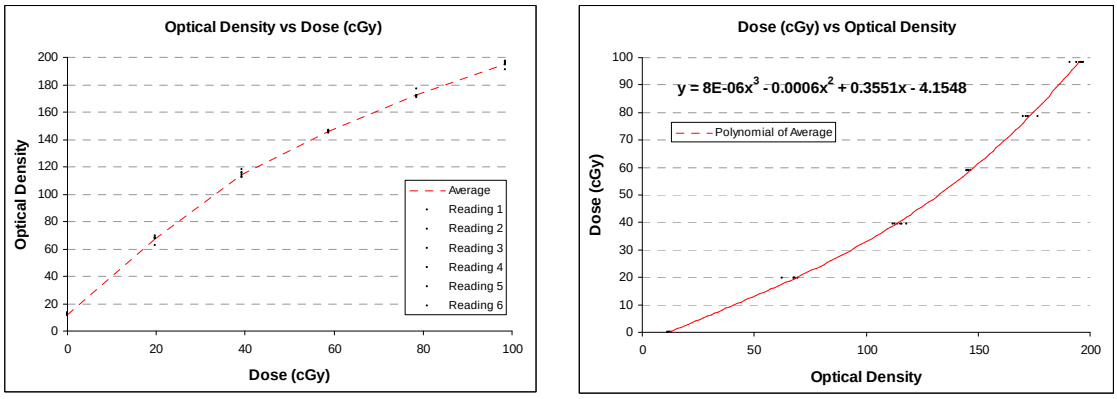

Fig 46 – Optical density and dose for HDR calibration film

It can be seen from Fig 46 that, within the range 20-100 cGy, optical densities can be converted into dose readings using the following equation:

$y = 8x10^{-6}\ x^3 - 0.0006\ x^2 + 0.3551\ x - 4.1548$

Where y = dose (cGy) and x = optical density.

The dose levels are reproduced with an accuracy of ± 2.1% for one standard deviation. Therefore, one would anticipate a reading of ± 2.1% to be representative of the actual dose with 95% confidence.

The calibration films were also generated for the other plans. The optical density to dose graphs for each of the plans is shown in Fig 47.

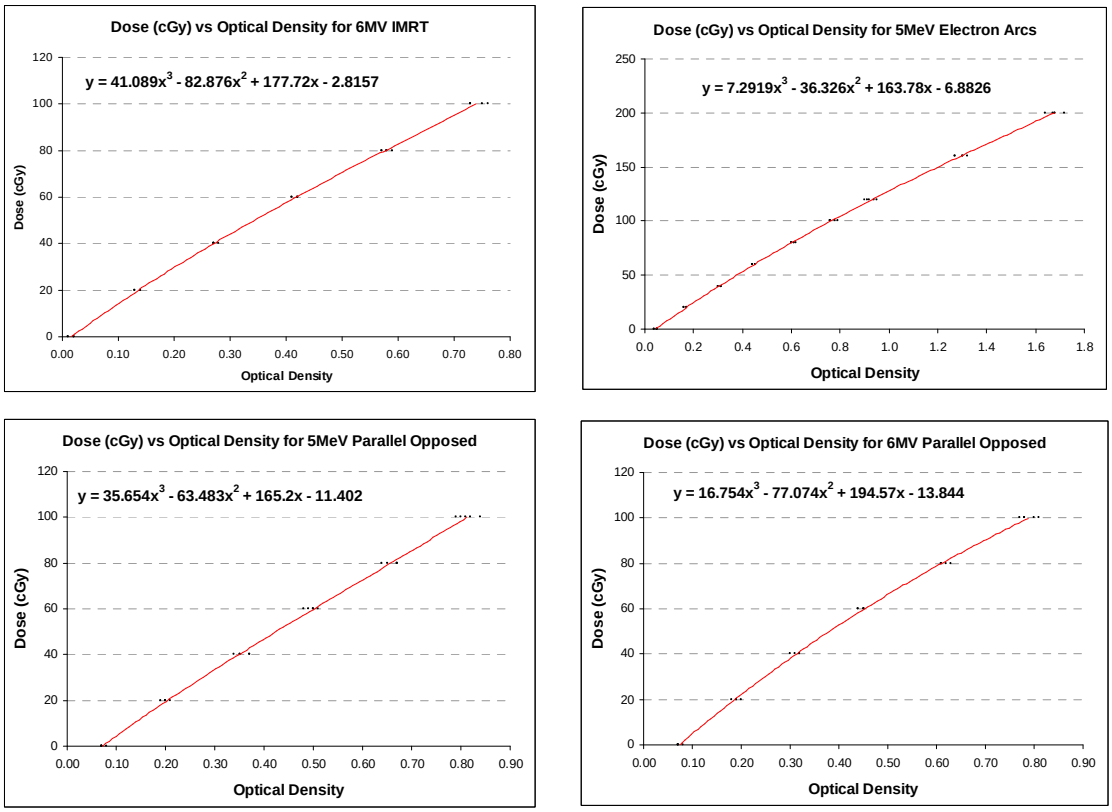

Fig 47 – Dose and optical density curves for external beam radiation films

There is little difference in the gradients observed on all of the graphs in Fig 47.

Fig 48 further illustrates the similarities between the calibration films despite a difference in modality. This graph shows the relationship between dose and the average optical density recorded for each calibration film.

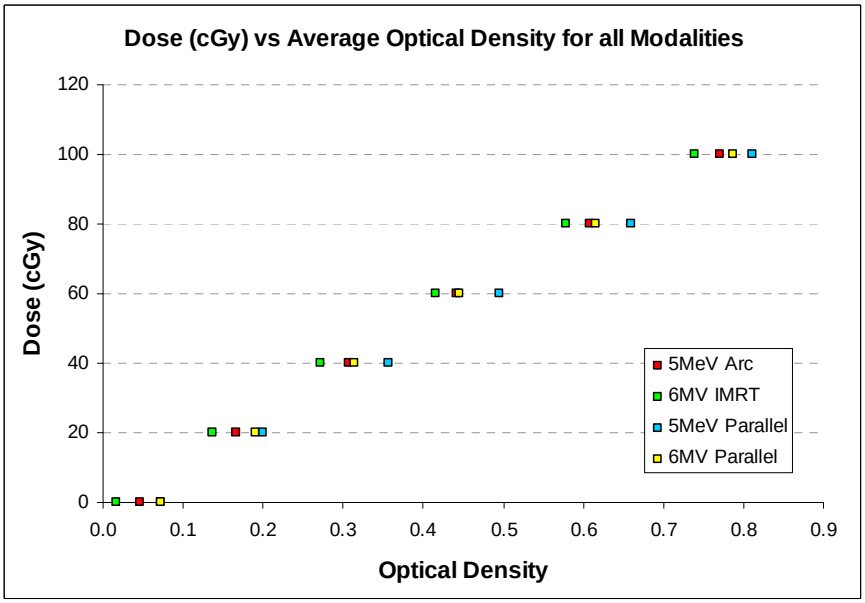

Fig 48 – Dose versus average optical density for all external beam modalities

A large difference in the fog density can be observed from Figs 47-48. This is probably because the films were processed and read on different days with resultant changes to the processor and dosimeter variables. All of the phantom films were processed and read at the same time as their calibration films so this difference in base and fog density is accounted for by the calibration conversion.

Table 17 shows the standard deviations of these readings as a percentage of the mean reading for each dose level for each modality.

Dose cGy	5MeV Arc	6MV IMRT	5MeV Parallel	6MV Parallel	Average
0	11.9	34.2	6.2	6.2	**14.6**
20	3.3	4.0	3.5	3.7	**3.6**
40	1.8	1.6	3.8	2.8	**2.5**
60	1.0	1.3	2.3	1.2	**1.5**
80	1.4	1.4	2.1	1.5	**1.6**
100	1.8	1.9	2.4	2.1	**2.1**
Average	**3.5**	**7.4**	**3.4**	**2.9**	**4.3**

Table 17 – Calibration film standard deviation of readings

Table 17 shows that a reading within 2.5 % of the planned dose, for dose values 40-100 cGy will be acceptable with 95 % confidence, or between 5 % with 90 % confidence. It is interesting to observe that there is much more variation in the optical densities recorded for low dose levels. This is due to the sensitivity of the densitometer at low levels, generally showing a variation of +-0.01 for a reading of approximately 0.02-0.08 optical density. Therefore it is anticipated that low dose regions will give a poorer agreement with the planned dose. A reading within 15 % of the planned dose for dose values lower than 20 cGy will be acceptable with 95 % confidence, or within 30 % of the planned dose with 90 % confidence.

CHAPTER III: RESULTS

2. FILM DOSIMETRY 2.2 HDR

The optical densities of the 250 grid points were measured on the films and were converted to dose values in cGy using the calibration optical density to dose conversion equation.

As discussed earlier, the film dosimetry technique for HDR brachytherapy has an accuracy of approximately ± 2.1%. It would therefore be expected that any larger variations in dose measurement would be due to the treatment delivery and technique. Fig 49 shows the difference between the dose measured and the dose calculated by the planning system for HDR brachytherapy. The results are displayed in terms of the frequency with which dose values occurred.

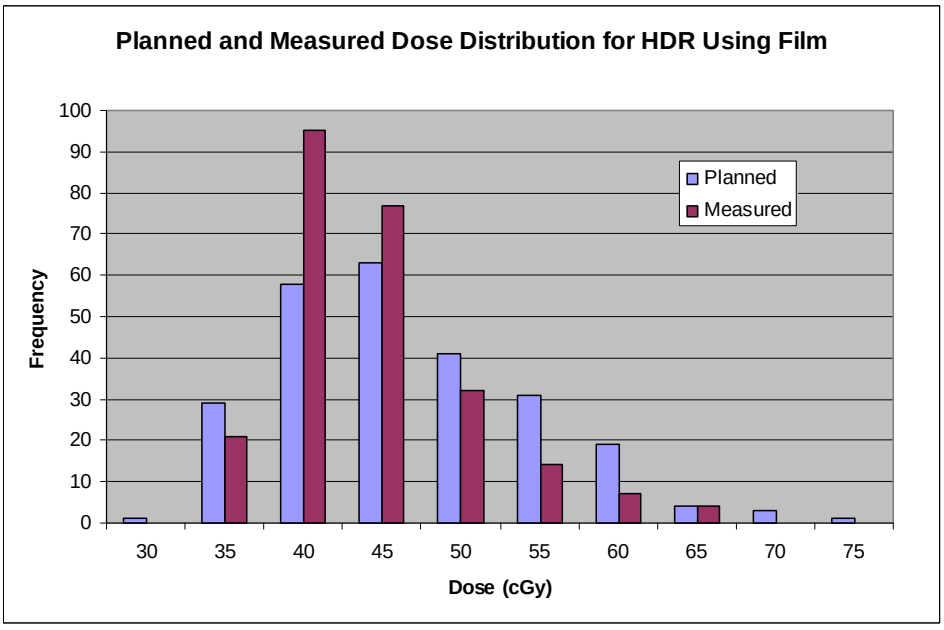

Fig 49 – Planned and measured dose distribution for HDR brachytherapy using film

Fig 49 shows a reasonable agreement between the two distributions and there was only a 2.3 cGy (4%) difference between the mean doses measured. However, it can be seen that the range of the planned doses was wider than the range of doses measured on the films.

When the dose results were analysed the results in Table 18 were found. This table shows the differences between all of the dose points measured on the film versus all of the dose points on the plan. The percentage differences column indicates the maximum, minimum and mean percentage difference between the plan and film observed for all points. The mean percentage difference should be zero if there is no shift between the plan and the film. The magnitude percentage difference column indicates the size of the percentage difference regardless of sign. This indicates the overall accuracy with which the doses were reproduced. For example, if percentage differences of 6 %, -4 % and -2 % were observed then the mean percentage difference would be 0 % but the mean magnitude percentage difference would be 3 %. The maximum and minimum percentage differences would be 6 % and -4 %, whereas the maximum and minimum magnitude percentage differences would be 6 % and 2 %.

	Dose Planned (cGy)	Dose Measured (cGy)	% Differences	Magnitude % Differences
Maximum	74.90	63.69	23.42	35.89
Minimum	29.54	31.12	-35.89	0.08
Mean	44.00	41.73	-4.22	7.21

Table 18 – Dose measurements on phantom film for HDR brachytherapy

There was a much higher percentage dose difference (7.2 %) between the measured doses and those planned than one would expect from the film dosimetry reproducibility. These films were processed at the same time as the calibration films, so these variations could not be explained by processor-related changes. The technique used to measure the optical density of the film had a geometrical accuracy of approximately 3 mm. This was due to the accuracy with which the densitometer could be positioned. In the regions of higher dose gradients, at the edges of the scalp, this would result in dose differences of up to 10 cGy (24 %). In the regions of lower dose gradients, at the centre of the brain, this variation would result in dose differences of approximately 2 cGy (5 %).

Fig 50 shows the percentage differences between the measured doses and those planned for the HDR brachytherapy technique.

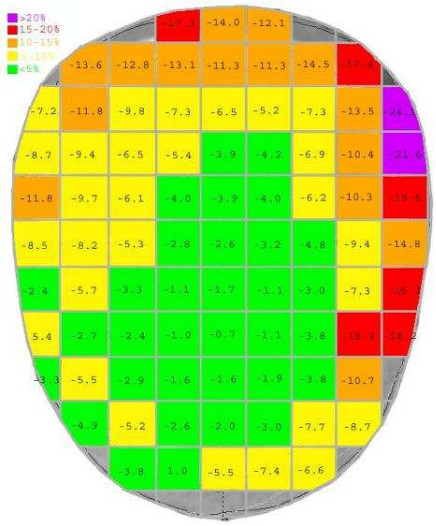

Slice 1

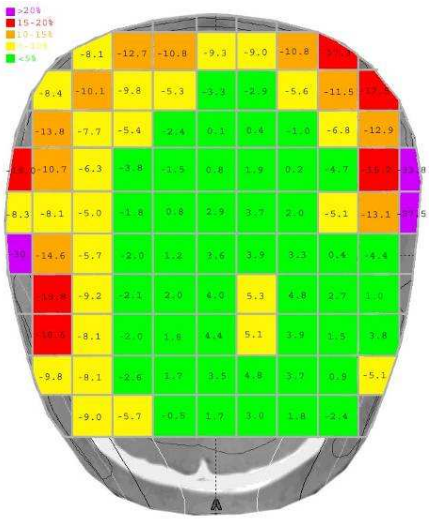

Slice 2

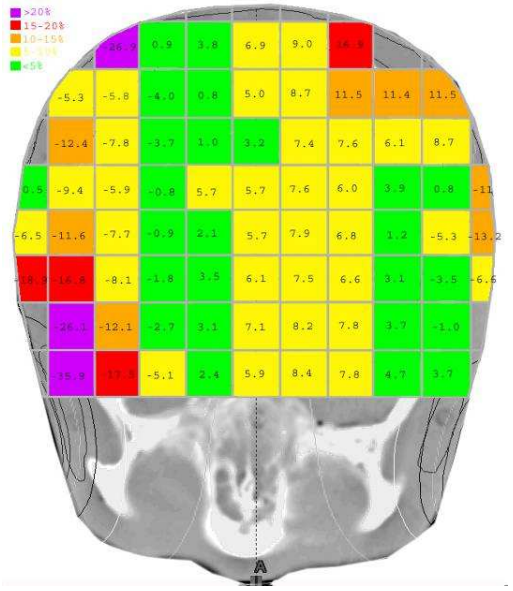

Slice 3

Fig 50 - Percentage dose difference between dose values measured and dose values planned for HDR brachytherapy plan

The coloured blocks show which regions show the greatest dose differences in terms of the magnitude of the percentage difference. These results are fairly consistent with the variability expected due to the accuracy of the film dosimetry technique employed, as previously outlined.

It was anticipated that film exposure due to light leakage at the film edges would have also contributed to the dose variability at the film edges. This would have resulted in an increase in the expected dose at the edges, which was not observed, as can be seen in Fig 50. Additionally, it was anticipated that if the mask was not secured to the head tightly then a lower dose over all regions would have been detected. However, this was not observed in Fig 50.

In conclusion, film dosimetry shows that the dose distribution predicted by the planning system can be reproduced in a phantom, using the catheter-mask HDR brachytherapy technique.

CHAPTER III: RESULTS
2. FILM DOSIMETRY 2.3 IMRT

It was anticipated for the external beam techniques that a reading within 2.5 % of the planned dose, for dose values 40-100 cGy, and a reading within 15 % of the planned dose, for dose values lower than 20 cGy, will be acceptable with 95 % confidence.

Fig 51 shows the difference between the dose measured and the dose calculated by the planning system for IMRT.

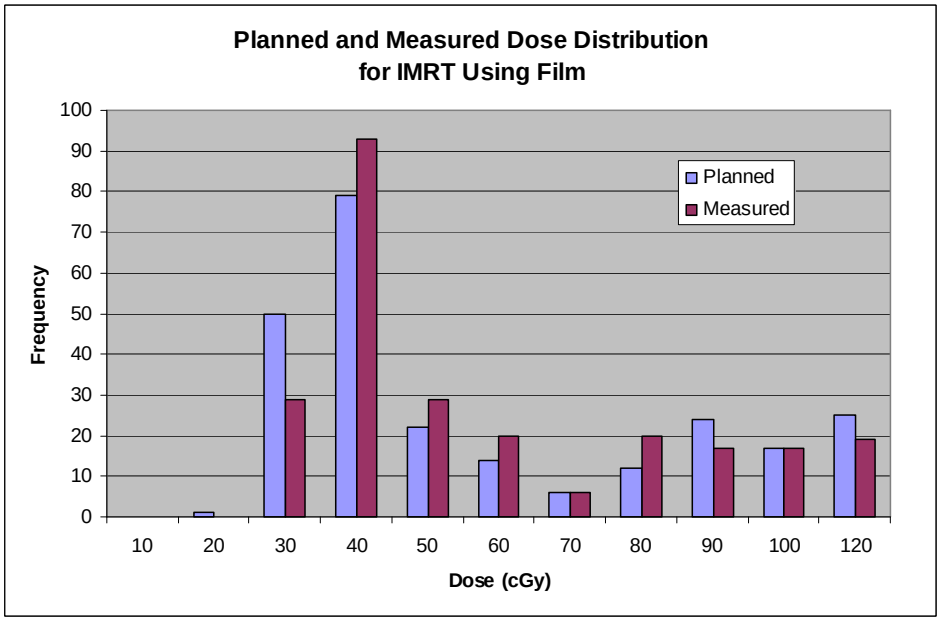

Fig 51 – Planned and measured dose distribution for IMRT using film

Fig 51 shows a reasonable agreement between the two distributions and shows less agreement for the lower dose values than for the higher dose values. When the results were analysed the results in Table 19 were found.

IMRT	Dose Planned (cGy)	Dose Measured (cGy)	% Differences	Magnitude % Differences
Maximum	110.00	117.40	18.77	40.61
Minimum	20.00	22.12	-40.61	0.01
Mean	55.88	53.60	-2.42	7.08

Table 19 – Dose measurement on a phantom film for IMRT

Some of the differences in dose were as high as 40 %. Fig 52 shows the percentage differences between the measured doses and those planned for the IMRT technique.

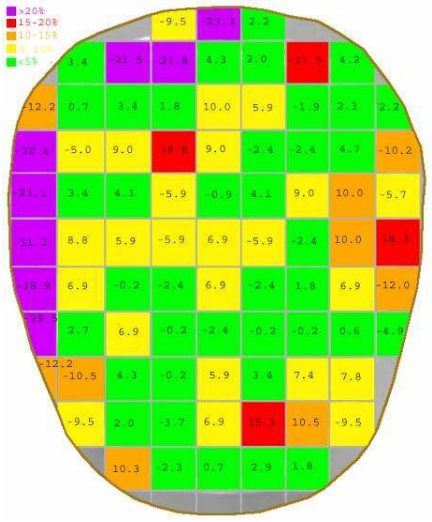

Slice 1

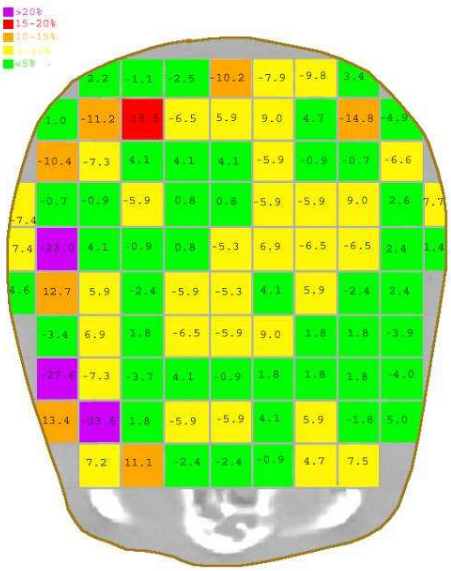

Slice 2

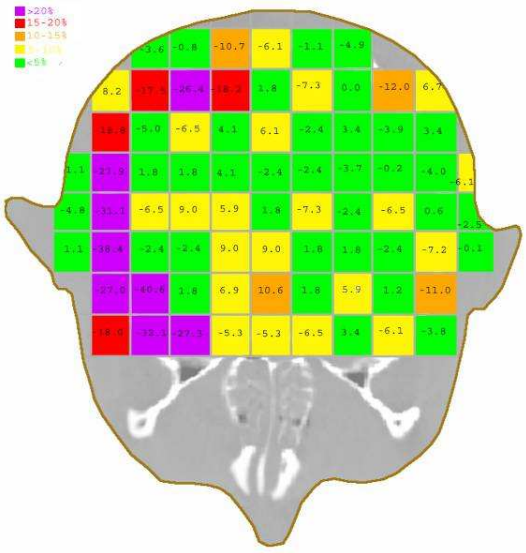

Slice 3

Fig 52 - Percentage dose difference between dose values measured and dose values planned for the IMRT plan

The IMRT plan has much higher steep dose gradients and the areas of worst agreement coincide with them. In the regions of high dose gradients, the 3 mm accuracy of the film dosimeter, could produce dose differences of approximately 20 cGy. In addition there is alignment variability in the placement of the film and grid which could further reduce the geometrical accuracy. The overall geometrical accuracy is estimated to be 5mm, which in

regions of high dose gradients for the IMRT plan can result in dose differences of 40 cGy. The images in Fig 52 further demonstrate the reduction in agreement in low dose regions. These results are therefore consistent with the variability expected due to the accuracy of the film dosimetry technique employed and the IMRT dose distribution has been accurately replicated within the phantom.

CHAPTER III: RESULTS
2. FILM DOSIMETRY 2.4 ELECTRON PHOTON PARALLEL OPPOSED

For the parallel opposed plans, the optical densities were converted to dose for the electron part of the plan then added to the optical densities converted to dose for the photon part of the plan. Fig 53 shows the difference between the dose measured and the dose calculated by the planning system for the parallel opposed plan.

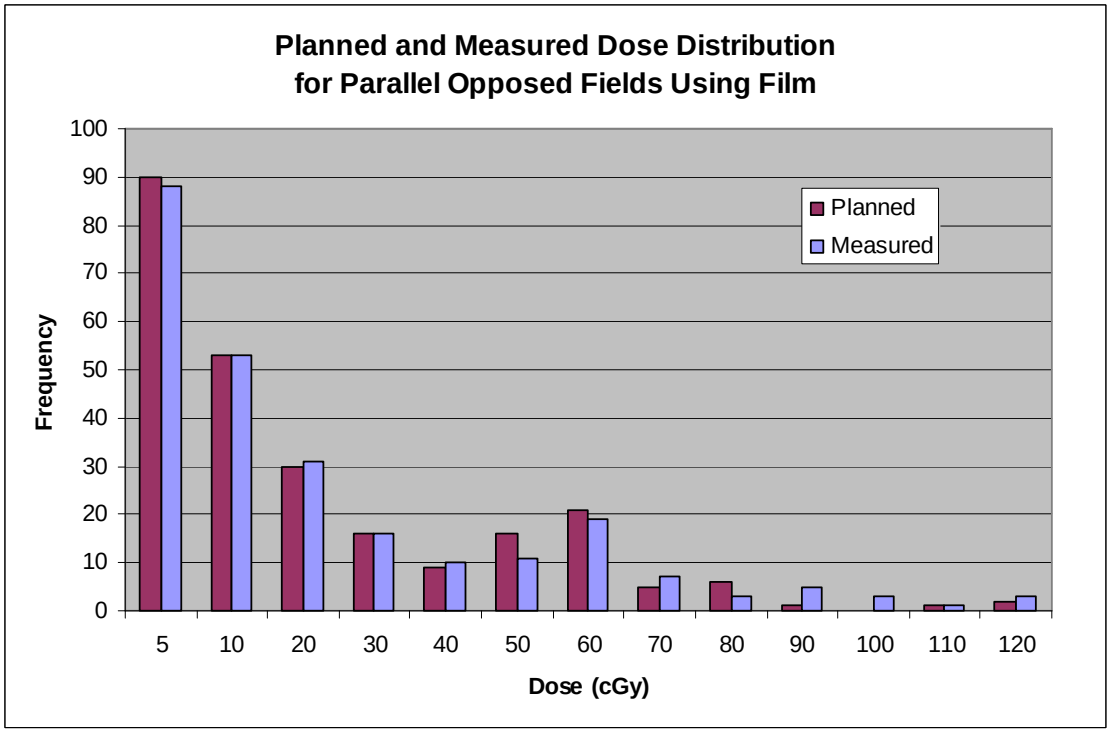

Fig 53 – Planned and measured dose distribution for parallel opposed fields using film

Fig 53 shows a good agreement between the two distributions. When the data was analysed the results in Table 20 were found.

Parallel Opposed	Dose Planned (cGy)	Dose Measured (cGy)	% Differences	Magnitude % Differences
Maximum	120.00	117.22	50.72	89.32
Minimum	1.00	0.85	-89.32	0.07
Mean	20.70	20.84	-1.82	9.10

Table 20 – Dose measurements on a phantom film for parallel opposed fields

There was an average dose difference of only -2%. Fig 54 shows the percentage differences between the measured doses and those planned for the parallel opposed technique.

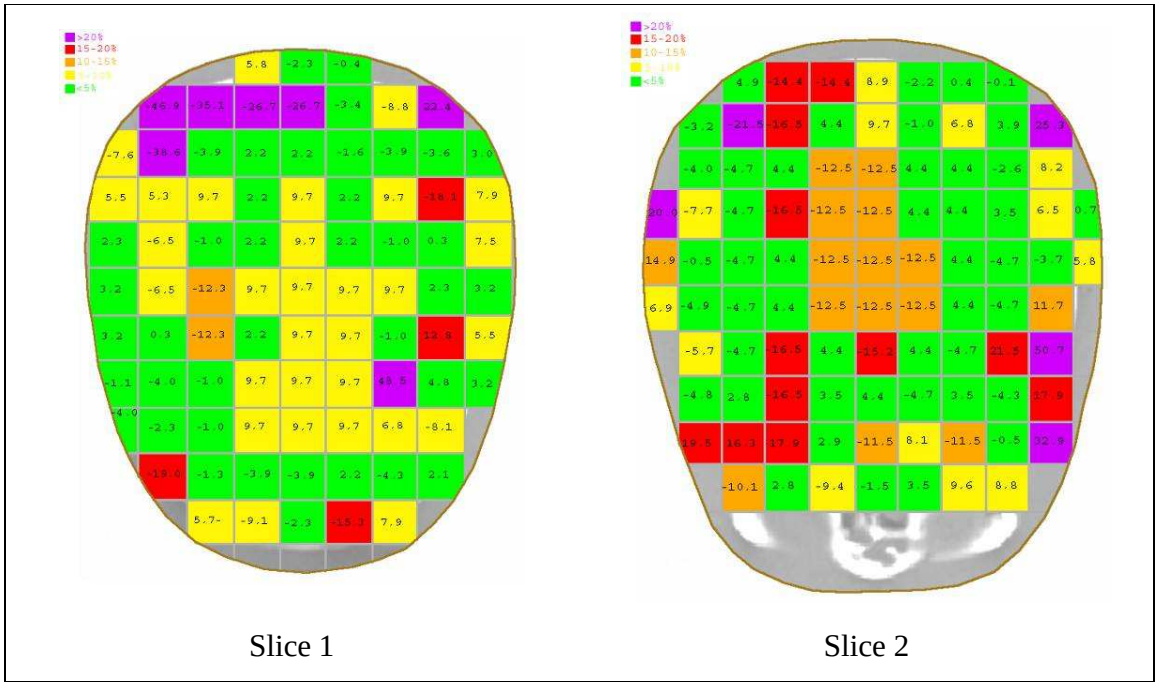

Slice 1 Slice 2

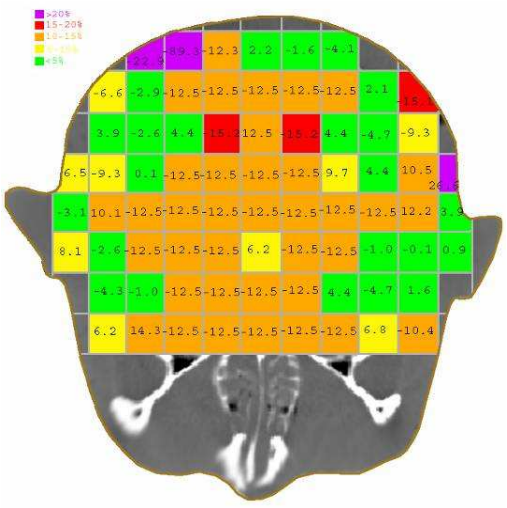

Slice 3

Fig 54 - Percentage dose difference between dose values measured and dose values planned for the parallel opposed plan

The parallel opposed plan has large regions of very low dose. It is these regions which show the worst agreement as is consistent with the standard deviation of 15 % shown by the calibration films for low dose levels.

There are some other regions of disagreement which coincide with the steep dose gradients. These are consistent with a distance to agreement equal to the geometrical accuracy of the film dosimetry technique. The film which was irradiated with both photons and electrons was assessed qualitatively. It did not have any obvious regions of overlap due to a misalignment of the fields. These results are therefore within the expected variability and the parallel opposed dose distribution has been accurately replicated within the phantom.

CHAPTER III: RESULTS

2. FILM DOSIMETRY 2.5 ELECTRON ARC

The electron arc plan evaluated for the film dosimetry was further optimised for the plan evaluation by the radiotherapy personnel. Therefore the dose values observed are inconsistent with those seen on the evaluated plan. Fig 55 shows the difference between the dose measured and the dose calculated by the planning system for the film irradiated electron arc plan.

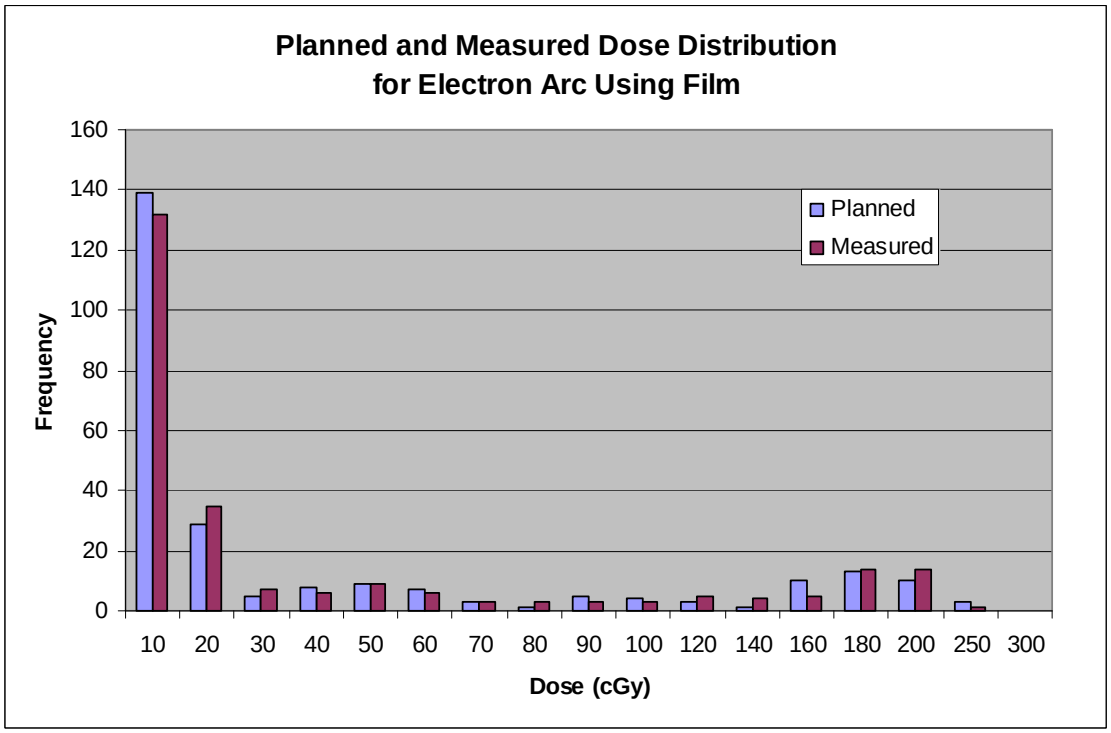

Fig 55 – Planned and measured dose distribution for electron arc using film

This graph shows an excellent agreement between the two distributions. When the data was analysed the results in Table 21 were found.

Electron Arc	Dose Planned (cGy)	Dose Measured (cGy)	% Differences	Magnitude % Differences
Maximum	210.00	205.49	73.18	73.18
Minimum	6.00	5.99	-63.16	0.10
Mean	43.17	42.04	-0.52	6.71

Table 21 – Dose measurements on a phantom film for an electron arc plan

There was an average dose difference of only -0.5 %. Fig 56 shows the percentage differences between the measured doses and those planned for the electron arc technique.

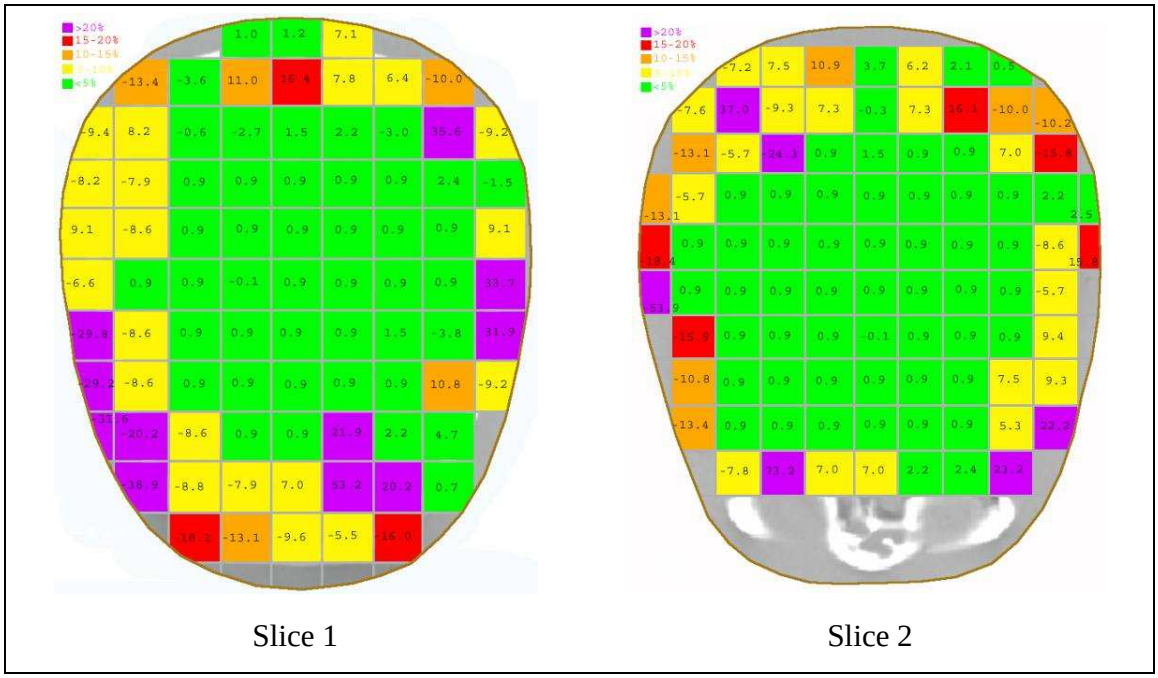

Slice 1 Slice 2

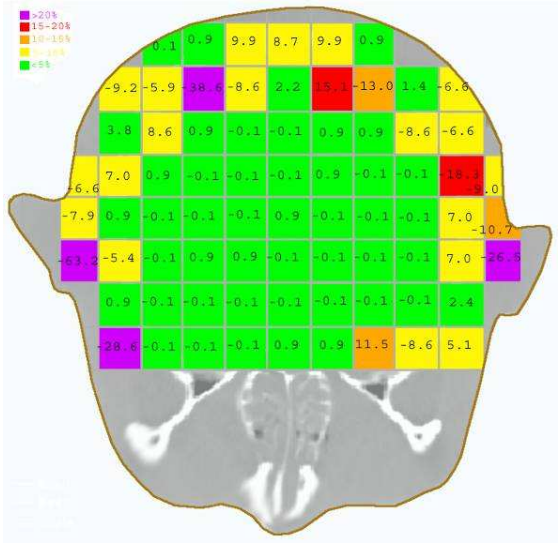

Slice 3

Fig 56 - Percentage dose difference between dose values measured and dose values planned for the electron arc plan

The electron arc plan has a distribution of relatively uniform dose without areas of low dose. It was therefore anticipated that this plan would show better agreement than the other techniques, as can be seen by these results. The attenuation by the foam cushion does not appear to have caused any measureable drop in dose. There are some regions of disagreement which coincide with the steep dose gradients. These results are within the geometrical accuracy of the technique and the electron arc dose distribution has been correctly reproduced within the phantom.

CHAPTER III: RESULTS

3. TLD DOSIMETRY 3.1 VARIABILITY

The TLDs were used to evaluate the reproducibility of the plans. Before using them to this end the variability of the TLD system was first investigated. The counts from the TLDs used to generate an HDR calibration file for 60 cGy are shown in Table 22.

Dose (cGy)	58.8	58.8	58.8	58.8	58.8	0.0	0.0	0.0	0.0
Counts	17176	14406	14509	14532	15068	86	40	19	157

Table 22 – TLD counts for HDR calibration

Once this calibration file had been generated, it was checked using three different doses, to establish the variability of the system. These results are shown in Table 23.

Dose cGy	39.2	39.2	39.2	39.2
Counts	11254	9055	12682	10179
Measured Dose (cGy)	44.3	35.4	49.9	39.9

Dose cGy	58.8	58.8	58.8	58.8
Counts	14453	(86991)	17209	13624
Measured Dose (cGy)	56.8	346.7	67.9	53.6

Dose cGy	78.4	78.4	78.4	78.4
Counts	(112653)	28796	21556	18125
Measured Dose (cGy)	449.4	114.3	85.3	71.5

Table 23 – TLD dose measurements to check the variability of the TLD system

The two TLD readings shown in brackets were not used for the analysis as their readings were approximately 5 times higher than the other TLD readings. Fig 57 shows the counts versus the dose with which the TLDs were irradiated.

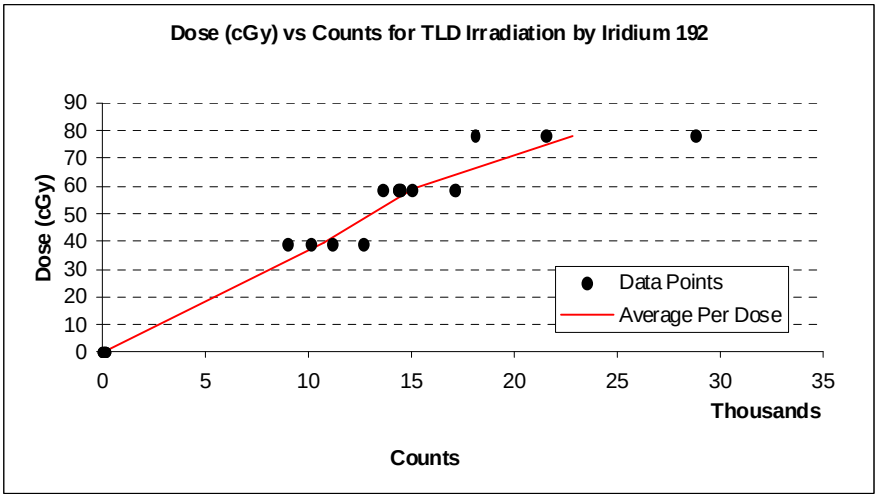

Fig 57 – Dose (cGy) versus counts for TLD irradiation by Iridium 192

12 of the TLDs were used to check the calibration file generated using the five TLDs irradiated to 60 cGy. The results of this check are shown in Fig 58 and Table 24.

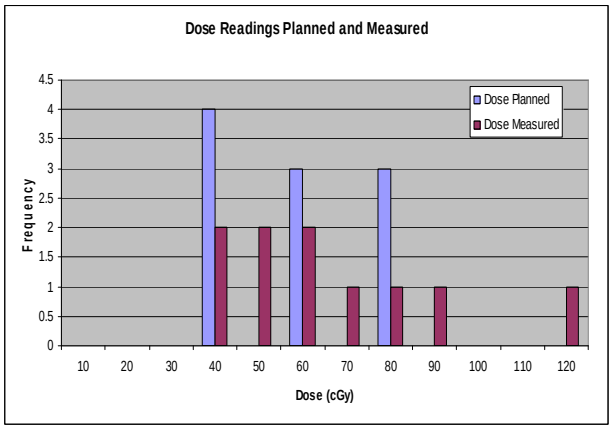

Fig 58 – Dose planned and measured for calibration TLDs with Iridium 192

Dose Planned (cGy)	Dose Measure (cGy)	% Difference
39.2	44.3	13.0
39.2	35.4	-9.7
39.2	49.9	27.3
39.2	39.9	1.8
58.8	56.8	-3.4
58.8	67.9	15.5
58.8	53.6	-8.8
78.4	114.3	45.8
78.4	85.3	8.8
78.4	71.5	-8.8

Table 24 – Dose differences for calibration TLDs with Iridium 192

It can be seen that even after the two outliers are removed, there is still a large variation in detected dose. These dose differences resulted in an average magnitude of the dose difference of ± 14%, an average dose difference of 8 % and a standard deviation of 13 %. Therefore TLD readings in the range +-13 % of the anticipated dose will be acceptable with a 95 % confidence and in the range +-26 % of the anticipated dose will be acceptable with a 90 % confidence.

For the external beam treatment techniques, eight TLDs were read to give the number of counts for an annealed reading and eight TLDs were read to give the number of counts for an irradiated reading of either 50 or 100 cGy. These counts were then used to generate a calibration file for that particular treatment modality and energy. The variability of these counts is shown in Table 25.

	Photon 6MV	Parallel Electron 5 MeV	Arc Electron 5MeV
Mean Annealed Reading	347	423	304
Annealed Standard Deviation as % of Mean	39%	21%	38%
Dose cGy	50	50	100
Mean Irradiated Reading	42598	39651	64358
Irradiated Standard Deviation as % of Mean	5%	4%	5%

Table 25 – TLD count readings for external beam calibration

From these results, it is expected that low dose readings will be within 30 % of the predicted values and high dose regions will be within 5 % of the planned values, with 95 % confidence.

CHAPTER III: RESULTS

3. TLD DOSIMETRY 3.2 HDR

A comparison was then made between the calculated dose and the dose measured using the 60 cGy calibration file. The results of this comparison are shown in Table 26.

Head Position	Counts	Measured Dose	Planned Dose	% Difference
A	9131	35.6	41.6	16.9
B	13306	52.6	42.9	-18.4
C	20355	80.4	44.3	-44.8
D	9085	35.6	43.5	22.2
E	17860	70.5	64.1	-9.1
F	24722	97.8	64.6	-33.9
G	11626	45.8	45.3	-1.0
H	9902	39.0	44.8	14.8
I	7621	29.8	31.4	5.2
J	8890	35.2	43.8	24.3
K	9486	37.4	37.9	1.3
L	9192	36.2	38.7	6.8
	Average	49.7	45.2	-1.3

Table 26 – TLD Dose differences for HDR phantom irradiation

It can be seen that there is some disagreement between the planned dose and the dose measured by the TLDs. However, the majority of readings are within the 90 % confidence interval. There are two readings, highlighted in grey, outside this range which can be explained by the incidence of outliers also observed in the calibration TLDs.

The histogram in Fig 59 shows that there is a uniform spread of results about the expected readings which is confirmed by the average percentage disagreement of only -1.3 %.

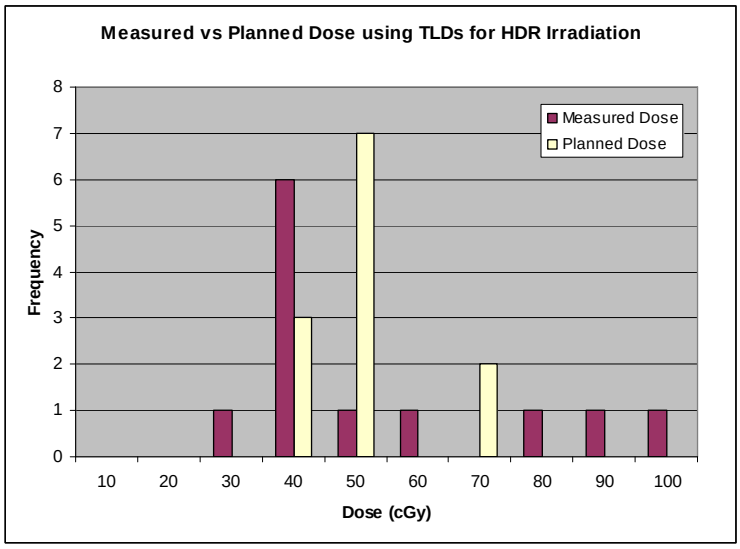

Fig 59 – Measured versus planned dose using TLDs for HDR irradiation

In general the TLDs therefore agree with the planned distribution within expected experimental variation.

CHAPTER III: RESULTS

3. TLD DOSIMETRY 3.3 EXTERNAL BEAM TECHNIQUES

The readings were repeated for the other plans with the results in Table 27.

	IMRT	Parallel Opposed	Electron Arc
% Difference Plan vs Measure	1.5%	-9.9%	-12.5%

Table 27 – TLD dose differences for external beam phantom irradiation

These average dose differences are well within the range anticipated from the standard deviation of the calibration readings. The higher dose difference between the planed dose and the measured dose for the electron arc is consistent with the lower doses delivered to the TLDs for this plan. A graphical representation of this comparison is shown in Figs 60-62. These graphs show that the TLD readings for all of the plans agree with the planned doses within the expected experimental variation.

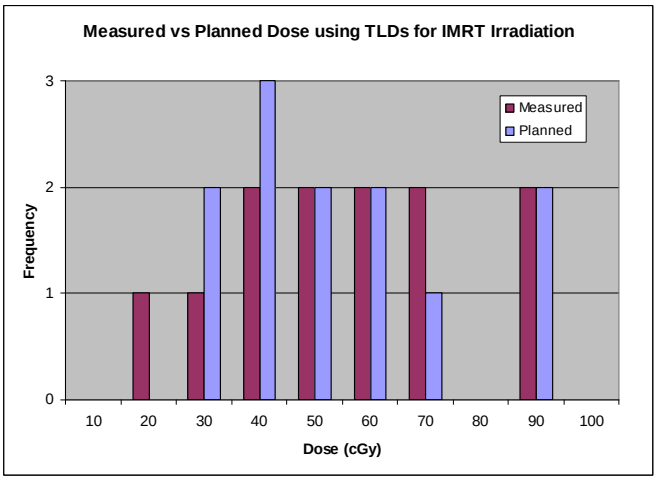

Fig 60 - A comparison of TLD readings for the IMRT Plan

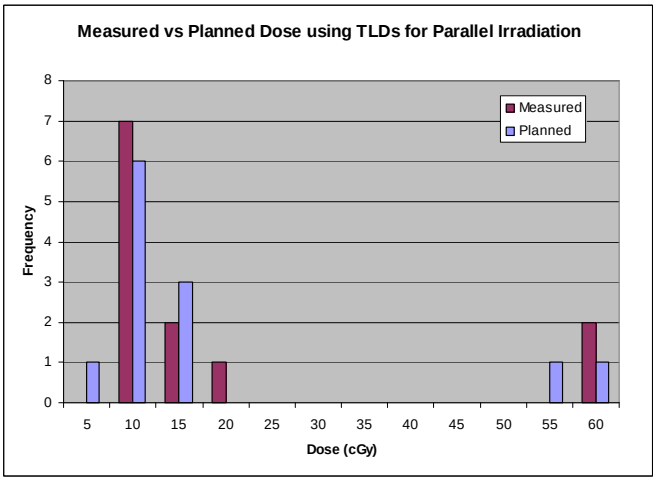

Fig 61 - A comparison of TLD readings for the X Ray and Electron Parallel Opposed Plan

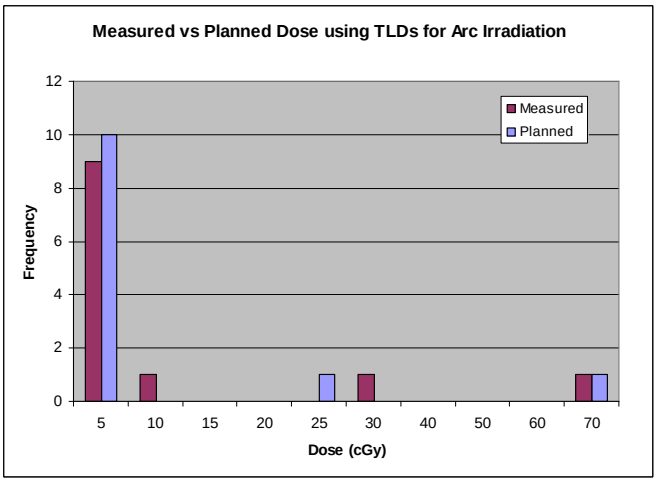

Fig 62 - A comparison of TLD readings for the Electron Arc Plan

CHAPTER III: RESULTS

4. PLAN EVALUATION

The plans were evaluated by 19 radiotherapy personnel who are regularly involved in planning. Plans were ranked from one to five in order of preference. The results of this survey are shown in the Fig 63.

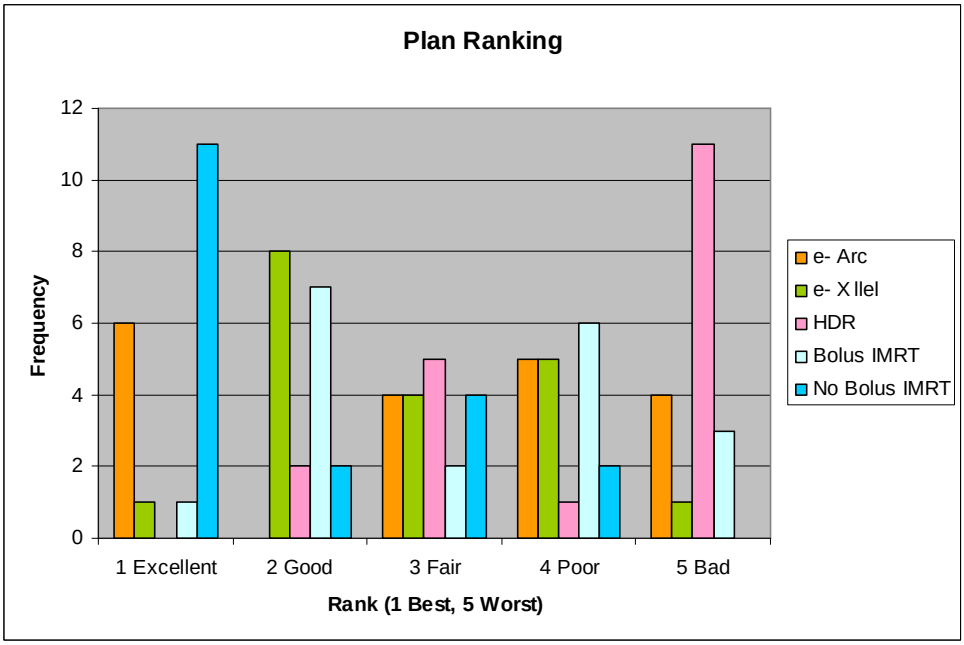

Fig 63 – Ranking of plans by radiotherapy personnel

The IMRT plan without bolus was evaluated as the best plan most often and the HDR plan was evaluated as the worst. The electron-photon opposed plan was ranked as between good and poor. It can be seen above that the electron arc received rankings fairly evenly from excellent to bad from all personnel. The HDR plan was seen to give a distribution which was fair to poor. The five plans evaluated were very different in terms of dose coverage, maximums and organ at risk doses. There is therefore quite a surprising spread of results from the assessment.

Fig 64 shows the total score from each plan relative to the worst possible score that it could have obtained. This gives an indication as to the overall plan popularity.

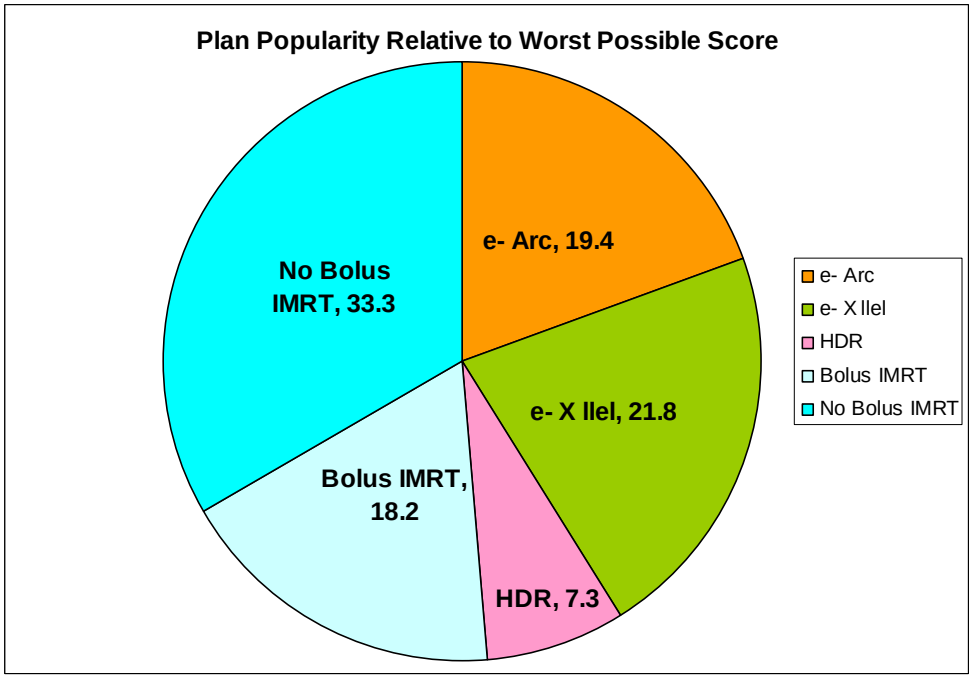

Fig 64 – Plan popularity relative to worst possible score

This graph shows that the IMRT plan without bolus was most popular overall. The next most popular was the electron and photon parallel opposed plan. The IMRT with bolus and the electron arc plans were considered similar, whilst the HDR plan was the least popular.

CHAPTER III: RESULTS

5. TIMING

The plans were additionally evaluated in terms of the time to make treatment aids, the time to plan and the time to execute the treatment delivery. The timing was normalised to the time taken to deliver a dose of 200 cGy in a single fraction. It was further noted if any specialist equipment or personnel skill was involved in the technique.

All plans required the following:
60 minutes to make thermoplastic mask
30 mins to perform and transfer CT scan
120 mins to digitize contours
5 mins patient setup for treatment
5 mins data transfer and verify

HDR

The HDR delivery time was slowed due to the availability of only two catheters. The actual time for delivery with two catheters was three minutes. The treatment time if 24 catheters were available is estimated based on the source transfer and delivery time.

360 mins catheter fixation
120 mins to digitize catheters
60 mins to optimize using inverse planning: select optimum parameters and calculate
30 mins to optimize plan manually after inverse planning
5 mins approx treatment time

IMRT Slow with bolus

120 mins bolus manufacture
30 mins to find optimal beam configuration
120 mins to optimize using inverse planning: select optimum parameters and calculate
5 mins additional data transfer and verify for IMRT
5 mins additional patient setup for bolus
50 mins linac delivery on Siemens Oncor Linac
120 mins additional IMRT QC

IMRT Slow no bolus

30 mins to find optimal beam configuration
120 mins to optimize using inverse planning: select optimum parameters and calculate
5 mins additional data transfer and verify for IMRT
50 mins linac delivery on Siemens Oncor Linac
120 mins additional IMRT QC

Quick IMRT with bolus

120 mins bolus manufacture
30 mins to find optimal beam configuration
120 mins to optimize using inverse planning: select optimum parameters and calculate
5 mins additional data transfer and verify for IMRT
5 mins additional patient setup for bolus
30 mins linac delivery on Siemens Oncor Linac
120 mins additional IMRT QC

e- and X Parallel Opposed

90 mins to make blocks for both electrons and photons.
360 mins wait for blocks to harden
30 mins to clean, file and sand blocks
15 mins to mount blocks
15 mins to check block setup on linac
30 mins to find optimal beam configuration
25 mins linac delivery including room entry for applicator

Electron Arc- ArcAP

The electron arc planning process took 120 minutes to find optimal beam configuration using simulated SAD Arced treatment. This was due to limitations of the planning system described previously. It is estimated that a planning system with an arced SAD treatment available would only take 10-15 minutes to plan. The plan took 55 minutes to deliver on the Hobbes linac as the gantry had to be rotated manually for 10º increments over the treatment angle. The delivery time for a true are treatment was estimated, based on the monitor units required, the dose rate and the gantry rotation rate.

10 mins to enter optimal beam configuration using real SAD Arced treatment
10 mins linac delivery using true arc treatment

With Bolus:

Add 10 mins bolus manufacture
Add 5 mins additional patient setup for bolus

With Blocks:

Add 60 mins to make blocks.
Add 360 mins wait for blocks to harden
Add 30 mins to clean, file and sand blocks
Add 15 mins to mount blocks
Add 15 mins to check block setup on linac

Electron Arc- ArcLRInfSup

60 mins to make blocks.
360 mins wait for blocks to harden
30 mins to clean, file and sand blocks
15 mins to mount blocks
15 mins to check block setup on linac
15 mins to enter optimal beam configuration using real SAD Arced treatment
15 mins linac delivery using true arc treatment including room entry for blocks

These times are summarised in Table 28 and Fig 65. The time in which the patient is involved during the preparation, such as during the manufacture of the bolus or thermoplastic mask, is considered separately from the time which is required for accessory preparation, which does not involve the patient, such as during the manufacture of the catheters or the blocks. In Table 28 and Fig 65 the times required to generate and deliver the arced plans which gave such poor distributions are not shown as these treatments were too poor to consider for patient delivery. The lead time is the additional time required for the blocks to harden, which does not involve any patient or personnel time.

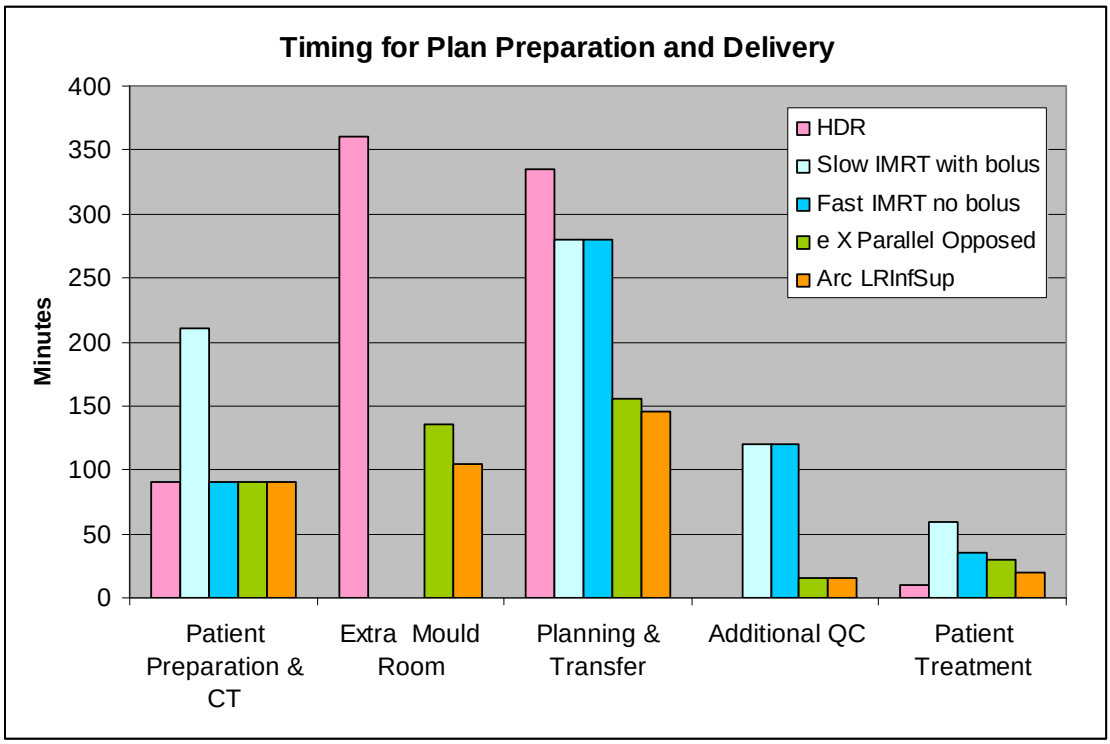

Fig 65 – Timing for plan preparation and delivery

Technique	Patient Preparation & CT	Extra Mould Room	Planning & Transfer	Lead Time	Additional QC	Treatment per Fraction
HDR	90	360	335	-	-	10
Slow IMRT with bolus	210	-	280	-	120	60
Slow IMRT no Bolus	90	-	280	-	120	55
Fast IMRT with bolus	210	-	280	-	120	40
e X Parallel Opposed	90	135	155	360	15	30
Arc LRInfSup	90	105	145	360	15	20

Table 28 – Timing for plan preparation and delivery

It can be seen that the patient involved preparation time was similar for all treatments. The planning time varied from 2.5-5.5 hours depending upon the complexity of the plan and the time required to optimise the inverse planning procedure. The treatment times varied considerably from 10 minutes to an hour per fraction. This variability could have a huge impact depending upon the patient cooperation and the overall patient throughput on the treatment machines.

In addition to the times taken for the treatment processes, it was necessary to consider the additional skills or equipment which each technique may require. These are summarised in Table 29.

Technique	Specialist Equipment	Specialist Skills
HDR	Multiple catheters	3D Planning
Slow IMRT with bolus	MLC, IMRT Inverse Planning	Inverse Planning
Slow IMRT no Bolus	MLC, IMRT Inverse Planning	Inverse Planning
Fast IMRT with bolus	MLC, IMRT Inverse Planning	Inverse Planning
e X Parallel Opposed	Block cutter	None
Arc LRInfSup	Block cutter, Arc Applicator, Arc Planning	None

Table 29 – Specialist skills and equipment required for treatment modalities

Each of the treatment plans also had problems specific to the technique which needed to be overcome before they could be delivered to the patient. Some of these obstacles were unique to the equipment and licenses available in the department in which these plans were generated but similar problems would be encountered in other departments. These problems are shown in Table 30.

Technique	Obstacles Encountered
HDR	Insufficient catheters for multiple catheter delivery. Catheter mask difficult to manufacture and deliver dose around ears
Slow IMRT with bolus	Bolus difficult to manufacture evenly and cumbersome and uncomfortable for patient
Slow IMRT no Bolus	None
Fast IMRT with bolus	Bolus difficult to manufacture evenly and cumbersome and uncomfortable for patient
e X Parallel Opposed	Block alignment and cold spot reduction

Arc LRInfSup	Arc licensing for planning and linac. Electron attenuation through head tray and cushion. Non-uniform head shape results in non-uniform distribution.

Table 30 – Obstacles encountered for treatment modalities

CHAPTER IV: CONCLUSIONS

The results from the TLD and film dosimetry show that all of the plans were reproduced accurately in the phantom. There are a number of factors to consider in the evaluation of these plans for the treatment of the whole scalp. A brief summary is shown in Table 31.

Technique	Patient Preparation	Planning, QC, Mould Room	Treatment per Fraction	Equipment	Plan Ranking
HDR	90	695	10	>20 catheters	5
Slow IMRT with bolus	210	400	60	IMRT	4
Slow IMRT no Bolus	90	400	55	IMRT	1
Fast IMRT with bolus	210	400	40	IMRT	-
e X Parallel Opposed	90	285	30	Blocks	2
Arc LRInfSup	90	265	20	e Arc	3

Table 31 – Summary of plan timing, equipment and ranking

Whilst the IMRT plan without bolus was evaluated to be the most popular by the radiotherapy planning personnel, the treatment times were very long. For a patient in the prone position in a mask this is very uncomfortable and additionally can prevent the ability to treat several 3D conformal patients in a busy department. The IMRT plans also required a lot of time during the planning process. The electron and photon blocked parallel opposed plan could be delivered in half the time on the linear accelerator and saved almost two hours during the planning process. The electron arc was also very quick to deliver and plan. Whilst the HDR plan could be delivered to the patient sitting in an upright position with little discomfort in only five minutes, the dose distribution was unfortunately too poor for it to be seriously considered for a patient treatment.

It is therefore concluded that if enough time is available on the linear accelerator and the planning system and the patient is able to lie in a prone position for an hour, then the IMRT plan without bolus can be considered the most appropriate for the treatment of the whole scalp. If a department has a very high patient throughput or the patient is unable to lie in a prone position for long, then the electron and photon parallel opposed plan also delivers a reasonable dose distribution to the whole scalp in a more acceptable time.

CHAPTER V: DISCUSSION

The measurements of the accuracy of the plan delivery required the use of film dosimetry inside a patient-like phantom in order to realistically represent the treatment that would be delivered to a real patient. Unfortunately this resulted in a dosimetry technique with very poor spatial resolution. It may therefore be advantageous to investigate the delivery of these plans in a phantom with calibration marks using film dosimetry software to more accurately measure the plan delivery. This would require the purchase of a dose export license for the brachytherapy system. Due to the insertion of film it was also not possible to verify the patient and block positions using portal imaging prior to treatment which could have added valuable insight into the reliability of the treatment setup.

Other groups have suggested the use of proton irradiation, tomotherapy or RapidArc treatment to irradiate the whole scalp. It would have been a valuable extension of this study to compare these techniques if the technology was available.

It was interesting to observe the huge range of responses to the plan evaluation by the radiotherapy personnel. This highlighted the subjective nature of plan assessment. From discussion with the personnel after the evaluation, it appeared that there were two opposing philosophies employed to determine the plan ranking. The first most conservative planning style was to disregard any plan with high hot spots even if they were restricted to the target. The second philosophy was more aggressive and the plans with the lowest organ at risk does were chosen regardless of how high the target dose was or how inhomogeneous the distribution.

Whilst the plan evaluation was very subjective it did still seem to be apparent the dose distribution achieved with the IMRT plan was superior to the other plans. However, each plan required the use of different planning systems or specialist equipment. The choice of plan for the irradiation of the whole scalp may therefore depend more upon the availability of techniques than the superiority of the resultant treatment.

CHAPTER VI: REFERENCES

ABLE C, Mills M, McNeese M, Hogstrom K. 1991.
Evaluation of a total scalp electron irradiation technique.
Int J Radiation Oncology Biology & Physics. 21(4):1063-72.

BEDFORD J, Childs P, Nordmark Hansen V, Warrington A, Mendes R, Glees J. 2005.
Treatment of extensive scalp lesions with segmental intensity-modulated photon therapy.
Int J Radiation Oncology Biology & Physics. 62(5):1549-1558.

DE BOER S, Khan I, Hackett R, Hales L, Jaggernauth W. 2005. The Dosimetric and Geometric analysis of a total scalp electron-photon irradiation technique.
Int J Radiation Oncology Biology & Physics. 63(Supp 1): S555.

HARDCASTLE N, Soisson E, Metcalfe P, Rosenfeld AB, Tome WA. 2008.
Dosimetric verification of helical tomotherapy for total scalp irradiation..
Medical Physics. 35(11):5061-8.

HOLMES T, Hudes R, Dziuba S, Kazi A. 2006.
Total Scalp and other circumferential large surface area mold irradiation technique for skin lesions using multi catheter HDR brachytherapy.
Brachytherapy. 5(2): 104.

KHAN F 2003.
The Physics of Radiation Therapy 3rd Edition.
Philadelphia:Lippincott Williams & Wilkins. 317.

KINARD J, Zwicker RD Schmidt-Ullrich R, Kaufman N, Pieters R. 1996.
Short Communication: Total craniofacial photon shell technique for radiotherapy of extensive angiosarcomas of the head.
British J Radiology. 69(820):351-5.

LIEBMANN A, Pohlmann S, Heinicke F, Hildebrandt G. 2007.
Helmet Mold-Based Surface Brachytherapy for Homogeneous Scalp Treatment: a Case Report.
Strahlentherapie und Onkologie. 183(4):211-214.

References

MELLENBERG D, Schoeppel S. 1991.

Total scalp treatment of mycosis fungiodes: the 4x4 technique.

Int J Radiation Oncology Biology & Physics. 21(4):1063-72.

NAKAMURA R, Harada S, Obara T, Ehara S, Yoshida A, Akasaka T. 2003.

Iridium 192 brachytherapy for hemorrhagic angiosarcoma of the scalp: a case report.

Japan J Clinical Oncology. 33(4):198-201.

OZYAR E, Gurdalli S. 2002.

Mold brachytherapy can be an optional technique for total scalp irradiation.

Int J Radiation Oncology Biology & Physics. 54(4):1286.

PEARCE A, Breitman C, Herring C, Rans K, Balogh A. 2005.

Total scalp irradiation using intensity modulated radiotherapy for scalp lymphoma.

Radiotherapy & Oncology. 76(Supp 1):S66.

TUNG S, Shui A, Starkschall G, Morrison W, Hogstrom K. 1993.

Dosimetric evaluation of total scalp irradiation using a lateral electron-photon technique.

Int J Radiation Oncology Biology & Physics. 27(1):153-60.

WOJCICKA J, Lasher D, McAfee S, Fortier G. 2009.

Dosimetric comparison of three different treatment techniques in extensive scalp lesion irradiation.

Radiotherapy & Oncology. 91(2):255-60.